AD NUMBER

AD885333

LIMITATION CHANGES

TO:

Approved for public release; distribution is unlimited.

FROM:

Distribution authorized to U.S. Gov't. agencies and their contractors; Critical Technology; APR 1971. Other requests shall be referred to Air Force Flight Dynamics Laboratory, Wright-Patterson AFB, OH 45433.

AUTHORITY

AFFDL ltr dtd 8 Mar 1972

AFFDL-TR-70-141

IMPROVEMENT OF A STRUCTURAL FATIGUE SENSOR

ROBERT S. HORNE

LOCKHEED - GEORGIA COMPANY

TECHNICAL REPORT AFFDL-TR-70-141

APRIL 1971

This document is subject to special export controls and each transmittal to foreign governments or foreign nationals may be made only with prior approval of the Air Force Flight Dynamics Laboratory (AFFDL/FEBT), Wright-Patterson Air Force Base, Ohio 45433.

AIR FORCE FLIGHT DYNAMICS LABORATORY
AIR FORCE SYSTEMS COMMAND
WRIGHT-PATTERSON AIR FORCE BASE, OHIO

NOTICE

When Government drawings, specifications, or other data are used for any purpose other than in connection with a definitely related Government procurement operation, the United States Government thereby incurs no responsibility nor any obligation whatsoever; and the fact that the government may have formulated, furnished, or in any way supplied the said drawings, specifications, or other data, is not to be regarded by implication or otherwise as in any manner licensing the holder or any other person or corporation, or conveying any rights or permission to manufacture, use, or sell any patented invention that may in any way be related thereto.

Copies of this report should not be returned unless return is required by security considerations, contractual obligations, or notice on a specific document.

300 - May 1971 - CO305 - 40-71-673

IMPROVEMENT OF A STRUCTURAL FATIGUE SENSOR

ROBERT S. HORNE

FOREWORD

This investigation was performed by Lockheed-Georgia Company at Marietta, Georgia under Air Force Contract No. F33(615)-69-C-1593. The contract was initiated under Project No. 1347, "Structural Testing of Flight Vehicles," and Task No. 134702, "Measurement of Structural Response."

The work was supervised and this report was prepared by Robert S. Horne, Project Engineer. This project was initiated by the Air Force Flight Dynamics Laboratory, and was administered under the technical coordination of Mr. Robert A. Crouch (AFFDL/FBT), Project Engineer.

Some of the items evaluated in this report were fabricated from commercial materials that were not developed or manufactured to meet government specifications, to withstand the tests to which they were subjected, or to operate as applied during this study. Any failure to meet the objectives of this investigation is no reflection on any of the items discussed herein or on any manufacturer.

Special acknowledgments are due to Dr. R. W. Newman, Dr. H. J. Rack, Mr. T. J. Headley, and Mr. C. D. Bailey of the Lockheed Research Center. Technical assistance was also provided by Mr. W. M. McGee, Specialist, Development Test Laboratory.

This report covers work conducted from April 1969 to April 1970 and constitutes the final report under Contract No. F33(615)-69-C-1593. It was submitted by the author in September, 1970. The contractor's report number is ER-10655.

This technical report has been reviewed and is approved.

Robert L. Cavanagh

ROBERT L. CAVANAGH
Chief, Experimental Branch
Structures Division
Air Force Flight Dynamics Laboratory

ABSTRACT

The annealed Constantan foil materials currently used in bonded fatigue sensing devices have fatigue life and sensitivity limitations which place restraints upon practical application to long life service aircraft. These restraints led to the requirement for further investigation and development of a more compatible material to meet present and future applications to fleet aircraft within the Air Force inventory. Since previous sensor development efforts have been centered around strain gage technology, a new approach oriented toward adapting the most favorable metallurgical and fatigue properties of a bondable resistive material to the fatigue behavior of an aircraft structure seemed the more appropriate course of action. Initially a group of alloys of the most promising thin foil resistive materials were evaluated. When the threshold sensitivity of the annealed foil materials proved inadequate, the effort was directed toward the development of a vacuum deposited sensor of a material having an ordered atomic structural arrangement. A selected composition of a copper-nickel-zinc material was vacuum deposited in a long-range order arrangement so that when disordered by cyclic deformation a relatively large, permanent electrical resistance change was produced. The test results indicated that the vacuum deposited sensor shows a substantially large improvement over annealed foil materials in the important areas of fatigue life and sensor sensitivity. The sensor performance obtained did represent a breakthrough in technology and indicates the potential for diversified application to fleet aircraft.

TABLE OF CONTENTS

ILLUSTRATIONS

The symbols and terms used in this report are peculiar to the nature of this activity and are listed here to help clarify what might otherwise be an ambiguous description. Where possible, the terms and symbols used are compatible with those in recognized standards and handbooks, such as the "8th Edition of the Properties and Selection of Metals." It is believed these definitions will permit a common basis for later communications.

Aging	Any change in properties with time at room or elevated temperatures
Annealing	Any heating cycle which serves to soften the alloy, or to reduce or eliminate the effects of cold work or previous heating cycles
Anneal, Full	A heating or quenching procedure for metals which leads to their maximum softness, ductility, and formability
Anneal, Stabilizing	Heating at a temperature which results in material properties less liable to be affected by other heating and cooling cycles
Anneal, Stress Relief	An anneal which reduces residual stresses present after forming, welding, or machining
Anneal, Strand (Bright Anneal)	Annealing thin foils in a protective medium to prevent oxidation and discoloration
Artificial Aging	Aging at elevated temperatures
Base Metal	The metal present in the largest proportion in an alloy
Bell Jar	A bell shaped glass enclosure used for vacuum experiments
Burning	Overheating to a temperature which produces incipient melting of one or more phases leading to embrittlement - evidenced as discoloration in thin foils
Carbonization	Conversion of a substance into elementary carbon

Cold Working	Deforming metal plastically at a temperature lower than recrystallization temperature
Cooling	Reducing the temperature of a foil in a gaseous environment rather than liquid quenching
Configuration	Grid geometry
Constantan	Most common alloy used in the manufacture of strain gages - known under various trade names, the most common of which is "Advance" composed of 43% nickel and 57% copper
Composition	Construction and materials for backing and grid elements
Coupon; Specimen	Test article or structure -terms used interchangeably
Deformation, Plastic	Elongation that remains after removal of the load which caused it
Diffusion	The spontaneous movement of atoms or molecules to new sites within a material
Die-Cut	Process for obtaining a particular sensor grid configuration by the use of precision dies
Discontinuity	An abrupt change in load path associated with holes, notches, contaminants, or other material defects
Discontinuous Yielding	Nonuniform plastic flow of a metal exhibiting a yield point in which plastic deformation is inhomogeneously distributed along the gage length
Dislocation	A linear defect in the structure of a crystal - misfits in atomic spacing
Disorder	Disturbance of the normal order of an atomic lattice

Equiaxed Grain	A structure in which the grains have approximately the same dimensions in all directions
Etch, Acid	A chemical process designed to dissolve or otherwise remove an unwanted portion of foil material leaving a particular grid configuration
Evaporant	The metal being vaporized
Hardened, Fully	Maximum hardness obtainable by strain hardening, cold rolling, drawing, or heat treatment
Flash Evaporation	Foil material transformed to a gaseous state by electrical vaporization
Fractionation	Separation of elements of the alloy into separate layers
Grain	An individual crystal in a polycrystalline metal or alloy
Heat Treatment	Any combination of heating and cooling operations for the purpose of changing the material properties
High Cycle Fatigue	Failure of specimen in more than 10^4 cycles
Homogenizing	Annealing or soaking at extreme temperature to reduce alloy segregation by diffusion
Kapton	A polyimide film manufactured by E. I. DuPont Co.- also known as "H" film
Karma	Trade name for a Driver Harris material which is composed of 74% nickel, 20% chromium, 3% aluminum, and 3% iron
Lattice	A geometric array in space so arranged that each point in the array has identical surroundings
Low Cycle Fatigue	Failure of specimen in less than 10^4 cycles
Mask	A device to cover parts to be protected and exposing parts to be coated

Metallograph	An optical instrument designed for both visual observation and photomicrography of opaque material surfaces
Ordering	A process consisting of a heating and quenching sequence to obtain a specific atomic arrangement in the lattice
Pinholes	Very minute holes in the deposited film exposing the substrate
Recovery	Reduction or removal of work hardening effects, without motion of large angle grain boundaries
Recrystallization	The formation of a new strain-free grain structure from that existing in cold worked metal - usually accomplished by heating
Sensitivity	The electrical change (ohms/ohm) of a sensor in response to a mechanical input
Sensor Grid	That portion of the sensor which is most sensitive to mechanical forces and produces an electrical resistance change
Substrate	An electrical insulating base material - sensor backing
Supersensitivity	Failure of electrical grid of a gage and consists of microscopic cracks in the strained portion of the foil which will intermittently open and close under dynamic conditions
Superlattice	An ordered arrangement of atoms in a solid solution to form a lattice superimposed on the normal solid solution lattice
Ternary Alloy	Alloy made of three elements
Thin Film	A process for materials vacuum deposited to a thickness ranging from several hundred angstroms to several microns
Thick Film	A process characterized by screen printing followed by firing in a furnace

Threshold Sensitivity	That completely reversed minimum strain level which will produce a resistance change of 0.05% or more within 50,000 cycles
Twinning	Plastic deformation causing a symmetrical shifting of grain parts with respect to each other
Vacuum Deposition	A process for vaporizing metals and condensing them on a designated spot in a vacuum chamber
Volumetric Resistivity	The electrical resistivity per unit volume - the unit used here is ohms per circular mil foot
Work Hardening	Mechanically induced hardening of ductile metals which are hardenable by plastic deformation

SYMBOLS

A°	Angstrom unit (10^{-8} cm) one thousand angstroms equals approximately 4.0 microinches
A_x	area of cross section
$A = \frac{F\ max - F\ min}{\frac{1}{2}(F\ max + F\ min)}$	ratio of alternating stress to mean stress in fatigue
bcc	body centered cubic
°C	degrees centigrade
cps (Hertz)	cycles per second
cpm	cycles per minute
e	elongation in percent - gage length given in ( ) following e
E	modulus of elasticity in tension
EV	electron volts
ϵ	strain $(\frac{\Delta L}{L})$
F	stress (psi)
F max	maximum stress
F min	minimum stress
fcc	face centered cubic
F alt	fatigue alternating stress
F_{tu}	tensile ultimate stress
F_{ty}	tensile yield stress
K	work hardening coefficient
Micron	one thousandth of a millimeter, approximately 40 microinches
MP	melting point
ϵ_p	plastic strain
L	length

R	strain ratio $\frac{\varepsilon \text{ min}}{\varepsilon \text{ max}}$
RT	room temperature
R_i	initial sensor resistance
RPM	revolutions per minute
S-N	S - stress N - number of cycles
TCR	temperature coefficient of resistance
ΔRs	resistance change of the sensor
μ	microunits or 10^{-6}
$\sim$	cycles
Δ	delta, incremental change
Ω	resistance in ohms

SECTION I

INTRODUCTION

The investigation and development of techniques for the determination of aircraft structural fatigue damage have been goals of the U. S. Air Force for many years. In 1965 the Air Force Flight Dynamics Laboratory initiated a feasibility investigation of an annealed foil type fatigue sensor and has reported the results in AFFDL-TR-66-113 dated January 1967 (Ref. 1). These thin foil sensors, configured in a manner similar to foil strain gages, are bonded to the structure using conventional strain gage attachment techniques. As the structure beneath the sensor "moves," the sensor foil material is cold-worked with a resulting electrical resistance change from a nominal value. The device can be used as a damage sensor if correlation factors can be adequately established to relate the resistance change to the damage induced in the structure. Since the resistance change is an irreversible process, within specific temperature limitations, the sensors have a "memory capacity" which eliminates the need for continuous connection to monitoring equipment. Ground-based monitoring instrumentation can be connected to the sensors at any convenient time to determine the sensor's resistance change and hence the structure's relative degree of fatigue exposure. A zero reference point (initial resistance value) of each sensor is required to represent the structures undamaged condition prior to test or usage.

The above mentioned investigation demonstrated that the presently used annealed Constantan alloy will change resistance measurably when bonded to structures which experience cyclic loading above specific strain levels. A number of controlled load fatigue tests were performed with sensors attached to test beams and a limited number of tests were conducted on structural panels. The results were encouraging and the feasibility of developing a practical system has been established. Some problems which remain are:

(a) The sensor will not respond effectively to alternating strain levels below 2000 microstrain peak-to-peak ($\pm$ 1000 microstrain or $\pm$ 10,000 psi stress range in aluminum);

(b) The sensor has a relatively short cyclic life at alternating loads of 3500 microstrain peak-to-peak ($\pm$ 1750 microstrain) and above;

(c) The sensor materials presently being used are limited to an operational temperature below approximately 200°F.

Additional sensor evaluations on C-5A production components (Ref. 2) have confirmed these limitations associated with annealed Constantan materials and the necessity for special considerations so as to derive reasonable success in their application. Recent investigations (Ref. 2) have made use of mechanical strain multipliers which serve to lower the apparent threshold sensitivity. Although 200 of the mechanically modified sensors are being used in a practical manner on the full-scale C-5A fatigue test specimens (Ref. 2) additional improvements appear possible and desirable.

1.1 TARGET REQUIREMENTS FOR AN IMPROVED FATIGUE SENSOR

For a practical application of the fatigue sensor to typical structural systems and components, the AFFDL has recognized the existence of some limitations with the annealed Constantan materials.

Continued evaluation and application of the fatigue sensor concept has permitted a more precise definition of the requirements necessary to obtain a more satisfactory sensor performance on fleet aircraft. The target specifications established by the AFFDL at the initiation of this program are listed as follows:

(1) The maximum sensor active length or width shall not exceed one inch including lead wire attachment tabs.

(2) The sensor nominal resistance value shall be between 60 ohms and 500 ohms at 75°F temperature and shall be reproducible within 1.0% sensor-to-sensor.

(3) The sensitivity threshold of the sensor shall be at a structural strain level of ± 500 microstrain (microinches per inch) or less (1000 microstrain peak-to-peak).

(4) The sensor sensitivity threshold is defined as the completely reversed structural strain level at which a 0.05% permanent change of the sensor nominal resistance value is obtained within 50,000 strain cycles <u>without</u> the use of a mechanical multiplier or amplification device. (Example: .03 ohms change from a 60 ohms nominal resistance). A desirable sensitivity threshold characteristic is one in which the sensitivity could be shifted up or down to suit the fatigue load spectra of the structure under surveillance.

(5) The sensor shall respond with a minimum permanent resistance change of 8.0% of the nominal resistance value over the usable strain-cycle life of the sensor. The strain-cycle life of the sensor, for structural materials application, shall approximate the figure shown below.

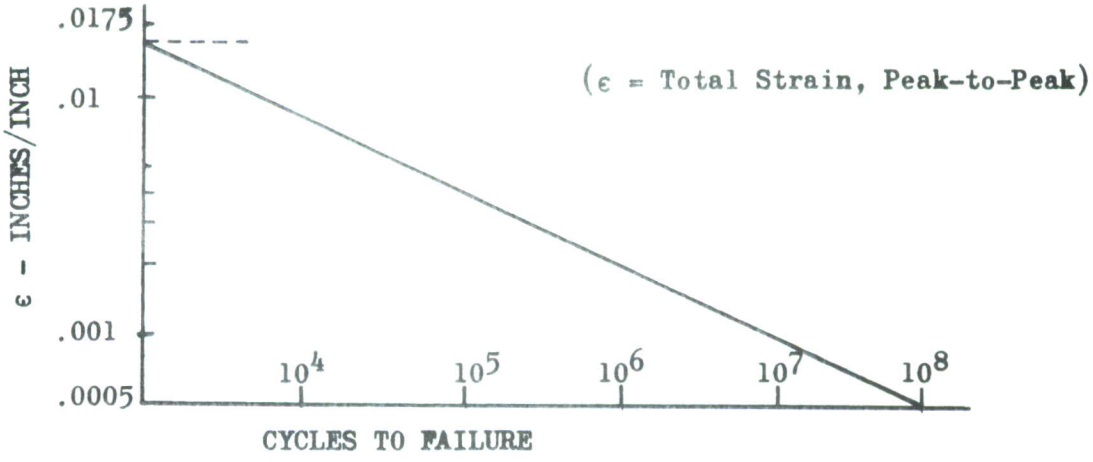

(6) Sensor-to-sensor strain-cycle repeatability variations shall not exceed a maximum bandwidth of 5.0% of the sensor total resistance change value.

(7) The sensor resistance change behavior shall be such that repeated strains of either tension or compression, or both, will cause a resistance change of the same polarity; that is, either positive or negative with respect to the nominal measured value but not both.

(8) Over the temperature range of $-65^{\circ}F$ to $+150^{\circ}F$, the sensor resistance change due to thermal effects will be minimized. The resistance-temperature characteristics of the sensor shall be determined during the sensor evaluation tests.

(9) The design and development of the sensor shall reflect the consideration of such variables as temperature, vibration, humidity, dust, and/or any other ambient conditions normally expected to be encountered under field service conditions.

(10) The sensor shall be capable of being installed, and lead wire attachments made, during the structural component fabrication process since many fatigue affected areas are inaccessible during an overall fatigue investigation. Access to the sensor shall not be required during operation.

(11) Changes in the nominal resistance of the sensor shall be produced by applied load cycles to the structural part, upon which the sensor is attached, and shall not be dependent upon connection to electronic equipment.

(12) The installation and operational reliability of the sensor shall be designed for long-time capabilities with usable life goals of 10 to 15 years desirable.

(13) The sensor resistance measuring network shall be compatible with, and have values that can be measured and/or recorded by use of standard commercially available electronic equipment that shall be ground based but can be packaged for easy transportability.

(14) The electronic measuring equipment required for sensor data acquisition shall be fully described as to manufacturer's model or type, functional operation, and other detailed descriptions, including a complete component and system interconnecting wiring diagram, as may be required for independent procurement actions. This data equipment procurement is not an objective or requirement of this program.

Although the above desired requirements were initially designated as target specifications, the limited funds available necessitated that some requirements be deleted from the program. High and low temperature test requirements were deleted as a result of contract negotiations, consequently all sensor evaluations were limited to room temperature exposure. The requirement for simulated long-life reliability evaluation involving humidity, salt fog, fuel soak, and similar environmental exposure was also deleted. Therefore no attempt was made to determine the sensor behavior as shown in target specification numbers 8 and 9.

SECTION II

TECHNICAL APPROACH

2.1 THEORETICAL CONSIDERATIONS

The ability of a metal to conduct electricity is a recognized characteristic and an important feature of a metal. Under the influence of an applied electric field, the quasi-free electrons present in the material will flow through the metallic lattice. Infinite conductivitiy would result if it were not for the presence of disturbing influences. These influences are chemical, physical and environmental in nature, and will impede the free flow of electrons, scattering them and causing an impedance better known as electrical resistance (ohms).

The chemical state of a metal and its influence on resistivity will depend upon the types and relative proportions of foreign impurity atoms present. Their effect on resistivity depends upon their distribution within the lattice, e.g., whether they are in solid solution, ordered, or present as compounds.

The physical state of even a chemically pure metal can be influenced by localized stresses produced by dislocations, vacancies, or interstitial atoms. Its electrical resistivity is dependent upon the quality and quantity of these defects which is related to the previous history of the metal including cold-work, annealing treatments, etc.

One obvious approach to development of a sensor is an exploitation of a material's best combined chemical and physical properties to produce the most desirable electrical behavior. For practical utilization, the selected sensor material must also possess suitable mechanical properties for bonding, soldering, and mechanical strength applicable to a fatigue environment.

Although it is generally found that the resistivity of annealed metals increases during plastic deformation, available reference material does not specify the exact relationship between resistivity change and the amount of deformation. The investigator is thus restricted to the measurement of the change of resistivity accompanying the alterations in the concentration and/or distribution of vacancies, interstitials, impurities, solute atoms, and dislocations which result from plastic deformation. Before proceeding to the type of materials that were investigated for possible use as fatigue sensors, it should be worthwhile to consider some of the salient features of experimental observations regarding materials which might be suitable for these devices.

With the exception of a very small number of alloys, it has been found that alloying results in a larger absolute increase in resistivity (Ref. 3) for a given amount of deformation than does the pure solvent metal. It has been shown (Ref. 4) that spectacular changes in resistivity may be due to the destruction of either long or short-range order. Alloys which undergo an order-disorder change can be made to transform completely from the ordered to the disordered state by heavy deformation. This destruction of order is accompanied by resistivity changes of approximately 50% for heavy deformation.

If one uses the concept of work hardening of annealed materials to produce an electrical resistance change, one may select between the face-centered-cubic (fcc) or body-centered-cubic (bcc) alloys. Although the fcc alloy Constantan is presently used for strain gages and fatigue sensors, it was felt that bcc materials might be better suited because of the work hardening requirement. Pure molybdenum, tungsten, and columbium were likely candidates in this respect and were therefore selected for a preliminary evaluation. The more promising of the fcc nickel-copper alloys, i.e., Monel 400, Nickel-Silver, and Chace 720, were also programmed for a materials evaluation. The use of semiconductor material was also a distinct possibility since they have both high resistivity and high modulus. Silicon has been used for strain gage applications; therefore, it was believed that modifications of this material or other alloys such as indium antimonide might be satisfactory for fatigue sensor applications. It was suspected that semiconductor materials might be either too temperature sensitive or too fragile for a fatigue environment; however, further examinations appeared desirable. Consequently, a thorough analysis of prospective semiconductor materials was programmed into the materials evaluation activities.

2.2 DESIRABLE OPERATING CHARACTERISTICS OF RESISTIVE MATERIALS

Previous experimental tests and evaluations of Karma, Constantan, and aluminum foils have provided a working knowledge of the most desirable characteristics for using the work hardening concept in a bonded foil sensor. Difficulties with aluminum foil were brought about by such characteristics as (1) low volumetric resistivity, (2) low resistance change from the soft to hard condition, and (3) difficulties in the attachment of lead wire. Refinements and improvements in Constantan and Karma necessary to comply with the requirements of Section 1.1 was considered unrealistic; therefore these materials were not subjected to further investigation or development. Without stating how high is high, or how low is low; suitable resistive materials were expected to have high volumetric resistivity, low yield strength, low TCR, but a large resistance change in going from the soft to hard metallurgical condition.

The characteristics believed more desirable for sensor resistive materials are shown in Figure 1. For a material to possess a threshold sensitivity of 500 $\mu\varepsilon$ or less it should have a low yield point. To produce a large resistive change it should have a high and uniform elongation range. The diagram in Figure 2 is typical of the relationship of the yield-to-tensile ultimate ratio to the work hardening coefficient of annealed metals. Basically, the materials with the higher work hardening coefficient (K) can be expected to produce the larger electrical resistance change. The lower yield-to-tensile strength ratio as illustrated in Figure 2, also results in a higher coefficient of strain hardening. These parameters combined with a low TCR , suitability for bonding, mechanical handling, etc., were considered essential to the selection of an annealed metal for sensor applications.

2.3 METAL DEFECT RESISTANCE DUE TO DEFORMATIONS

An electrical resistance change will occur in metals due to the introduction of imperfections in the crystal lattice by way of vacancies, interstitials, and dislocations. The principal way in which imperfections are introduced into metal are (1) plastic deformation by cold rolling, drawing, etc., (2) heat treatment, such as quenching from a high to a very low temperature, (3) thermal cycling through phase transformation, and (4) irradiation of the material with high energy particles.

Since the defects introduced by any of these techniques may be sensed by electrical means, the electrical resistance change produced by strain hardening is the particular area of interest. To promote the greatest resistance change from defects introduced by strain hardening, the cyclic strain exposure of the sensor should begin with the material in the fully annealed condition. Although the foil material has been hardened by cold rolling, the subsequent strand annealing removes the defects and the initial excess resistivity disappears.

Even greater resistance changes may be obtained by strain hardening ordered alloys, since the strain hardening characteristics of intermetallic compounds are dependent on the state of order. In general, ordered alloys work harden more rapidly than do equivalent alloys in the disordered state. Upon deformation at room temperature the ordered state is destroyed and defects are produced which do not recover at room temperature. Therefore, within temperature limitations the resistance change produced by these mechanisms can be considered permanent and irreversible.

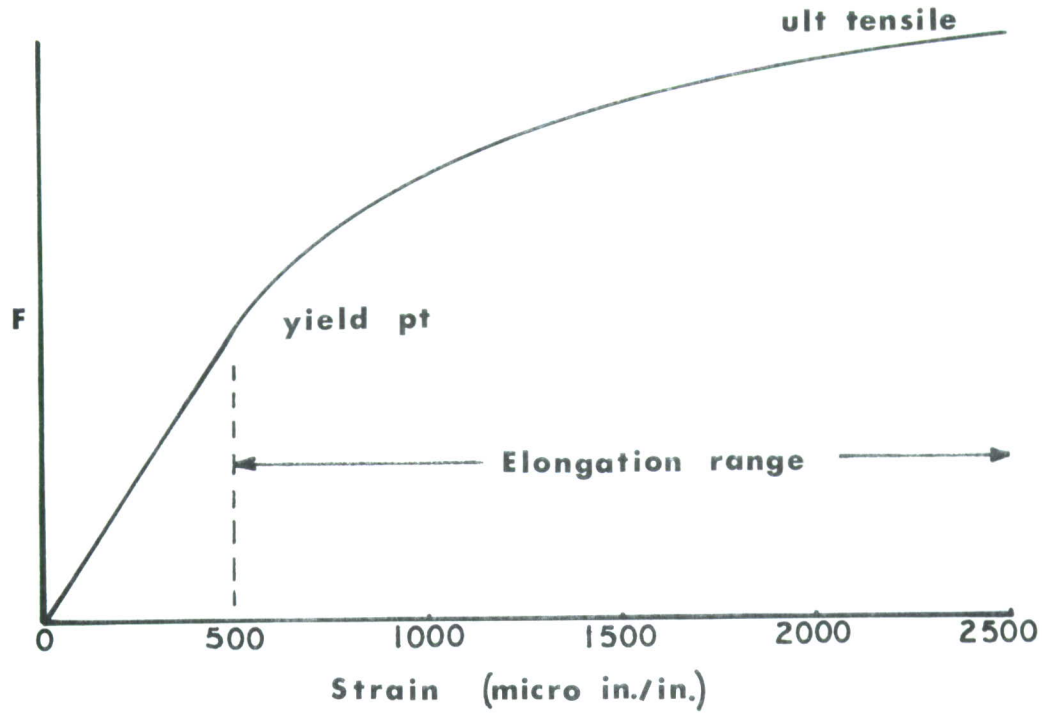

FIGURE 1. DESIRABLE CHARACTERISTICS OF A SENSOR MATERIAL

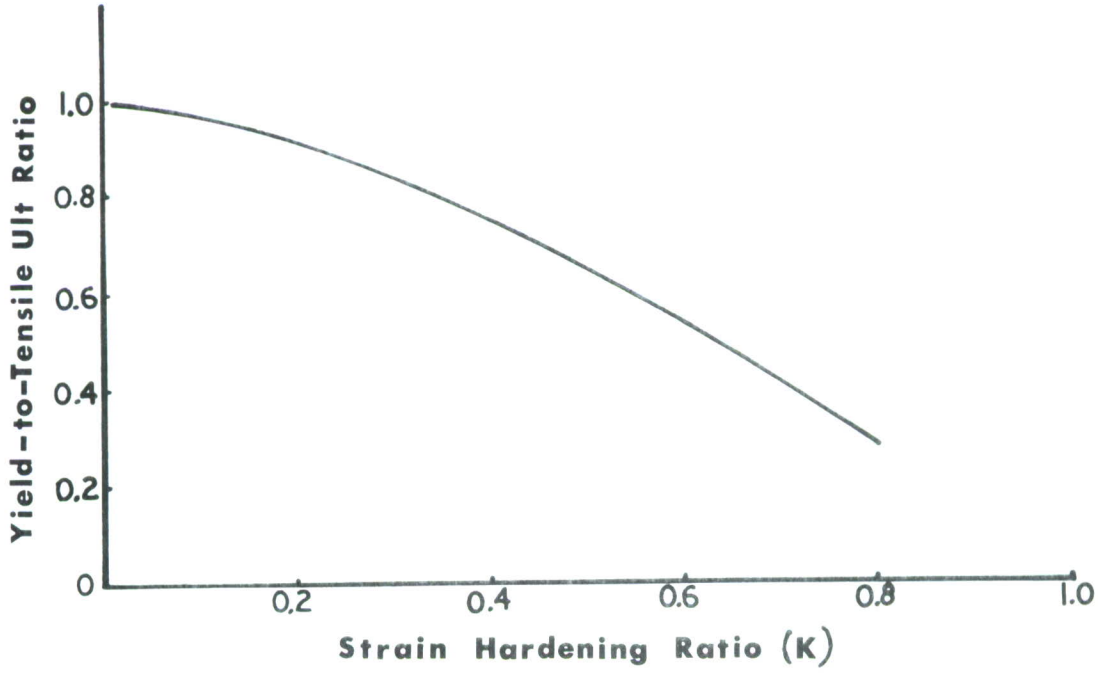

FIGURE 2. RELATIONSHIP OF YIELD-TO-TENSILE ULTIMATE RATIO TO MATERIAL WORK HARDENING COEFFICIENT

2.4 APPROACH SEQUENCE

Since previous investigations have been geared to strain gage technology, it was determined that a new approach oriented toward a "marriage" of metallurgical and fatigue properties of selected materials offered the potential for a significant breakthrough. In this respect a personnel task force composed of physical metallurgy, instrumentation, and stress disciplines was established and directed toward the development of an improved sensing device.

The program was designed to follow a sequence of activities as shown in Figure 3. The analytical evaluation of candidate resistive materials included a literature survey of material behavior characteristics in view of desired sensor performance. The materials showing the most promise were then procured in rolls of annealed foil or wire. Microscopic examinations of the candidate materials were then conducted to determine (1) the degree of anneal, (2) the extent and type of foil contaminants, (3) grain orientation, (4) precise foil thickness or variations in thickness, and (5) general overall appearance. The preliminary inspection and evaluation of the basic materials also included a determination of the suitability of each material for (1) soft soldering, (2) bonding to a flexible substrate, and (3) general material workability.

The evaluation was planned to progress through two basic stages, i.e., a materials evaluation followed by a sensor evaluation as shown in Figure 3. If a material proved unsuitable and an unlikely candidate for sensor fabrication, it was rejected from further evaluation. The acceptable materials were subjected to an evaluation of their suitability for fabrication into a sensing element, followed by an evaluation of sensor behavior upon exposure to cyclic strains. The cyclic strains were produced by screening tests and served to eliminate those sensors which could not meet the target requirements in regard to sensitivity, fatigue life, etc., as specified in Section 1.1. Sensor compliance with the first target requirement, i.e., threshold sensitivity, was a prerequisite for proceeding to further evaluations. Failure to comply with the first requirement was cause for rejection as an unacceptable sensor.

The sensor which best conformed to or exceeded the target requirements as a result of screening was then to be subjected to possible improvements and more extensive tests. Testing of the optimized sensor involved exposure to axial strains over a wide range of strain ratios and strain levels, more representative of the fatigue environment to be expected on service aircraft. One hundred of the optimized sensors were then to be submitted to the program initiating agency (AFFDL) for evaluation.

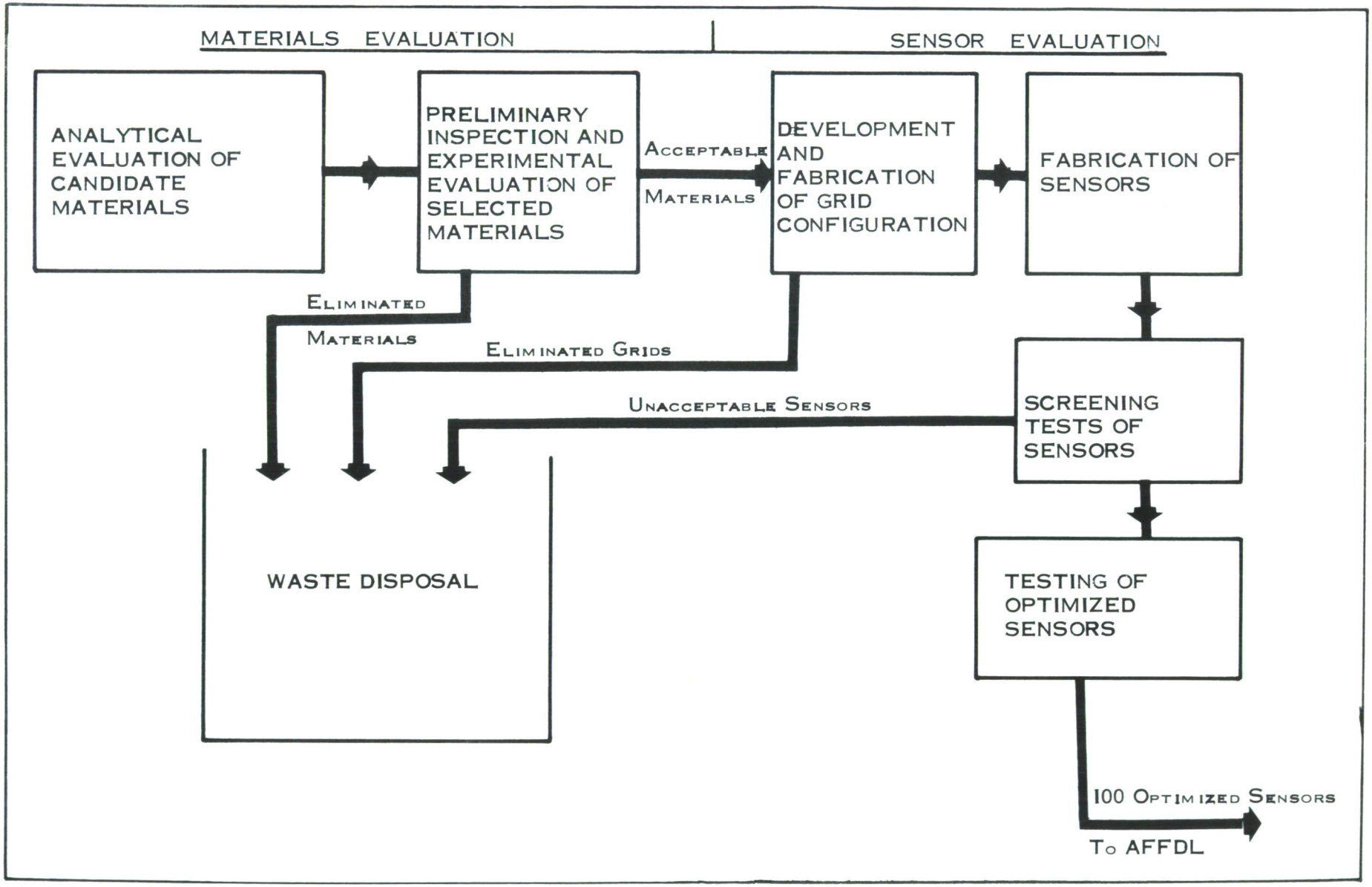

FIGURE 3. SEQUENCE OF ACTIVITY FOR THE DEVELOPMENT OF AN IMPROVED SENSOR

SECTION III

SENSOR DEVELOPMENT PROGRAM

3.1 PHASE I ACTIVITIES - ANNEALED WIRE AND FOIL SENSORS

3.1.1 SELECTION OF CANDIDATE MATERIALS

A literature survey was pursued to assist in the selection of candidate materials with the more desirable behavior characteristics. It was preferred to establish some criteria for selecting the most suitable materials and forecasting their performance rather than testing every possible combination of alloys, state of anneal, etc. The surveyed reference material (Refs. 3 through 9) did not always relate material mechanical properties to electrical properties; however the references usually discussed the material behavior characteristics. Some data such as threshold sensitivity had to be established by laboratory test.

The approximate percentage electrical resistance change of the material resulting from a change in its metallurgical condition (hard to soft) was obtained by a resistance measurement of a sample in each condition. That is, the resistivity of a specimen sample was measured in the cold rolled condition (hard) and then again after strand annealing (soft). The percent resistance change of the material is indicative of the sensor resistance change to be expected upon exposure to a fatigue environment.

The pertinent mechanical and electrical properties of the more promising materials were tabulated as shown in Table I. The data shown on the material analysis chart were collected from either the material manufacturer, handbook sources, or compiled as a result of laboratory tests. The literature survey (Refs. 3 through 9) covered a review and analysis of resistive materials in the semiconductor, wire, and foil form. Some materials such as tungsten and Manganin were available and more convenient to handle in the wire form. The selected semiconductor materials (silicon and indium antimonide) were given a laboratory analysis and rejected as being too temperature sensitive and erratic for a practical fatigue environment.

To comply with the target requirements outlined in Section 1.1 an order of priority regarding material characteristics was established. The physical and performance parameters in the order of their importance are listed as follows:

(1) Threshold Sensitivity
(2) Percent Resistance Change
(3) Fatigue Life
(4) Repeatability, Stability, TCR
(5) Mechanical Suitability
(6) Volumetric Resistivity

TABLE I

MATERIAL ANALYSES CHART

Commerical Designation	MECHANICAL AND PHYSICAL PROPERTIES (1) — PERCENT CHEMICAL COMPOSITION						Thermal Expansion ppm	Modulus of Elasticity psi x 10^6	Annealed Tensile Strength psi	Annealed Yield Strength psi	Ratio of Yield-to-Tensile Ultimate	ELECTRICAL PROPERTIES (1) — Volumetric Resistivity Ω/CMF	Threshold Sensitivity in (2) με	% Resistance Change (2) Soft - Hard	Temp. Coeff. of Resistivity (TCR) per °F	Adaptability (3)
	Ni	Cu	Mn	Zn	Fe	other										
Constantan (4)	45	55					8.7	28	60,000	28,000	.47	294	1,000	8.7	± .00001	A
Monel 400	66	31.6	.90		1.35		7.7	26	70,000	25,000	.36	307	700	12.5	.0001	B
Inconel 600	76	.10	.20		7.20	Cr 15.8	7.4	31	80,000	30,000	.38	620	1,100	6.0	.0015	B
Nickel-Silver	18	65		17			9.3	18	58,000	20,000	.34	172	800	10.	.000013	A
Chace 720	20	60	20				11.0	21	54,000	22,000	.40	360	1,150	6.0	.00002	B
Manganin (5)	4	84	12.0				10.9	—	80,000	45,000	.56	290	1,500	—	.000001	B
Molybdenum Permalloy	79	.05	.50		16.3	Mo 4.0	12.9	33.7	63,000	30,000	.47	349	700—900	12.	.00013	A
Pure Metals																
Columbium							3.82	15	40,000	30,000	.75	90.0	1,400	3.2	.000197	C
Molybdenum (5)							2.7	47	70,000	50,000	.71	31.4	1,200	18.	.000225	C
Tungsten							2.4	56	140,000	99,000	.71	33.0	1,100	50.	.000220	C

NOTES:

(1) AT ROOM TEMPERATURE OF 70° F
(2) DATA COMPILED FROM RESULTS OF LABORATORY TESTS; ALL OTHER DATA COLLECTED FROM HANDBOOK SOURCES AND REPRESENTS PROPERTIES OF THE BULK MATERIAL.
(3) ADAPTABILITY INCLUDES EASE OF LEAD WIRE ATTACHMENT BONDING, HANDLING, FABRICATION, ETC., AND IS RATED (A) EXCELLENT, (B) ACCEPTABLE, (C) DIFFICULT.
(4) DATA ON CONSTANTAN INCLUDED AS A BASIS FOR COMPARISON—IT WAS NOT EVALUATED ON THIS PROGRAM.
(5) EVALUATED IN WIRE FORM ONLY; ALL OTHER MATERIALS EVALUATED IN FOIL FORM.

If any sensor resistive materials failed to conform to the first requirement it was cause for rejection of that material without determining its performance characteristics in regard to the remaining parameters. If the threshold sensitivity of a resistive material closely approached requirements, further evaluation and refinements were considered.

3.1.2 PREPARATION AND ANALYSES OF RESISTIVE MATERIALS

To promote a maximum resistance change (ΔR) and also a low threshold sensitivity, special preparation of the selected candidate materials was required. Therefore, special consideration was given to rolling the foil, cleaning, annealing, and overall handling to produce annealed foil materials more likely to meet the target performance requirements. A microscopic analysis of the raw materials was also performed prior to fabrication of any material into a sensor grid.

3.1.2.1 Forming and Annealing

The selected resistive materials were rolled into the required thin foils by a commercial supplier. The foils were rolled to a thickness of 0.2 mil, $\pm$ 5% tolerance, a convenient width of 2 to 4 inches, and to minimum order lengths of 100 feet. In the case of strand annealing, the foil was unwound from its roll, moved through a slot in the furnace at a selected rate and back on to another roll in a manner similar to that shown in the diagram below.

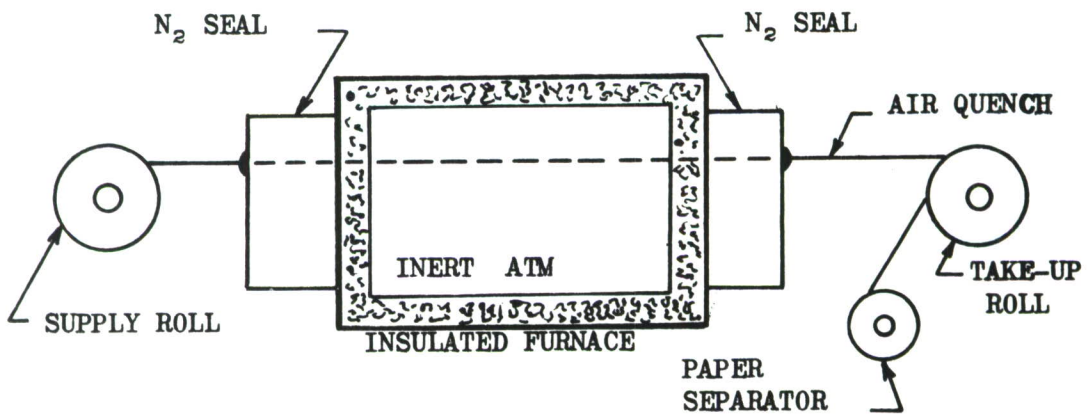

The term "strand anneal" has sometimes been misinterpreted as meaning annealing of the material after construction of the grid. This is not practical. The strand in this case is about four inches wide as opposed to the narrow strands associated with strain gage grids. All annealing or heat treatment of gage material was accomplished prior to their fabrication into conventional grids.

Some resistive materials (tungsten and Manganin) were more conveniently handled in the wire form. Tungsten is particularly difficult to die-cut, so one mil annealed bare wire was procured. The Manganin wire had a total diameter of 10 mil including the insulation coating and had a questionable degree of anneal.

3.1.2.2 Cleaning of Foil Materials

Preliminary examination of foil materials from four principal suppliers indicated that the supplier chosen produced the cleaner foil. Even the cleanest available foils, however, contained carbonized oil on the foil surface and embedded foreign particles which were strung out during rolling. The very nature of the foil rolling procedure introduces some contamination; consequently additional cleaning was attempted by Lockheed.

Attempts by the Lockheed Research Center to clean the foil ultrasonically did not remove the embedded particles; however it did alter the metallurgical characteristic of the foil in a detrimental manner. Ultrasonic cleaning was abandoned as unsuitable. Cleaning solvents were also applied to the foil surface with marginal results. Microscopic examinations revealed preferable areas of the foil could be selected, but the additional handling required to do this was considered inadvisable. As a result, die-cut grids were fabricated into sensors from the foil material "as received" from the supplier.

3.1.2.3 Laboratory Analyses of Materials

The annealed foil materials as received from the supplier were microscopically examined and preliminary tests were conducted for material flaws and discrepancies. A Bausch and Lomb Metallograph was used to identify any flaws or material conditions which would be detrimental to the fabrication of a sensor grid. The surface condition of the candidate foils were very similar to that of the Constantan materials as previously examined and discussed in Reference 2. That is, the foils showed surface finish lines, foreign particles rolled into the foil, and some variation in foil thickness. The photomicrographs in Figures 4 through 11 illustrate (1) the general surface condition, (2) that the foil is annealed as evidenced by equiaxed grains, and (3) that intermetallic or oxide inclusions were strung out during rolling and did not dissolve during annealing.

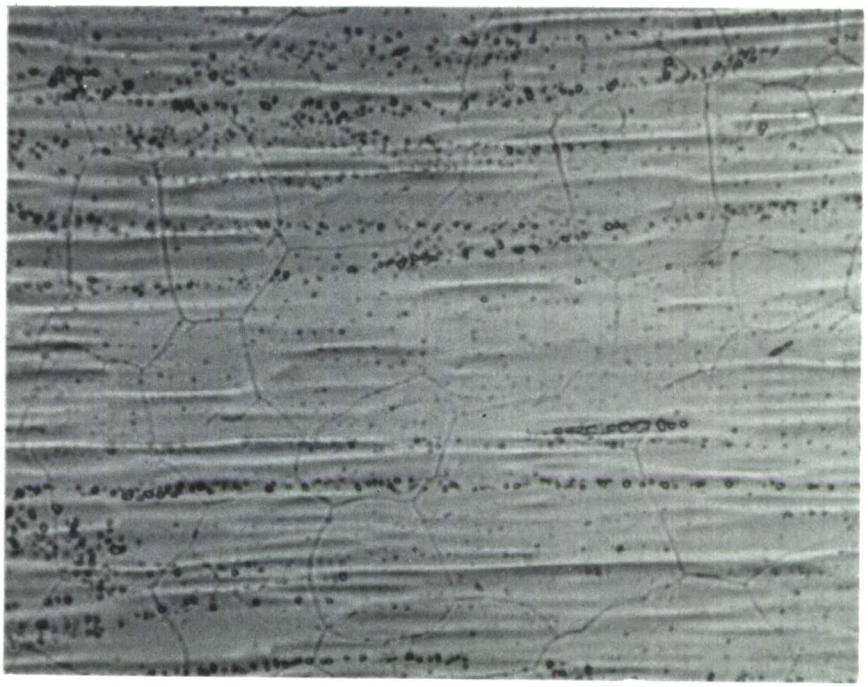

FIGURE 4. PHOTOMICROGRAPH OF ANNEALED MONEL 400 AS RECEIVED FROM THE SUPPLIER (1000X)

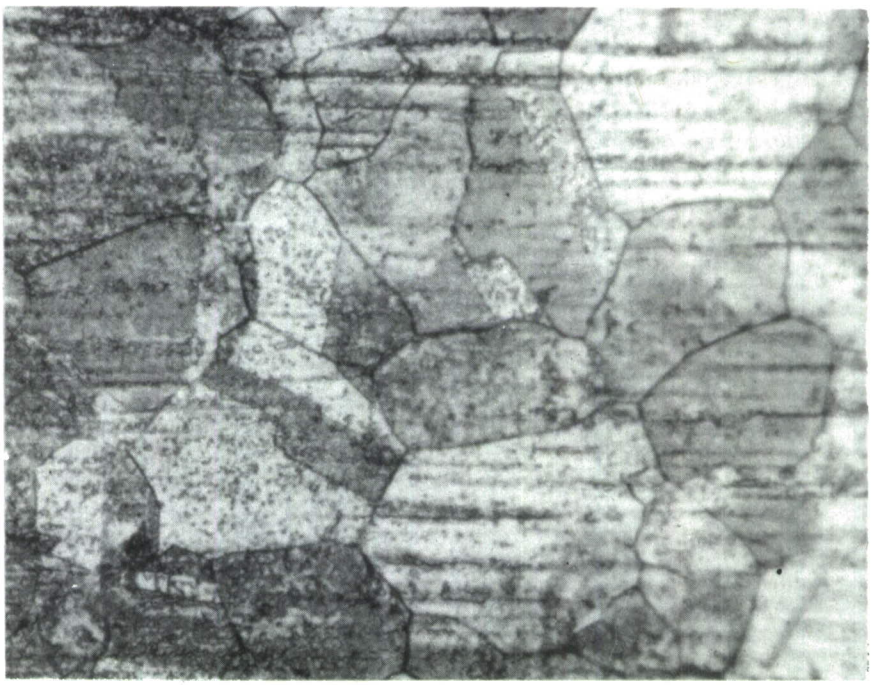

FIGURE 5. THE SAME FOIL AFTER ETCHING TO HIGHLIGHT GRAIN STRUCTURE (1000X)

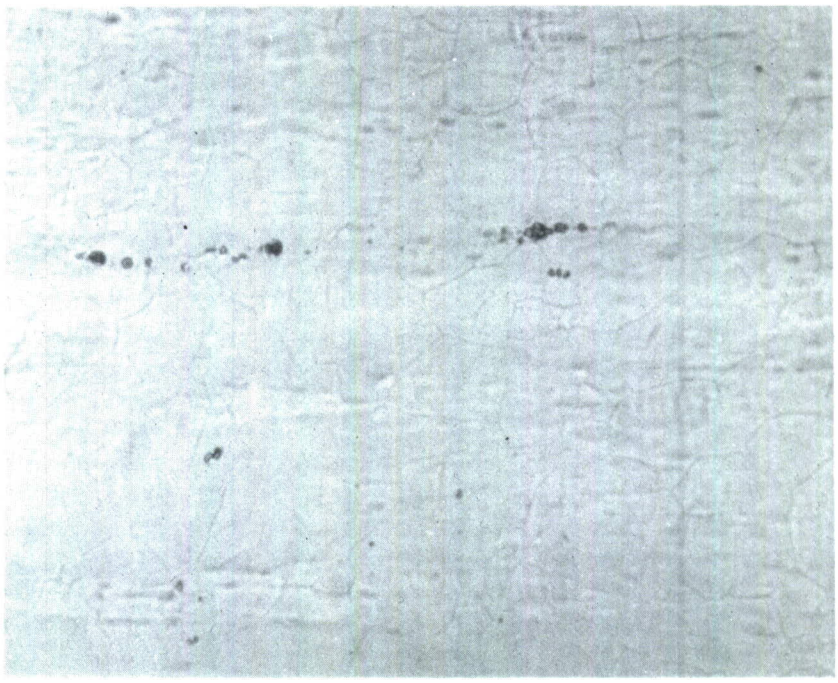

FIGURE 6. PHOTOMICROGRAPH OF FULLY ANNEALED MOLYBDENUM PERMALLOY PRIOR TO ETCHING (1000X)

FIGURE 7. PHOTOMICROGRAPH OF THE SAME FOIL AFTER ACID ETCHING (1000X)

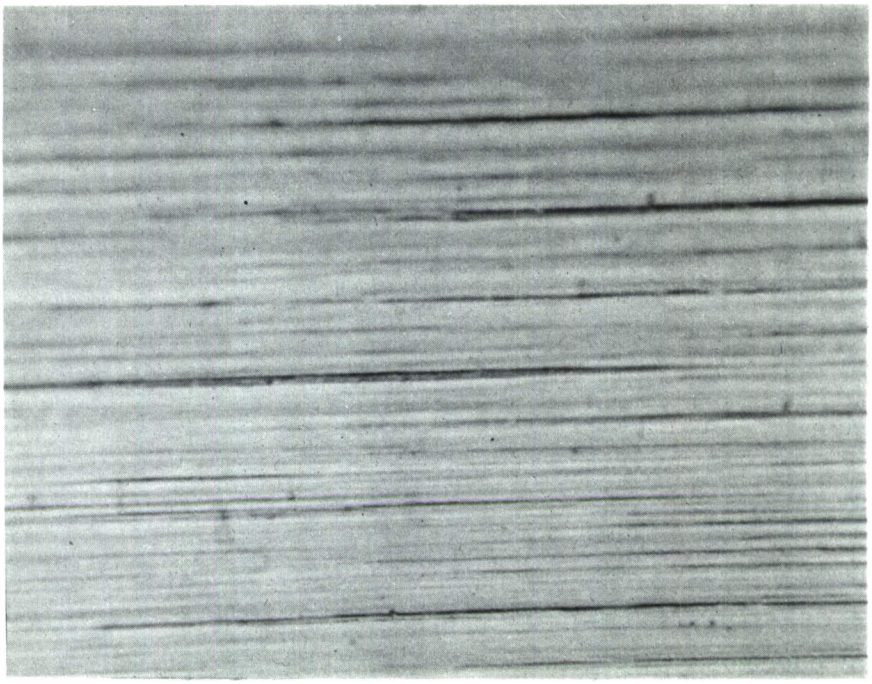

FIGURE 8. PHOTOMICROGRAPH OF 0.0002" THICK NICKEL-SILVER FOIL AS RECEIVED FROM THE SUPPLIER (1000X)

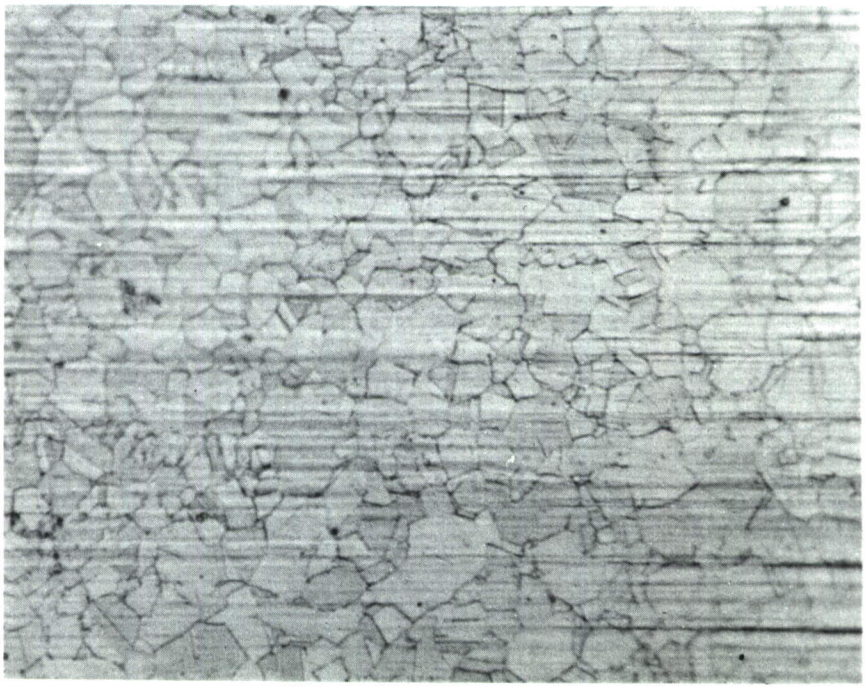

FIGURE 9. THE SAME FOIL AFTER ETCHING TO SHOW GRAIN STRUCTURE (1000X)

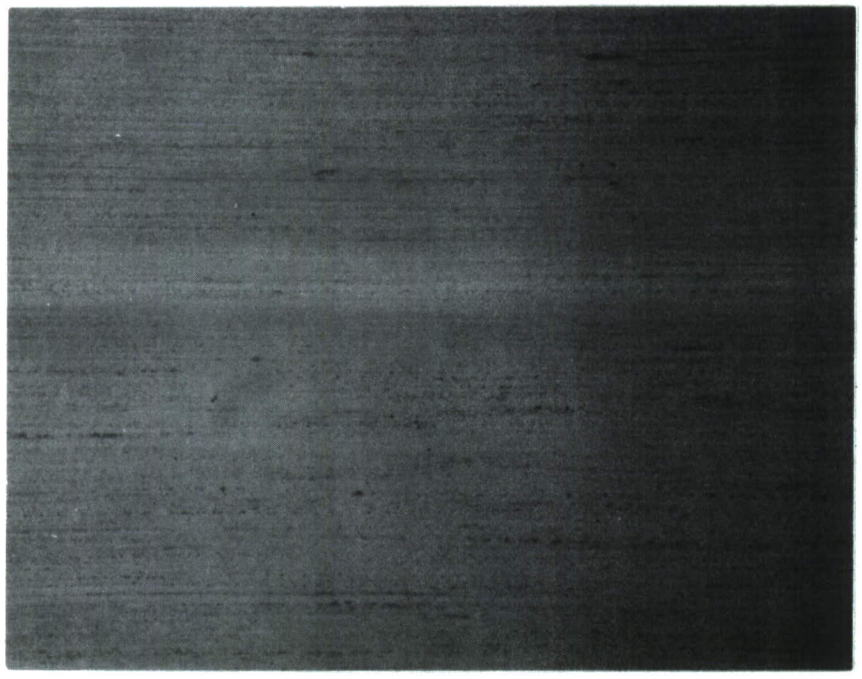

FIGURE 10. UNETCHED CHACE 720 ANNEALED FOIL (1000X)

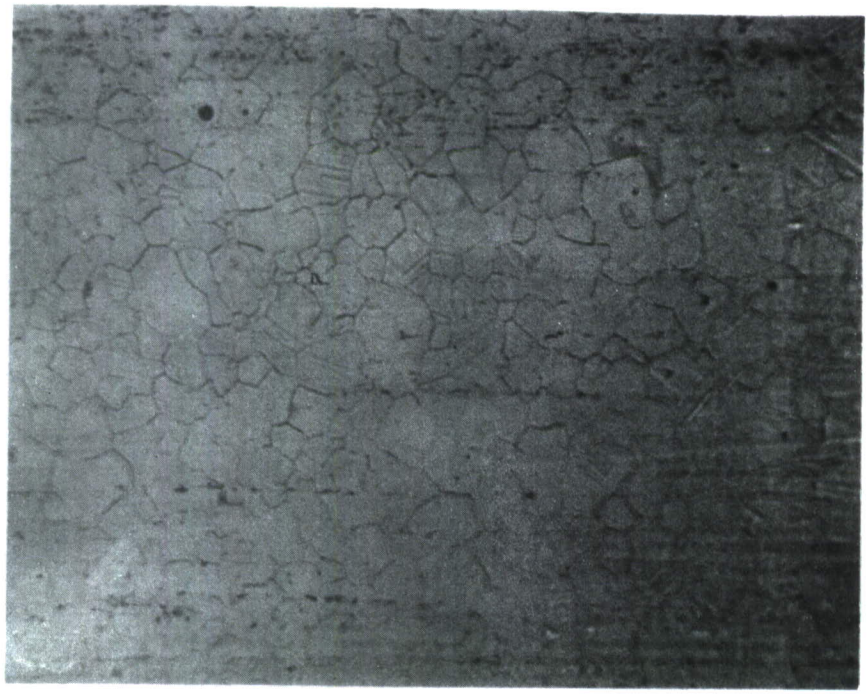

FIGURE 11. CHACE 720 FOIL AFTER A LIGHT SURFACE ETCH - THE INTERMETALLIC OR OXIDE INCLUSIONS WERE STRUNG OUT DURING ROLLING (1000X)

Of all the foils examined, the Nickel-Silver was the cleanest and possessed the minimum of microscopic flaws. All the foil and wire materials listed in Table I, however, were considered acceptable and suitable for a "first cut" fabrication into a sensor grid.

3.1.3 SENSOR FABRICATION TECHNIQUES

3.1.3.1 Acid Etch Vs the Die-Cut Method

Experience with strain gage fatigue performance as a function of fabrication techniques indicated that the strand edge condition is a most important factor for a long fatigue life. The uncontrolled notching of a gage strand edge characteristic of the acid etching process, while satisfactory for gages used in static measurements, is not conducive to a long gage life in a fatigue environment. Metallurgical examinations of fatigue failure of annealed Constantan foils (Ref. 1) confirmed that the notching and undercutting of the foil in the annealed condition is even more severe than when in the "as-rolled" or "heat-treat" condition.

The selected sensor fabrication subcontractor, Dentronics Inc., has demonstrated the capability of precision die-cutting of almost any material which can be rolled into a foil. The die-cutting state of the art has been extended to the use of carbide hardened dies for fabricating such difficult materials as stainless steel, monel, and columbium. A vernier adjustment is included in the dies for resistance correction as a result of variations in foil thickness. Although the etching and neutralizing processes for conventional strain gage foils such as Karma and Constantan have been satisfactorily developed, sensor fabrication from new resistive materials would require the concurrent development of new chemical treatments. The introduction of different chemicals for different materials with their required variations in acid concentrations, time in baths, post etching, etc., all constituted potential problem areas which would be eliminated by the dry fabrication technique. Acid etching is a random process and every grid of the same type gage will be different even though on a microscopic scale. This is not to say that the die-cut gage will not have imperfections but, simply, that each grid cut by the same die will have the same imperfections. Consequently there is not only less scatter in fatigue life, but also fewer variations in sensor output.

Although the Lockheed Microcircuit Laboratory has considerable experience and success with etching microminiature printed circuits, it was elected to by-pass the customary technique of acid etching grid configurations. It was felt that die-cutting, laser cutting, or vapor deposition offered the most expeditious method for fabricating sensor grids from all of the various metals to be evaluated.

The first attempt at fabricating a sensor was accomplished by the precision die-cutting technique. A minimum of 10 sensors were fabricated by Dentronics Inc., from each of the candidate foil materials, i.e., Monel 400, Inconel 600, Nickel-Silver, Chace 720, Molybdenum Permalloy, pure molybdenum and columbium. The sensor grids were die-cut to 1/4 inch grid length using either a 120 ohm or 350 ohm standard strain gage die, depending upon the volumetric resistivity of the material. This resulted in sensor resistances ranging from 60 to 260 ohms; however, this presented no problem since the parameter to be measured was ohms/ohm resistance change. Sensor fabrication was completed using conventional backings, adhesives, curing procedures, and solder dots. No difficulties were encountered in this phase of the program.

The fatigue sensors that were die-cut from the rolled and annealed foil materials were microscopically examined prior to testing. Typical sensors are shown in Figures 12 through 17. The nickel-silver foil was definitely the cleanest of all foils received from the foil supplier. Figure 8 shows a representative surface condition of the nickel-silver foil at a magnification of 1000X prior to etching. A surface etch of the foil is shown in Figure 9 and the material was judged to be annealed as evidenced by the equiaxed grains. The end loop sections shown are only a small portion of the photos made; however, they represent typical sensor sections. The Kapton encapsulating film is very transparent, as compared with the conventional cellulose filled epoxy encapsulation so it was not necessary to remove the Kapton to view the foil surface. Generally speaking, deformation of even the most difficult foils as a result of die-cutting a grid is limited to a slight burring at the end loop to no burring of the strand edge. No twinning was produced in any of the alloys. A large number of photomicrographs of die-cut sensors were studied to analyze and improve fabrication techniques. The end loop section of the more difficult foils like columbium and pure molybdenum (Figures 12 and 15) indicated some irregularities. A variety of radius dies were tried with these materials, resulting in very little improvement from the sharp cornered variety to the rounded ones. Prior to sensor installation all sensors were microscopically examined and none was rejected on the basis of microscopic flaws. Subsequent fatigue testing of the die-cut sensors produced no fatigue failures, consequently no additional microscopic examinations were conducted.

When it was desired to surface etch the foil strands, the Kapton encapsulation had to be removed. The most convenient method of removing the Kapton from the foil appeared to be a warm caustic solution (less than 180°F). This is the technique recommended by the Kapton manufacturer (DuPont Company) although a hydrazine treatment can also be used with some risk to the foil.

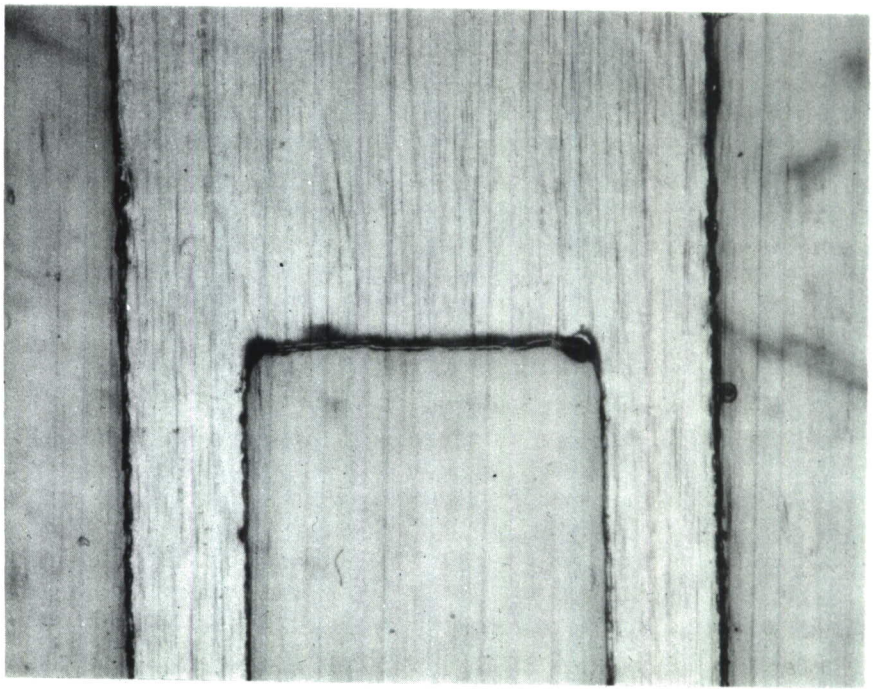

FIGURE 12. END LOOP SECTION OF PURE MOLYBDENUM SENSOR (200X)

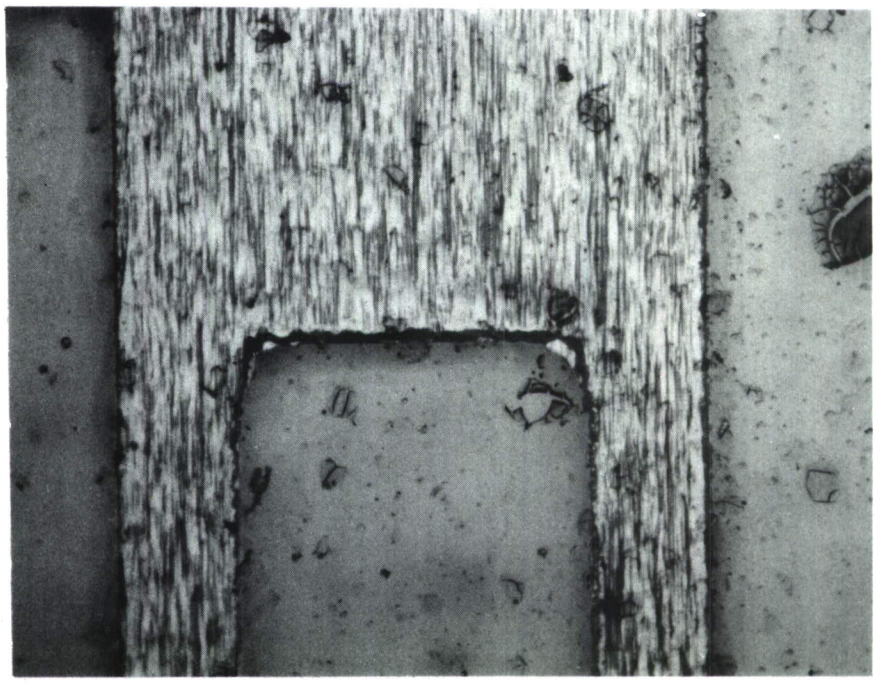

FIGURE 13. END LOOP SECTION OF MONEL SENSOR (200X)
(PHOTO TAKEN THROUGH THE KAPTON ENCAPSULATION)

FIGURE 14. END LOOP SECTION OF INCONEL 600 SENSOR (200X)
(MOST OF THE ENCAPSULATION HAS BEEN REMOVED.)

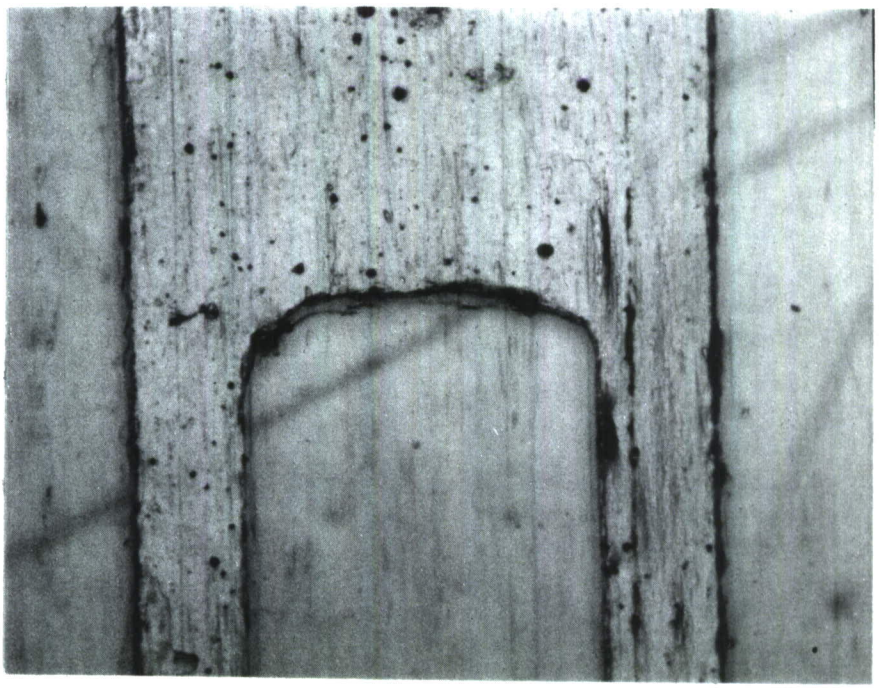

FIGURE 15. END LOOP SECTION OF COLUMBIUM SENSOR (200X)

FIGURE 16. END LOOP SECTION OF A MOLYBDENUM PERMALLOY SENSOR (200X) (FOREIGN OBJECT IS LINT TRAPPED INSIDE THE KAPTON ENCAPSULATION.)

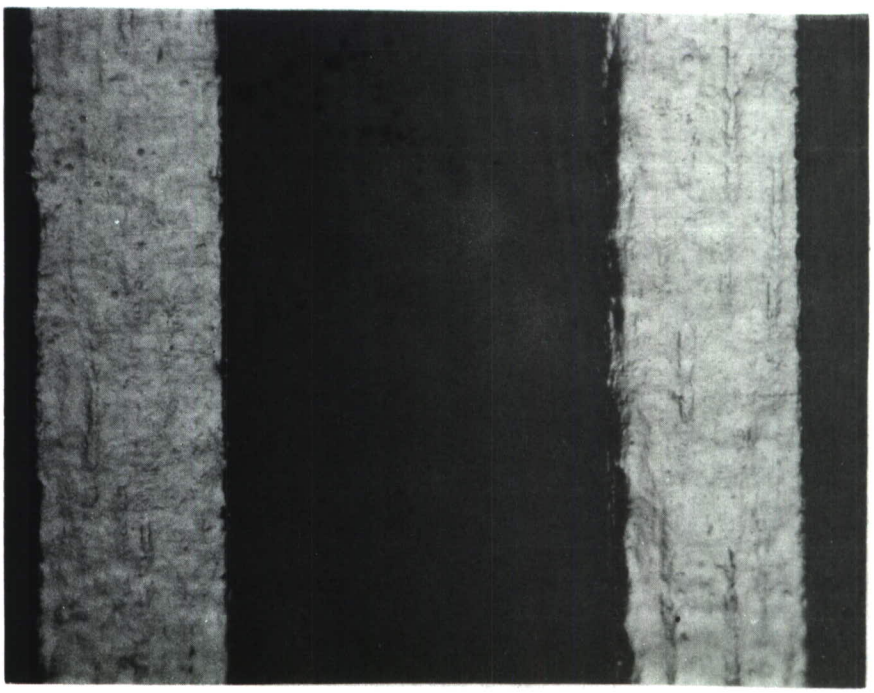

FIGURE 17. CENTER SECTION OF MOLYBDENUM PERMALLOY STRAND (FOIL SURFACE ROUGHNESS IS EVIDENT AT A MAGNIFICATION OF 200X.)

3.1.3.2 Laser Cutting Evaluation

The manufacturing specifications regarding commercial laser metal cutting equipment indicated the potential for cutting thin metal foils into a sensor grid. Manufacturer performance claims of a CO_2 laser beam diameter of 5 microns with an edge definition of one micron and a work rate of 5 inches per second were particularly attractive for the envisioned application. Therefore a CO_2 continuous beam laser was selected as the most feasible for cutting the 0.2 mil foils into the desired configuration.

Constantan and Karma foils were immediately available so these were selected for the "pioneer" effort. These foils were backed up by a ceramic substrate and the composite was then placed upon an X-Y table. The machining operation consisted of drilling holes and cutting slots in the foil. A typical hole produced by the laser beam is shown in Figures 18 and 19, at a magnification of 500X. A microscopic examination of a cross section of the hole indicated a wedge shaped cut with oxidation at the hole edge. The black rings shown in Figures 18 and 19 are due to carbonizing of the residual oil remaining on the foil as a result of manufacturer rolling techniques. Although it might have been possible to remove the rings by cleaning, it was not considered economically feasible at this stage of evaluation. An inert gas blanket during the cutting operation may have prevented oxidation; however this also represented an additional effort not warranted by the results. It was noted that considerable edge puddling occurred while cutting the Karma foil, leading to the conclusion that similar results could be expected with Monel 400, Inconel 600, and also Molybdenum Permalloy. It was felt that the correction of these difficulties would constitute a complexity that would prolong fabrication; consequently a complete grid was never constructed. When all the problems of laser cutting were objectively reviewed it was deemed advisable to abandon this technique in favor of the more familiar and proven methods of grid fabrication. If significant improvements in laser equipment capabilities and machining techniques ever became an accomplished fact, it should then be reconsidered as a possible method for fabricating a grid.

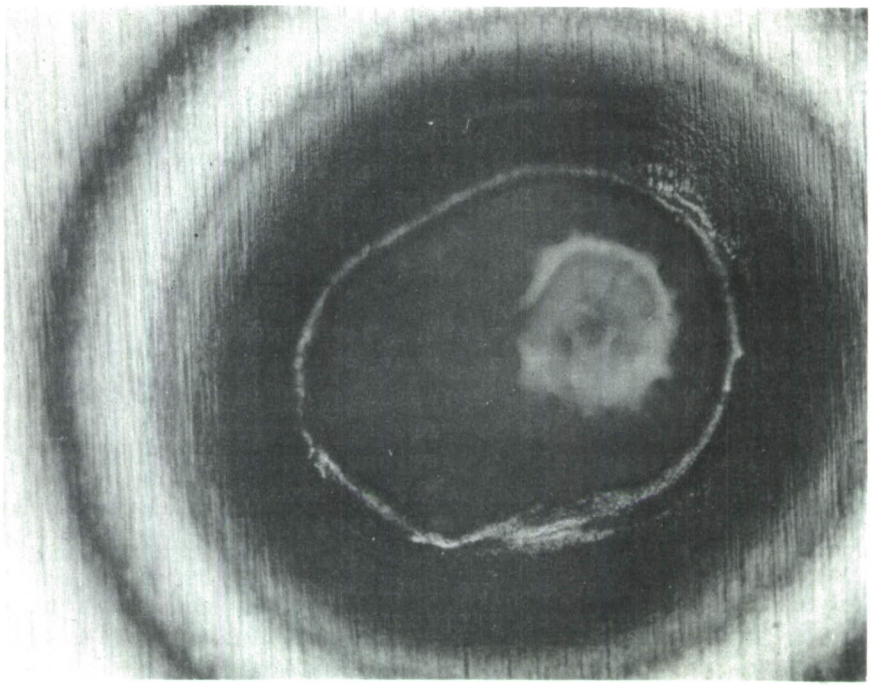

FIGURE 18. MICROPHOTOGRAPH OF LASER BEAM PENETRATION OF 0.00018" THICK CONSTANTAN FOIL (BLACK RINGS ARE CARBONIZED OIL) (500X)

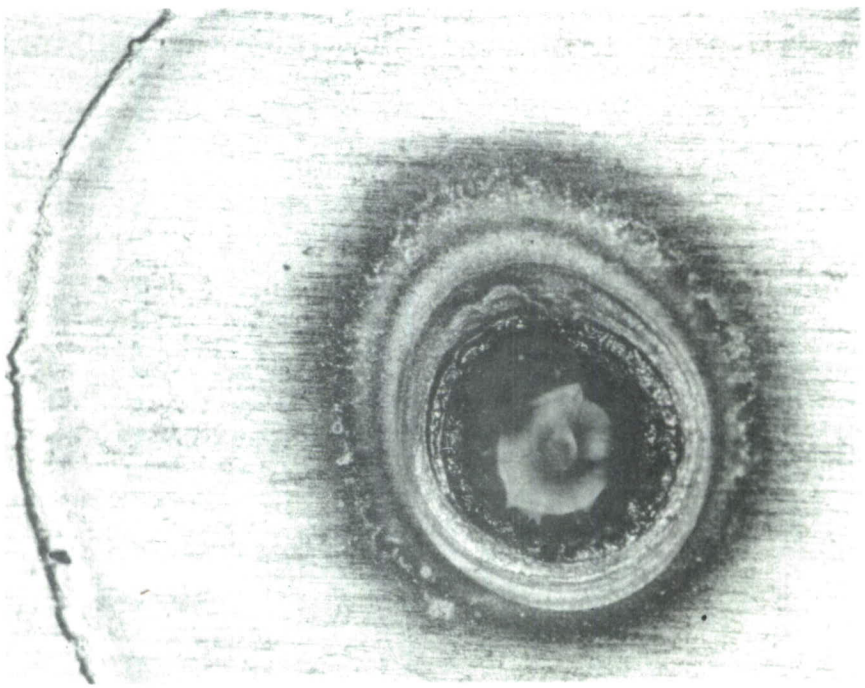

FIGURE 19. LASER BEAM PENETRATION OF KARMA FOIL 0.000185" THICK (500X)

3.1.4 TEST PROCEDURES AND EQUIPMENT

3.1.4.1 Screening Tests

The purpose of the screening tests was to collect data necessary to define the following:

- o Threshold sensitivity
- o Repeatability
- o Total resistance change within the approximate lifeline defined in Figure 20.
- o Sensor fatigue life with respect to the approximate lifeline defined in Figure 20.

These data were used to guide development with respect to optimizing sensor configuration and installation techniques, and most important to isolate sensors which met a predetermined or targeted set of performance criteria, and thus qualify for further refinement and more extensive fatigue evaluations.

3.1.4.2 Test Specimens

Since data from the screening tests were to be used for decisions relative to sensor selection and development, the associated test methods were designed to be simple and rapid, yet accurate and repeatable. The method used employed a constant stress cantilever beam loaded in completely reversed bending. This method not only meets the above requirements but is also consistent with methods used on previous fatigue sensor evaluations as reported in References 1 and 2. The data obtained on the current program could thus be linked directly to those obtained on previous programs.

Once installation techniques had been established, sensors representing each unique group were applied to constant stress type cantilever beam fatigue specimens machined from bare 7075-T6 aluminum alloy sheet. A typical installation is shown in Figure 23. Beams of two different lengths were employed as illustrated in Figure 21. The long beam was used for evaluations involving peak-to-peak strains up to approximately 6000 microstrain and from 6000 microstrain to 10,000 microstrain the shorter specimen was used. It would have been desirable to use the longer beam in all cases since the larger surface area would allow more sensors to be installed and evaluated on the same beam at the same time. The wide strain range to be investigated combined with load and deflection limits of the test equipment, however, required the two different beams.

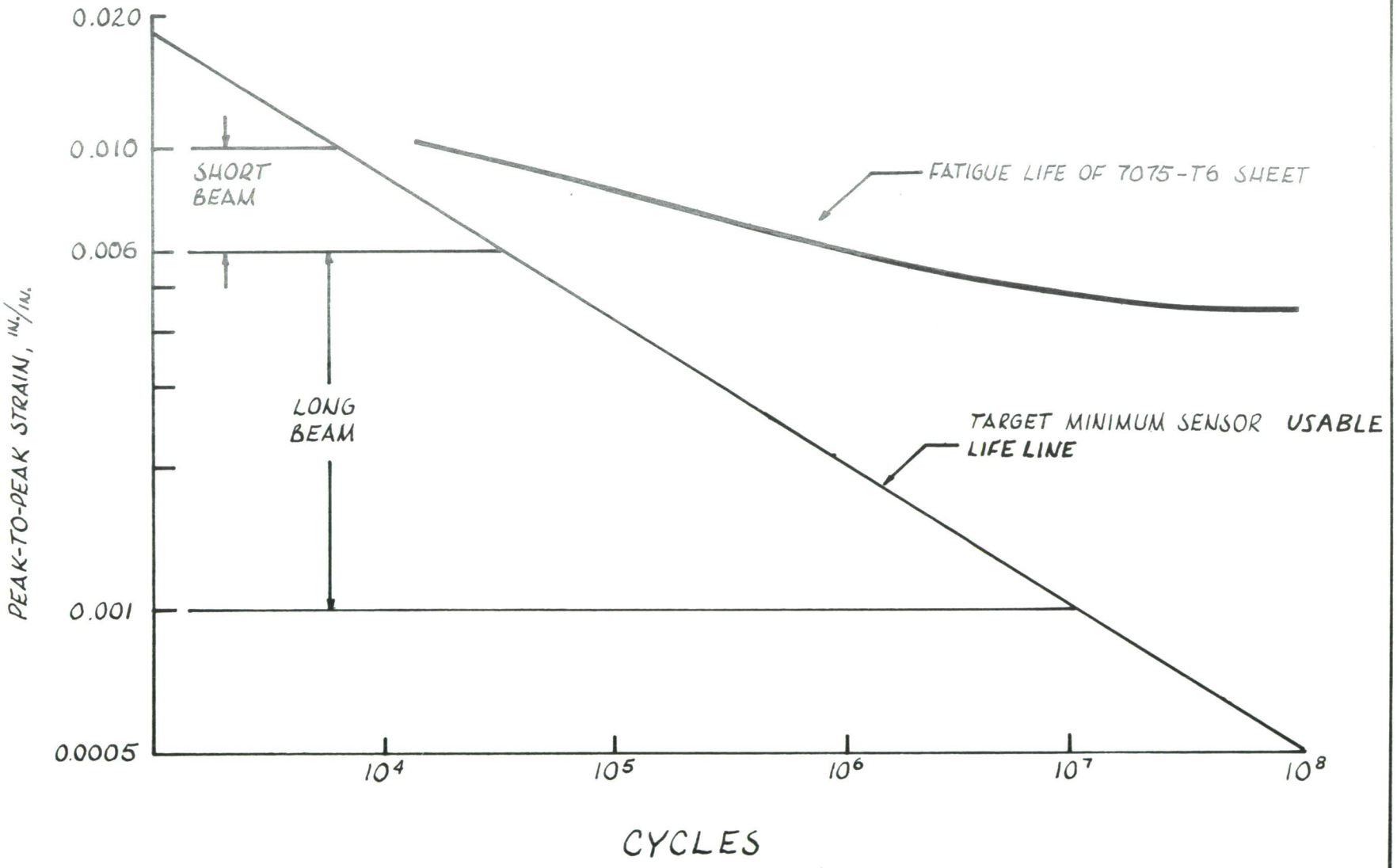

FIGURE 20. TARGET PERFORMANCE AND TEST RANGE FOR SCREENING TESTS

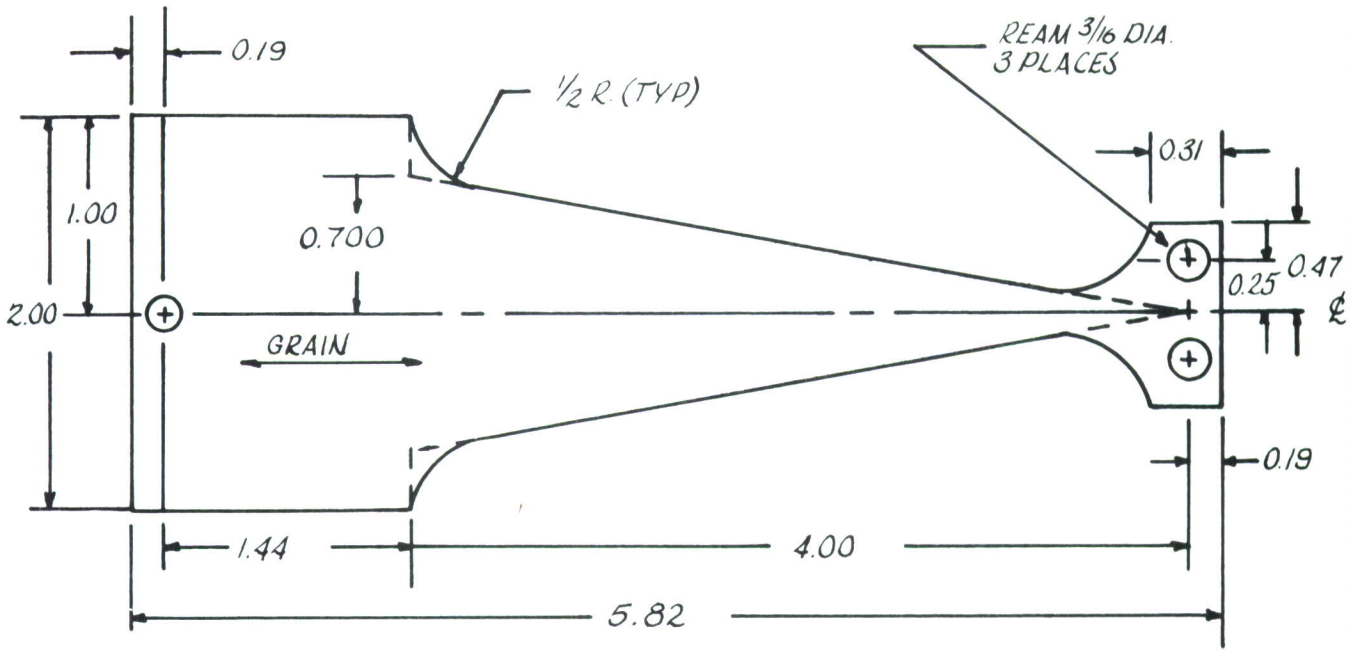

LONG BEAM

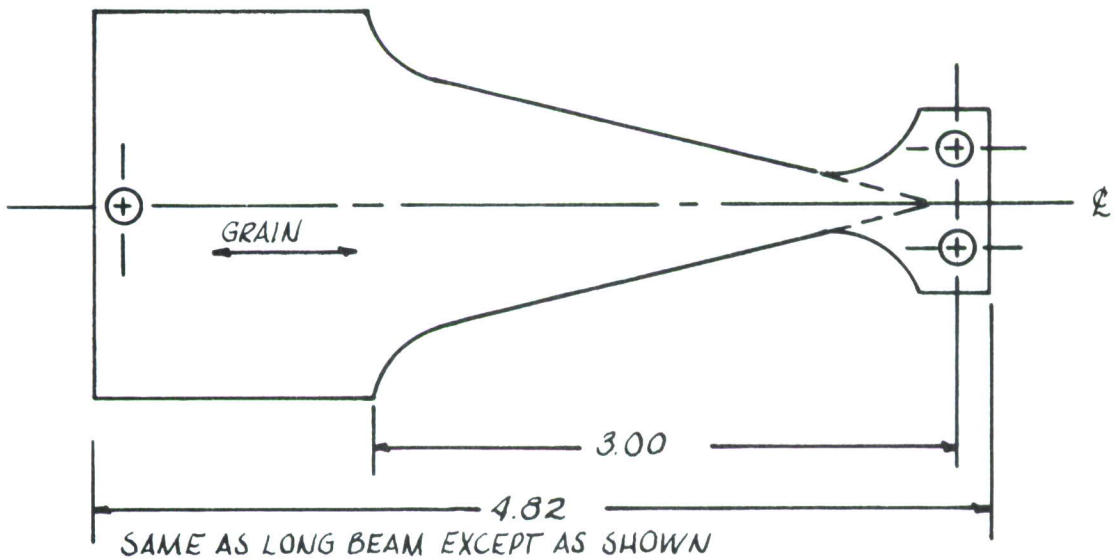

SAME AS LONG BEAM EXCEPT AS SHOWN

SHORT BEAM (DIMENSIONS IN INCHES)

FIGURE 21. CONSTANT STRAIN CANTILEVER BEAMS FOR SCREENING TESTS— 0.100 INCH THICK 7075—T6 ALUMINUM ALLOY SHEET

3.1.4.3 Test Equipment

Reversed bending fatigue tests were performed in Sonntag flexural fatigue machines having full-scale load capacities of ± 25 pounds and ± 50 pounds. These machines, shown in Figure 22, apply constant amplitude loads infinitely variable up to maximum capacity. The applied load is varied by a calibrated screw which changes eccentricity of a mass up to a maximum beam deflection of ± 0.50 inch. Load form is sinusoidal and is applied at a uniform rate of 30 cycles per second.

In initiating a particular test, the load required to produce a given strain on the beam surface was analytically determined using standard beam equations and dimensions of the particular beam. The eccentric mass was then adjusted to produce the desired load. Prior to initiating the screening tests, however, a cross-check on eccentric position versus beam strain was made to insure that correlation was achieved to at least ± 1%. This was performed using strain gaged beams exposed to dynamic loads. Signals from the strain gages were measured with a strain indicator, and an oscilloscope was used as a null indicator. Calibration of the instrumentation was performed in accordance with MIL-C-45662A (Ref. 10).

During screening the maximum strain was 5000 microstrain or 10,000 microstrain peak-to-peak. A greater strain would be significantly above the proportional limit of the beam and could influence the results. At the lower end, testing was performed at a peak-to-peak strain of 1000 microstrain. These boundaries are defined in Figure 20 along with the strain ranges for the two different beams. Also shown in Figure 20 are fatigue data from Reference 11 for the 7075-T6 sheet. These points fall sufficiently outside the envelope of interest to indicate that beam failure would not occur until the desired sensor information has been collected.

Measurements of sensor permanent resistance change was periodically made during the fatigue tests. A standard SR-4 type strain indicator or a conventional wheatstone bridge (as shown in Figure 22) was used to make these measurements, and in the case of the strain indicator the standard gage factor definition was used to convert microstrain to ohms. When available the same type sensor mounted on another test specimen was used as the "dummy" or bridge completion resistor. After serving the bridge completion function it was then evaluated. In the absence of a like sensor, a precision resistor of appropriate value was used.

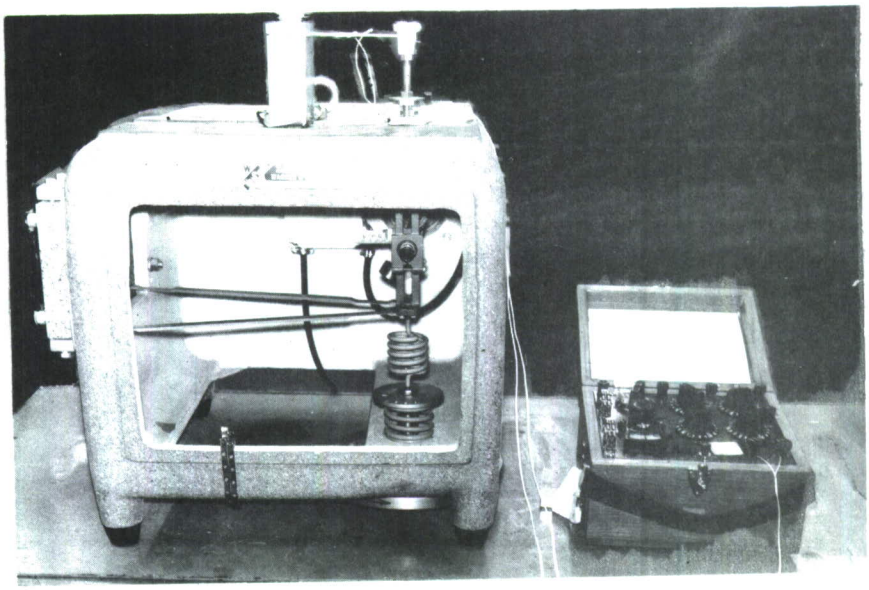

FIGURE 22. FATIGUE TEST MACHINE USED IN SCREENING TESTS

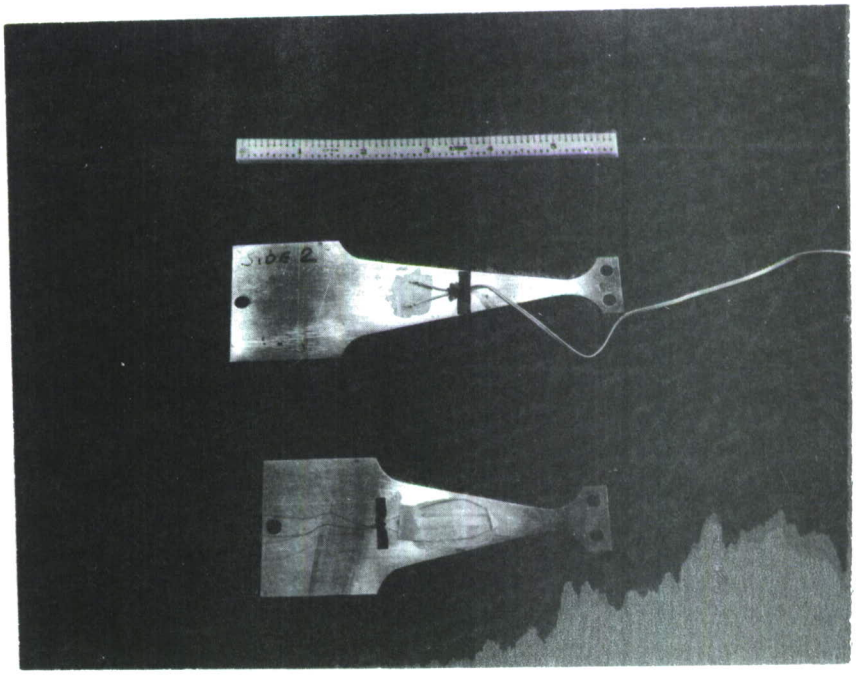

FIGURE 23. CONSTANT STRAIN BENDING BEAMS USED FOR SCREENING TESTS

3.1.5 TEST RESULTS

3.1.5.1 Die-Cut Sensors

Table I shows that the volumetric resistivity of each of the selected resistive materials was somewhat different. To expedite and simplify the preliminary evaluations, the sub-contractor used conventional strain gage dies to produce a grid configuration. Therefore, a standard 120 ohm strain gage die would produce a grid resistance either more or less than that of Constantan, depending upon the selected material's ratio of volumetric resistivity to that of Constantan. Scatter in initial sensor resistance did not present a problem since the data readout equipment was basically responsive to resistance (ohms/ohm) change.

The die-cut sensors were bonded in back-to-back installations on the constant strain bending beams only. All sensors were bonded with the heat cured epoxy adhesive, and all indicated an electrical resistance to ground of 10 K megohms or greater. Each type of sensor was tested to determine compliance with an established order of priority (Section 3.1.1) i.e., to first determine its threshold sensitivity. Initially, sensors of each type were first cycled at a strain level of $\pm$ 500 $\mu\epsilon$ for 50,000 cycles and the resistance change measured. If the required 0.05% resistance change was not obtained, the cyclic strain level was increased until the material threshold sensitivity level could be established. The data (Figures 24 through 27) are graphically presented as a curve showing sensor percent resistance change versus number of strain cycles. Several runs on each sensor type were made to verify its threshold sensitivity, and to evaluate the possibility of refinements to further improve sensitivity. A consolidation of the sensitivities established for the various materials is shown in Table I. The response characteristics of the more suitable materials (Monel 400 and Molybdenum Permalloy) are shown in Figures 24, 25, and 26. Although these materials are an improvement over Constantan, they still did not meet the target requirements. The die-cut sensors were also checked at a constant amplitude strain level of $\pm$ 2000 $\mu\epsilon$. A summary of the behavior characteristics of the various materials as shown in Figure 28 can be compared with that of Constantan as well as each other. The data for constructing the Constantan curve was taken from Reference 2.

The response curves of Inconel 600 and Chace 720 materials were very similar to each other in regard to threshold sensitivity, shape of output curve, and fatigue life. Since these materials did not meet the first priority of sensitivity, statistical averages for all the other customary behavior characteristics were not established. The response curve for Inconel 600 at a strain level of $\pm$ 1000 $\mu\epsilon$ is shown in Figure 27. The response curve for the Chace 720 material at the $\pm$ 1000 $\mu\epsilon$ level is not shown since it was essentially a duplicate of Inconel 600. The resistance change of the Inconel 600, Chace 720, and pure molybdenum was so low at the $\pm$ 1000 $\mu\epsilon$ level that variations in temperature and zero load obscured the resistance change

produced by work hardening. The change in resistance of these foils at the higher strain level ($\pm$ 2000 $\mu\epsilon$) was more precisely defined, therefore they are more realistically displayed in the curve summary shown in Figure 28. It is assumed that the ratio of resistance change of one metal to another would be similarly related at the lower strain levels.

The ease of installation, the bonding, and general mechanical adaptability of each sensor were also evaluated during the test phase. Since all the die-cut material utilized a treated Kapton backing all were equally easy to bond and no bond failures were encountered. The primary difficulties were encountered in the attachment of lead wire to the pure metals.

Although the nickel-copper alloys were easy to soft solder, the columbium and molybdenum foils were particularly difficult to solder or to attach solder dots. Various compositions of indium solder and fluxes were used in an attempt to attach a tinned copper lead wire. A conductive silver filled epoxy was also evaluated. None of these methods, however, produced a suitable connection satisfactory for a fatigue environment.

3.1.5.2 Wire Sensors

Historically, wire strain gages have not displayed the same "supersensitivity" characteristic as foil gages when subjected to a long term fatigue environment. Certain materials in the wire form were more adaptable when compared to the same material in a foil form. The preliminary materials evaluation activity indicated that tungsten and Manganin should produce a reasonable resistance change as a result of changes in its metallurgical state. The temperature characteristics of Manganin differed greatly from that of tungsten, however tungsten held forth the promise of a large resistance change if its threshold of sensitivity was acceptable. To evaluate the behavior characteristics of these two selected materials, sensors were fabricated from the annealed tungsten and Manganin wires. Approximately 22 inches of the one mil diameter tungsten wire was required to produce a 60 ohm sensor of approximately one square inch area. To keep the sensor within the targeted one square inch area, the wire was formed into a two layer flat grid with a one mil Kapton separator in between. Since the one mil tungsten wire was uninsulated, special care was exercised to avoid "shorting" one loop against an adjacent one. An additional difficulty included the attachment of a lead wire to the tungsten filament which required a "swaged" mechanical connector as opposed to conventional soldering.

Two sensors were also constructed from the 10 mil diameter varnish insulated Manganin wire. The grid was of a three layer flat wound construction with 1 mil Kapton separators and epoxy adhesive for bonding. From the standpoint of sensor fabrication, the construction of the composite, and attachment of lead wires were very difficult.

The threshold sensitivity of the resulting sensor was approximately 1500 $\mu\varepsilon$ which did not comply with the target requirement.

Performance curves for the tungsten wire gages are shown in Figure 29, and since this erratic operation was also typical of Manganin wire, curves for Manganin are not shown. Although the resistance change of tungsten was relatively high after exceeding its threshold sensitivity (1100 $\mu\varepsilon$) its temperature sensitivity was also high, with the end result being unsatisfactory performance. The preliminary tests indicated the two wire materials were unsatisfactory so no further evaluations were performed.

The mechanical adaptability, sensitivity, and general overall performance of wire sensors indicated that this approach should be abandoned and an evaluation of vacuum deposited materials should be considered. Therefore, the test program regarding the investigation of sensor materials was logically separated into two phases, i.e., Phase I concerning the wire and foil sensors, and Phase II concerning the vacuum deposited sensors. Phase II activities were undertaken when it became apparent that annealed foils or wires of various alloys were not going to satisfy AFFDL requirements.

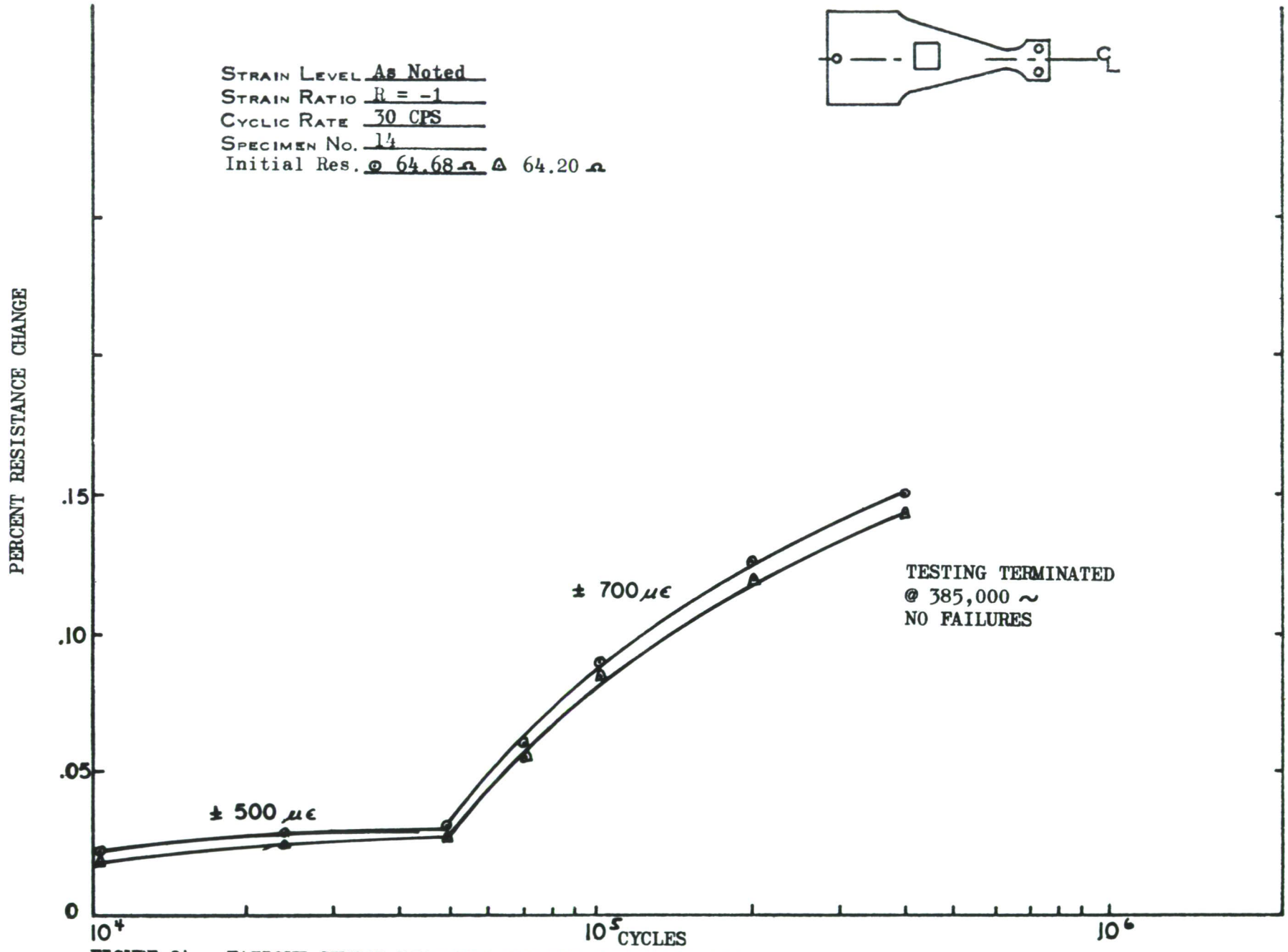

FIGURE 24. FATIGUE SENSOR RESPONSE FOR DIE-CUT MONEL 400

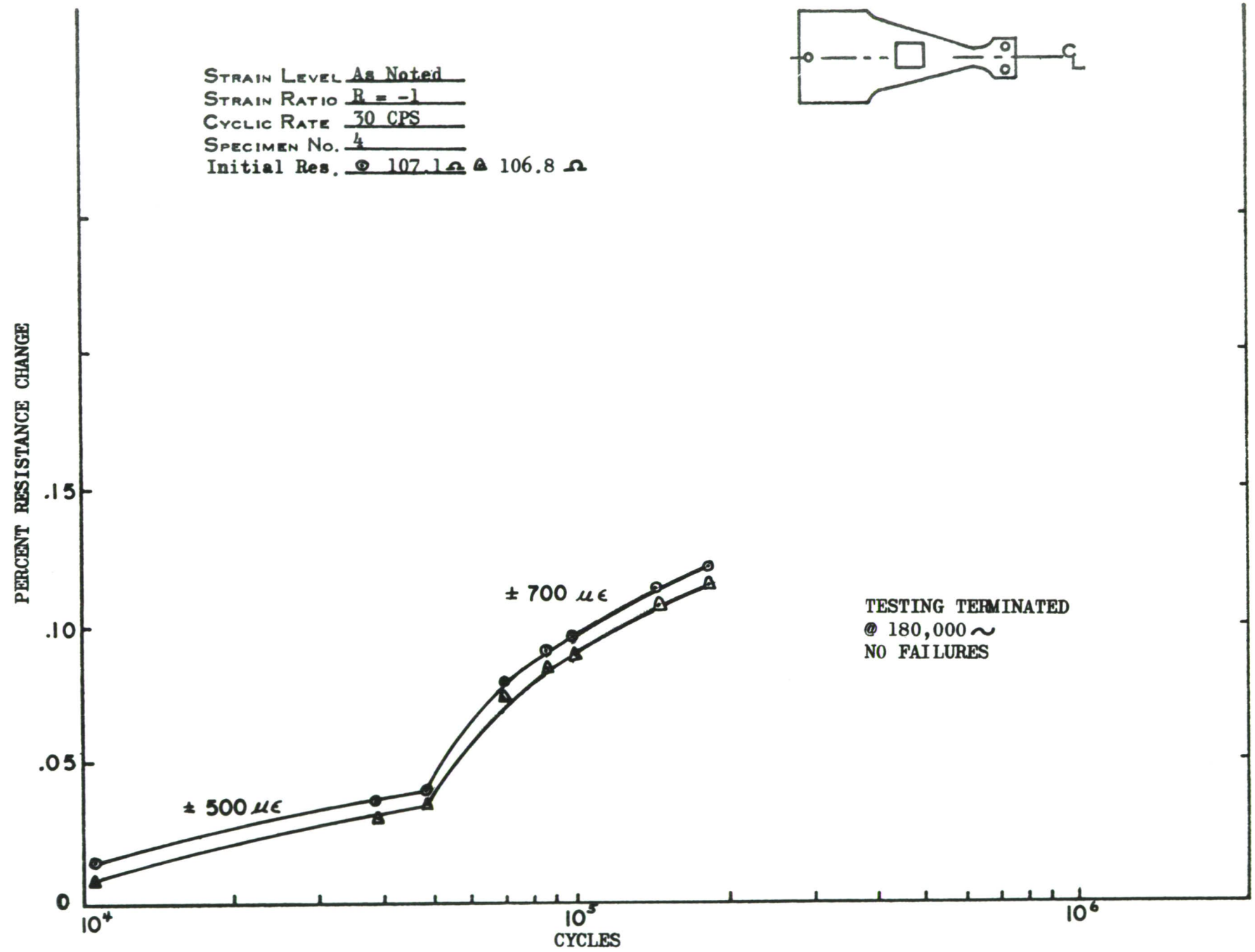

FIGURE 25. FATIGUE SENSOR RESPONSE FOR DIE-CUT MOLYBDENUM PERMALLOY

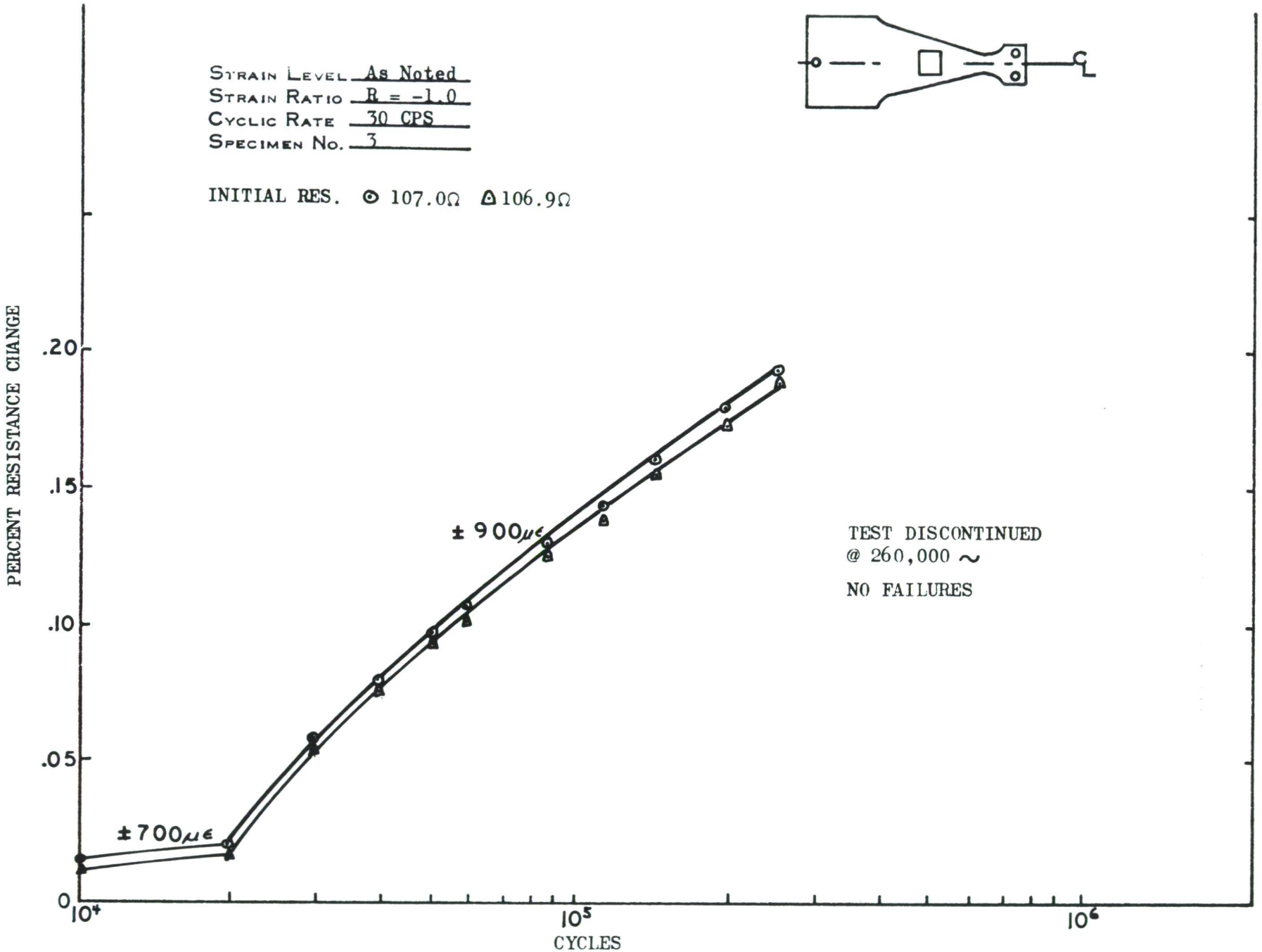

FIGURE 26. FATIGUE SENSOR RESPONSE FOR DIE-CUT MOLYBDENUM PERMALLOY

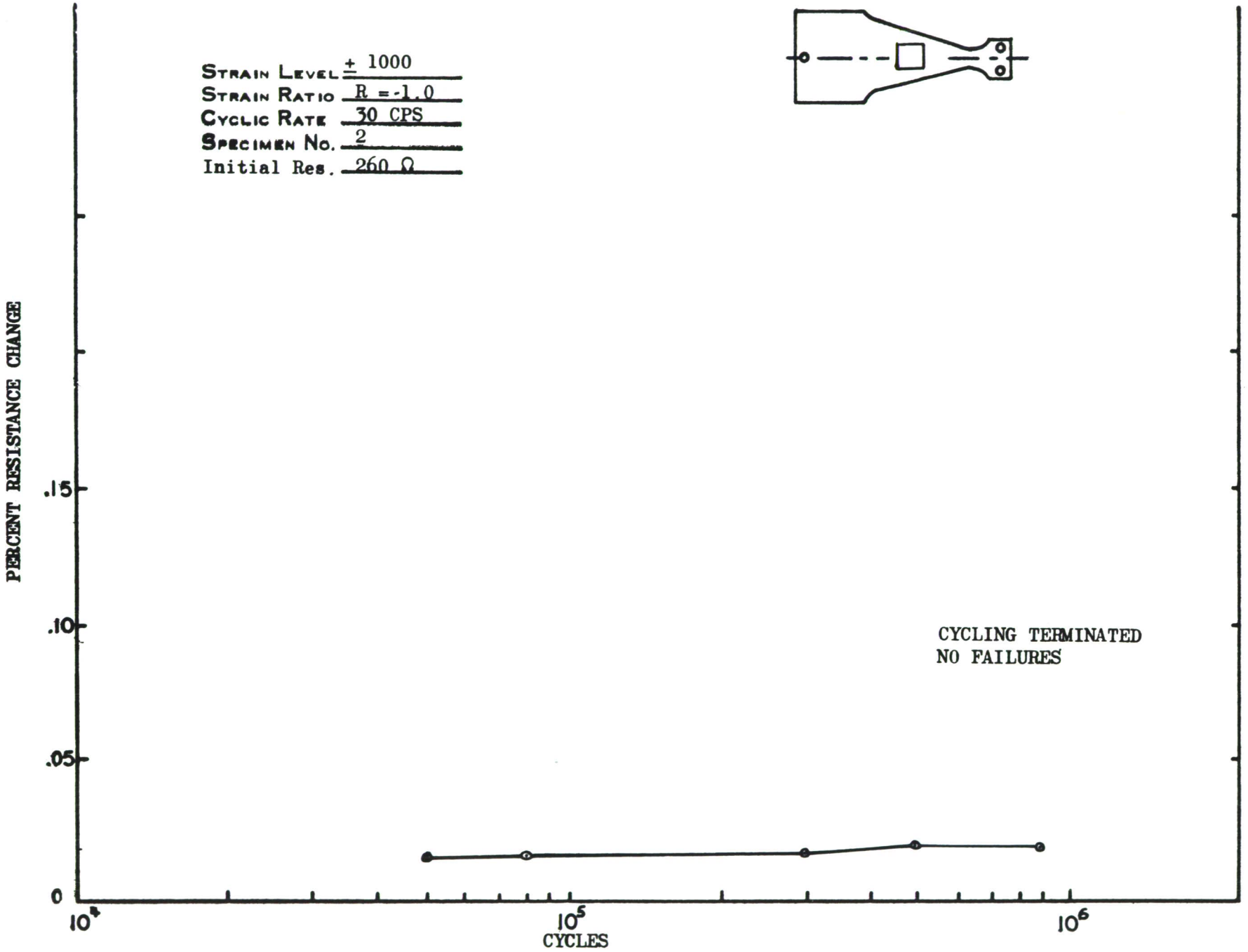

FIGURE 27. FATIGUE SENSOR RESPONSE FOR DIE-CUT INCONEL 600

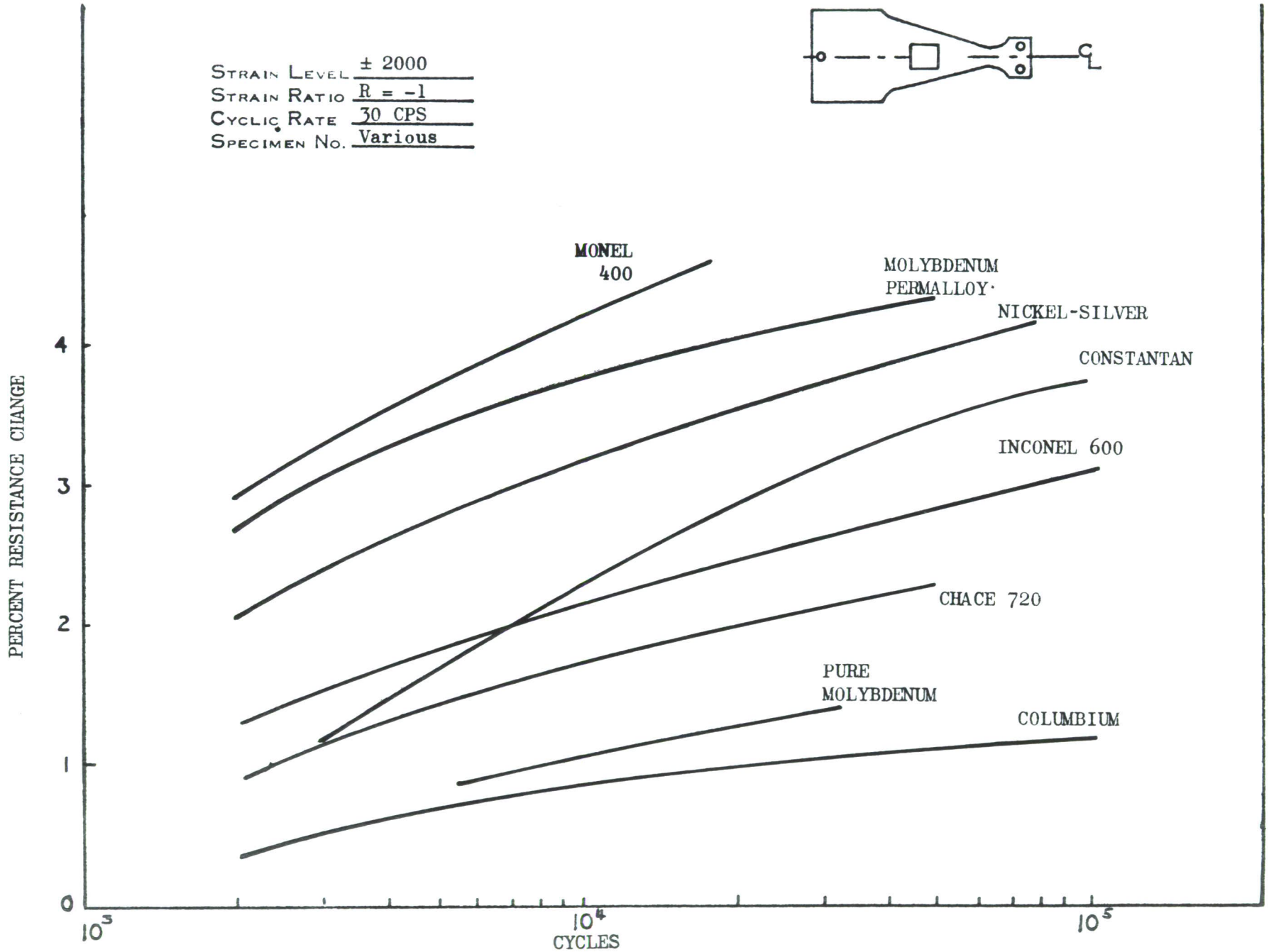

FIGURE 28 FATIGUE SENSOR RESPONSE FOR VARIOUS DIE-CUT MATERIALS

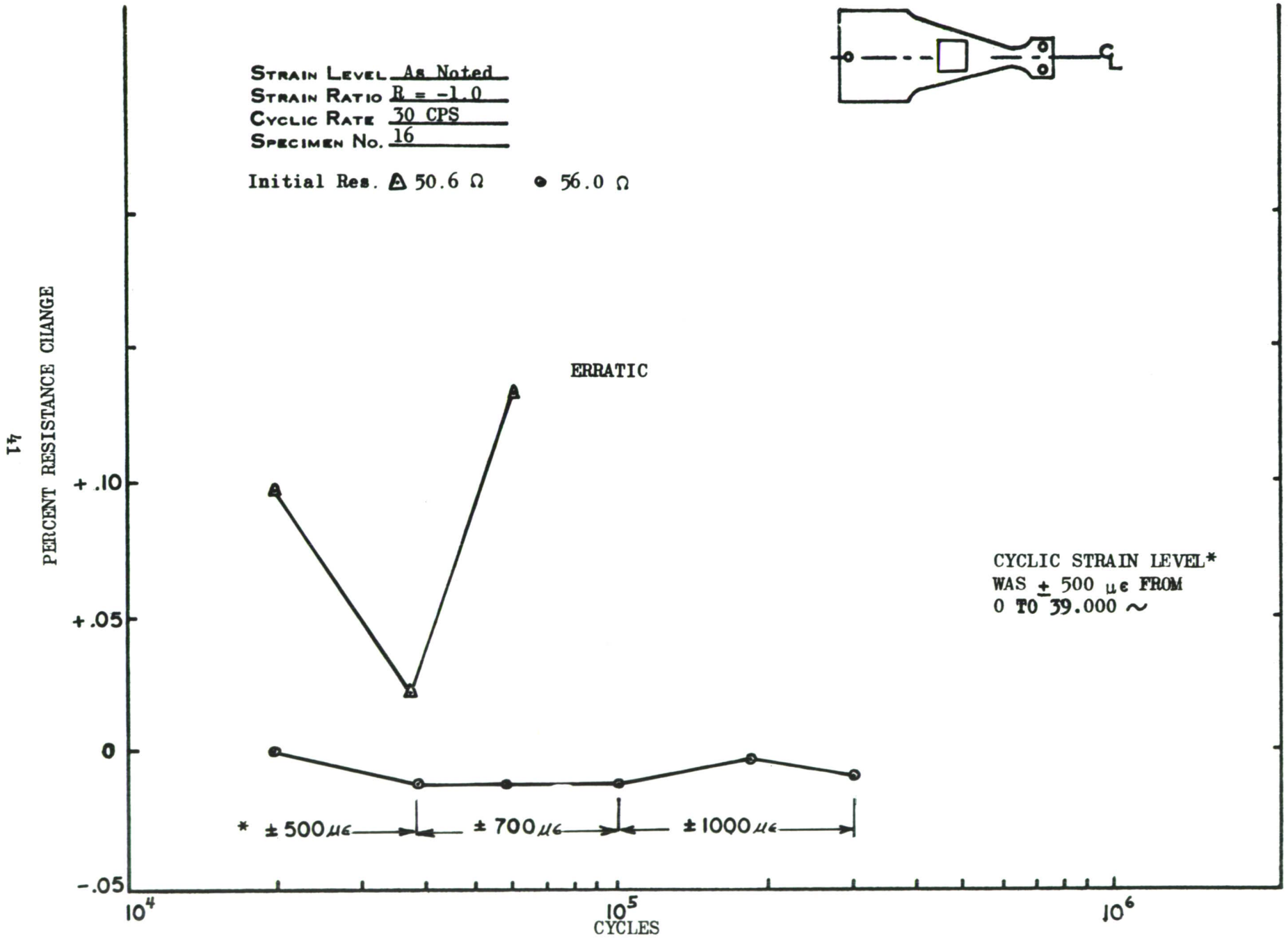

FIGURE 29. FATIGUE SENSOR RESPONSE FOR TUNGSTEN WIRE

3.2 PHASE II ACTIVITIES - VACUUM DEPOSITED SENSORS

3.2.1 BASIC APPROACH

The vacuum deposition technique and the order-disorder phenomena were programmed to be investigated only if the other approaches proved inadequate. Vacuum deposition held forth the promise of a miniature sensor with a uniform and clean film as the sensing element. The vacuum deposition technique also was suitable for producing materials with an ordered atomic structure. Atomic ordering exists in alloys where atoms of the component elements occupy special positions throughout the crystalline lattice. Particular alloys which undergo an order-disorder change can be made to transform from the ordered to varying degrees of the disordered state by cyclic deformation. This destruction of order is accompanied by resistivity changes of up to over 50% for heavy deformation. The ordering phenomenon is especially attractive since the resistivity change obtained by the disordering process is irreversible. Initially it was thought that a selection could be made from any of the limited number of alloys which could be ordered (Ag_3 Mg, Cu_3 Au, Ni_3 Mn, Cu_3 Zn); however, many do not possess the desirable and necessary physical or mechanical properties either for vapor deposition or for application as a fatigue sensor. The electrical and mechanical properties which have the greatest influence on sensor fabrication and application are (1) volumetric resistivity, (2) TCR, (3) soft soldering capability, and (4) bonding to a flexible substrate.

Broom (Ref. 4) concludes that a chemical reaction of the elements Cu-Ni-Zn causes no change in the nature of their atoms, but results merely in their rearrangement. He also states that combinations between atoms take place in the ratio of simplest numbers preferably AB, then AB_2 and so on. Ordering of the atomic structure of alloys can best be accomplished by the A_3B ratio; hence by vapor deposition of a selected Cu-Ni-Zn alloy, a deposited film of Cu_3 (Ni, Zn,) with an ordered atomic structure can be produced.

The basic properties of the individual elements pertinent to vapor deposition are shown below.

ELEMENT	AT NO	AT WT	MP (°C)	FIRST IONIZATION POTENTIAL (EV)
Nickel	28	58.7	1455	7.61
Copper	29	63.5	1083	7.68
Zinc	30	65.4	419	9.36

Although there is a considerable spread in the melting points of these elements, the specific alloy used has a melting point of 1110°C. The variation in vapor pressure of the three elements was a factor considered in the vacuum deposition techniques applied. The desired composition was obtained and fractionation was never a problem. The ordering of the deposited film was accomplished by a controlled "cool down" after condensation on the substrate.

3.2.2 ORDER - DISORDER PHENOMENA

According to the wave theory of matter, an electron has an associated wave function as it travels through a metal lattice. Thus a current of electrons acts as a group of waves traveling through the lattice. The positive metal ions arranged on the lattice sites represent a periodic potential field acting on the passing electrons. As they accelerate through the lattice under the force of an applied voltage, the electrons experience collisions with the positive ions. Theoretically, in a perfect lattice of a pure metal at 0°K, the individual waves scattered by the collisions at each lattice point reinforce one another coherently so that the electrons travel through the lattice without being deflected or disturbed in any way. Resistance in real metal crystals arises from the departure of the perfect regularity in the periodic lattice resulting in collisions which cause incoherent scattering. Such departure from the perfect lattice is created by (1) thermal vibrations of the atoms about the lattice sites, and (2) lattice imperfections such as dislocations, vacancies, interstitials or foreign atoms introduced by deformation, heat treatment, and alloying.

In solid solution alloys, an ordered alloy represents less departure from a perfect periodic lattice than does a random solid solution and, therefore, has less electrical resistance. Consider the simplest case of a solid solution of A and B atoms. If the atomic forces are such that each atom is indifferent to the type of its neighbors, the solution will be a random solid solution with A and B atoms arranged randomly on the lattice sites. If, however, the atomic forces are such that dissimilar atoms attract, i.e., AB bonds have lower energy than AA or BB bonds, then the solution can achieve its state of lowest energy when an atom moves to a lattice position such that it will have dissimilar nearest neighbors. Such rearrangement results in two or more interpenetrating lattices, termed a "superlattice" as shown in the following diagram.

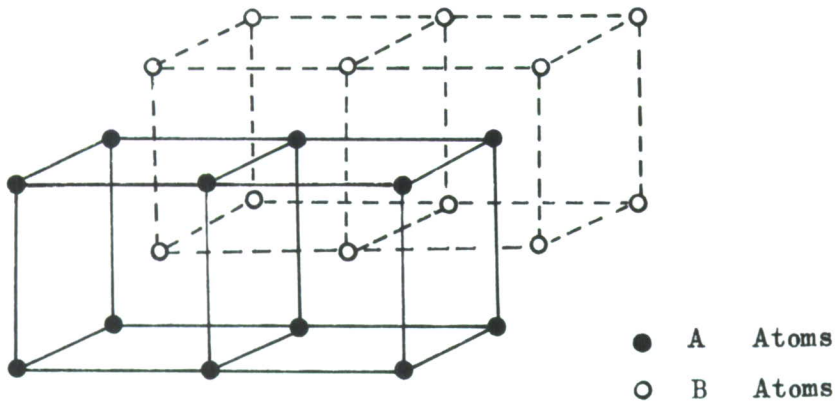

If the superlattice extends over long distances, the alloy is said to possess long range order. A perfect superlattice (or complete long range order) is possible only at critical and simple proportions of the solute and solvent atoms, such as 1:1 and 3:1. Alloy systems which exhibit perfect long range order at the critical composition ratios will exhibit partial or imperfect order at neighboring compositions. A substantial increase in resistivity is known to occur as a solution transforms from the ordered to the disordered state. This is caused by the transformation from the more perfect periodicity of the superlattice to the irregularity of the random solution resulting in increased collisions of the kind which cause incoherent scattering of electrons.

Any deformation, static or dynamic, of an ordered solution which destroys this order will give rise to an increase in resistivity as previously explained. In an unordered solution, single dislocations, known as unit dislocations, travel along through the lattice. In a perfectly ordered solution, dislocations move in pairs separated by a number of atomic distances. Such a pair of dislocations is known as a superdislocation and the passage of a superdislocation through a perfect ordered lattice does not create disorder. The first dislocation moves the atoms one atomic spacing thereby creating like bonds. Passage of the second dislocation moves the atoms one more spacing, restoring the unlike bonds so that the superlattice remains intact. In a partially ordered solution, however, both unit dislocations and superdislocations move through the lattice during plastic deformation and both create unfavorable bonds which decrease the degree of order. As the degree of order decreases, the separation of the paired dislocations in a superdislocation increases. It then becomes easier for one to become pinned while the other passes on through the lattice as a unit dislocation with concomitant increase in resistivity.

In relation to an annealed fatigue sensor, the "threshold sensitivity" is described as the strain level at which the sensor foil yields, resulting in a measurable permanent resistance change. The resistance change sensitivity of an ordered or partially ordered alloy as a function of cyclic deformation is related directly to its degree of order. The "measurable" resistance change will still occur at some specific cyclic strain level; therefore, the terminology remains valid for an atomically ordered sensor material.

3.2.3 OPERATIONAL REQUIREMENTS

The possibility of devising sensor material with an ordered atomic structure and the subsequent large resistance change upon destruction of that order was especially attractive. It was decided that the direction the vapor deposition effort should take was determined by the following requirements.

(1) The sensitive film material must be deposited on a flexible substrate. (Kapton)

(2) The deposited film must possess a high degree of atomic order.

(3) Precise material composition must be maintained for all sensors.

(4) The bond between the Kapton and the deposited film must not peel or creep with repeated strain.

(5) The sensor material must be mechanically suitable for fabricating, bonding, and soldering.

(6) The sensor material must show a uniformity of film thickness for each sensor.

3.2.4 ADHESION OF EVAPORATED FILMS TO FLEXIBLE SUBSTRATES

For the intended sensor application it was deemed necessary that a flexible substrate be used with the deposited film as opposed to the ceramic type substrate as used in some applications (Ref. 12). Although other investigators (Ref. 13) had developed a portable device for vacuum deposition directly on primary structure this procedure was considered impractical for service application.

The successful adhesion of vacuum deposited materials to a Kapton substrate remains one of the most critical steps. A uniform and tenacious bond between the film and the substrate is desired. Initial failure to obtain this was

evidenced by common "peeling." The factors which are known to influence the adhesion of Cu-Ni-Zn alloy to the Kapton are noted as follows:

1. Contamination of the substrate surface is recognized as the major cause of peeling. The presence of foreign materials, or any irregular surface can contribute to poor adhesion. Foreign materials include water, organics, fingerprints, dust or even a residue left on the surface from the cleaning process. Also, materials absorbed below the substrate surface may be expelled during the deposition phase.

2. Residual stress sometimes occurs when a metal underlay or overlay is deposited on the basic film. A silver overlay on the strand ends has produced curling and subsequent peeling. An external force such as flexing or straightening the "curl" is usually required to peel the film. This residual stress may also influence electrical properties as well as the mechanical properties of the composite. The stress-induced peeling is probably insignificant for films less than 500 Å thick but becomes more pronounced for films 1000 Å or more. A mismatch in the coefficient of expansion was considered pertinent. Both a pure copper overlay and underlay have been evaluated. The copper underlay has proven the most peel resistant and generally the more feasible. The copper underlay on the strand end is necessary to provide an adequate heat sink during soldering of the lead attachments.

3. Finish lines or other irregularities in the Kapton substrate, even on a microscopic scale, may contribute to peeling. Microscopic examinations (Figure 32) have indicated that the deposited film follows the impressions on the Kapton producing minor irregularities in the finished film.

Despite precautionary measures occasional peeling did occur on the initial material specimens. As more experience was gained this problem was eliminated. The bond offers many advantages over the conventional chemical bond utilized in strain gage fabrication, e.g., there is "no cure" required with the deposited film. Therefore, one should not experience the creep or dimensional instability that is sometimes present between a foil grid and backing in customary strain gages. Figures 30 and 31 show the basic work area where the vacuum deposition of the Cu-Ni-Zn alloy occurred. The electrical feed-through connectors in the base of the chamber supports the dual filaments and carries the current necessary to heat the filaments.

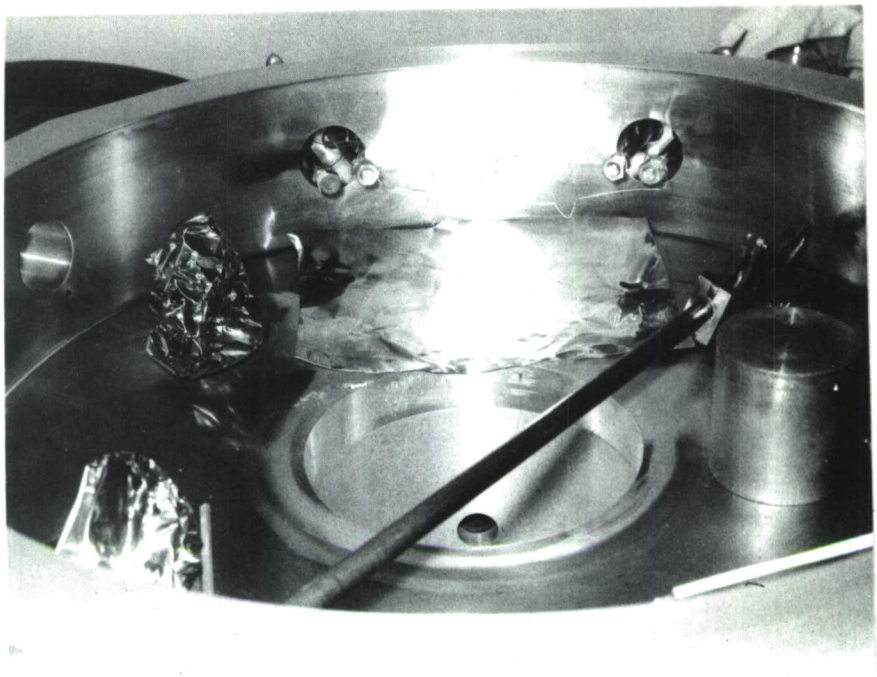

FIGURE 30. SETUP FOR VACUUM DEPOSITION OF NICKEL-SILVER, SHOWING FILAMENTS, MECHANICAL FINGERS, AND BASE OF VACUUM CHAMBER

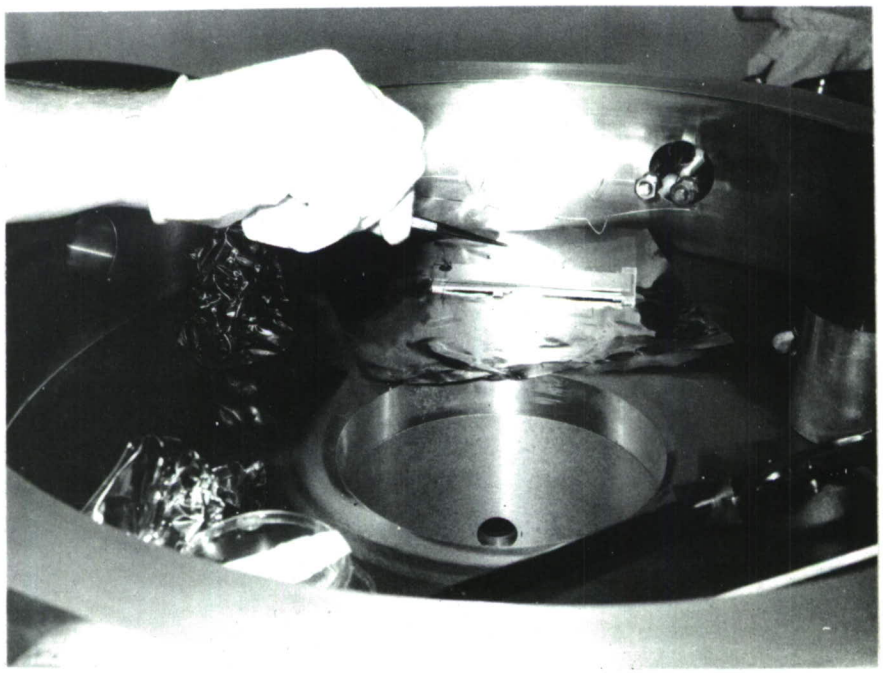

FIGURE 31. FILM AFTER DEPOSITION ON KAPTON SUBSTRATE (ALUMINUM CARRIER BENEATH FILM USED FOR HANDLING)

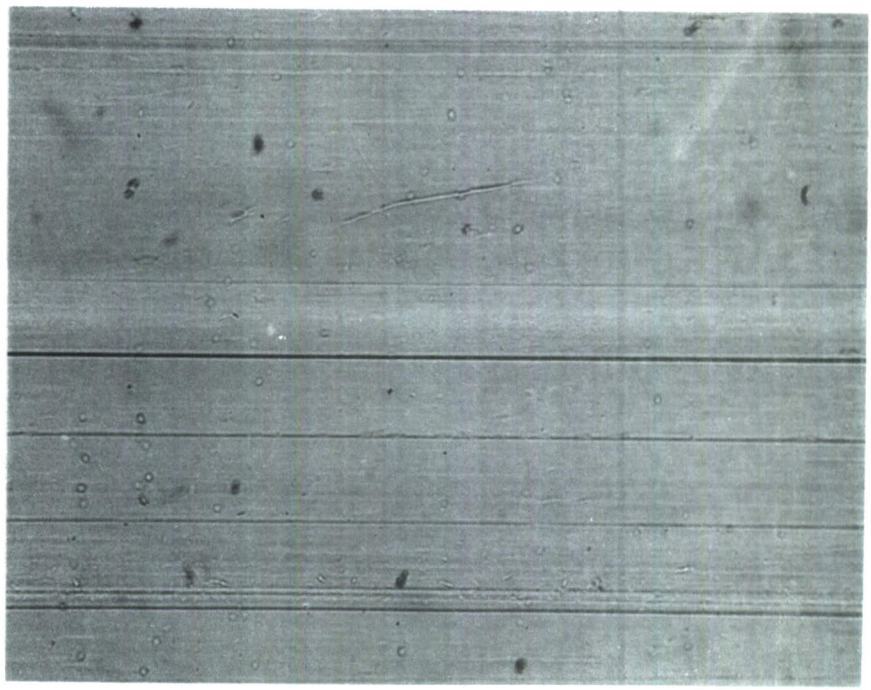

FIGURE 32. NICKEL-SILVER DEPOSITED ON KAPTON SUBTRATE: BACK LIGHTED (NOTE FILM FOLLOWS FINISH LINES AND OTHER IMPERFECTIONS OF THE KAPTON.) (500X)

FIGURE 33. PHOTO SHOWING UNUSUAL SURFACE DIRT WHICH CAN BE REMOVED BY CLEANING (ILLUMINATED BY REFLECTED LIGHT) (500X)

3.2.5 QUALITY ANALYSIS

The quality control of the vacuum deposited film in regard to composition and atomic order was considered to be important if performance repeatability was to be obtained. Some problems were encountered in obtaining a precise analysis of the film, however, because of the physical dimensions. The deposited film was in the range of 4 to 12 microinches thick and a 1/2 inch diameter chemical analysis sample weighed only 0.08 to 0.25 milligrams. The following techniques were used in analyzing the thin films; (1) x-ray fluorescence, (2) atomic absorption, and (3) electron diffraction. The equipment and techniques employed are described in more detail in Appendix I of this document.

A precise quantitative chemical analysis was obtained by atomic absorption techniques. A sample for analysis was deposited on a 1/2 inch diameter coverglass at the same time the sensor material was deposited. The glass was weighed with a Cahn microbalance before and after coating to determine the quantity of film per unit area which was deposited. The film was removed from the glass by dissolving in acid and the resulting solution was analyzed for copper and nickel. Zinc was determined by difference. The results of chemical analysis by atomic absorption techniques on eight different samples are presented below.

CHEMICAL COMPOSITION BY ATOMIC ABSORPTION

Sample Number	Sample Weight (milligrams/in.^{2})	Chemical Composition % Cu	% Ni	% Zn
1	0.50	53	17	30
2	0.50	57	15	28
3	0.65	57	21	22
4	1.00	53	18	29
5	1.05	55	15	30
6	0.85	54	16	30
7	0.50	60	20	20
8	0.35	62	15	23

A total of 26 batches of the deposited films were prepared and samples of each were quantitatively analyzed for composition. Of the samples shown, number seven was more ideal since it produced a composition of 60% Cu, 20% Ni, 20% Zn which is more in line with the desired A_3B ratio previously discussed in Section 3.2.1. Preliminary experiments indicated some copper was being "lost" in the deposition process; therefore, an alloy with excess copper seemed appropriate. The scatter in chemical composition shown here for the initial samples was considered excessive and as the deposition techniques improved with experience, less scatter was noted. A foil alloy of 65% Cu, 18% Ni, 17% Zn was the final alloy selected to produce the desired deposited composition.

A microscopic examination of the Kapton substrate revealed finish lines and microscopic imperfections in the thin film. A very tight bond was obtained between the deposited alloy and the Kapton although the deposited metal would follow original impressions in the Kapton as shown in Figure 32.

The contaminants present in the nickel-silver foil as received from the supplier were greatly reduced by the flash evaporation process. Figure 33 illustrates a strip of deposited film with an unusual quantity of surface impurities. These contaminants are not embedded as occurs with the rolled foil; consequently the foreign particles may be removed by solvents.

The preliminary metallographic studies of the deposited film have shown very small grain structure (Figure 34) when compared with the grain structure of the annealed nickel-silver foil (Figure 9) as supplied by the manufacturer. It can be noted that the deposited film is no longer in the annealed condition; consequently the large resistance change resulting from strain cycling must have been produced by a disordering of atoms.

Electron diffraction patterns (Figure 35) of the Cu-Ni-Zn film were produced in an attempt to determine the degree of atomic order. The selected area ring pattern verifies that the material is polycrystalline with a very fine grain size. The grain size is approximately 200 A° in diameter. Because the grain size was so small the minimal information obtained regarding ordered domains was considered inconclusive.

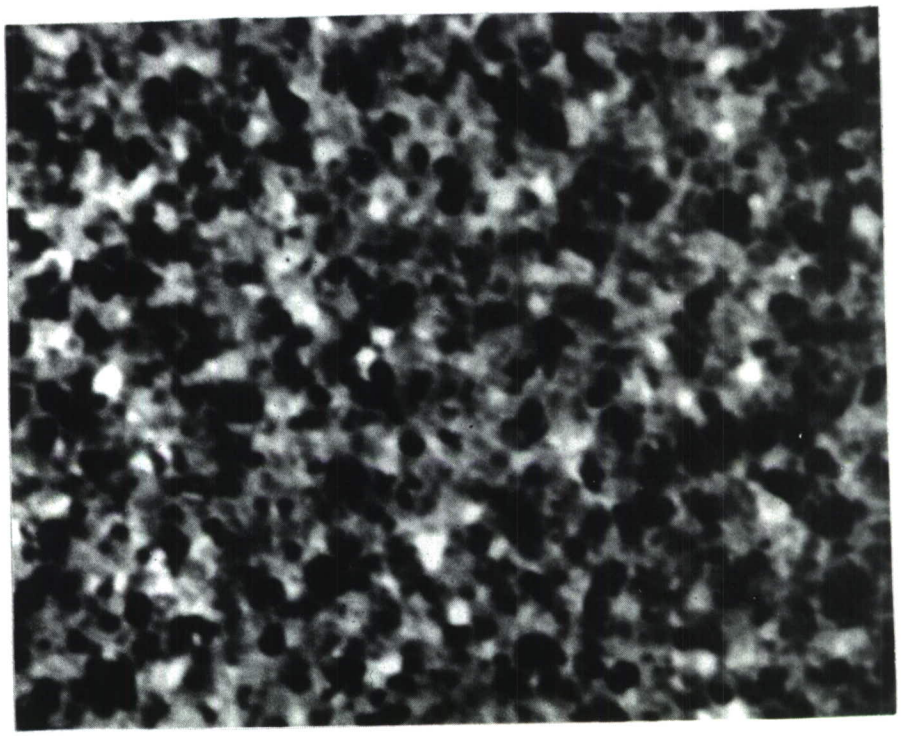

FIGURE 34. ELECTRON MICROGRAPH OF VACUUM DEPOSITED CU - NI - ZN FILM (TAKEN BY A JEM 7 TRANSMISSION ELECTRON MICROSCOPE) (190,000X)

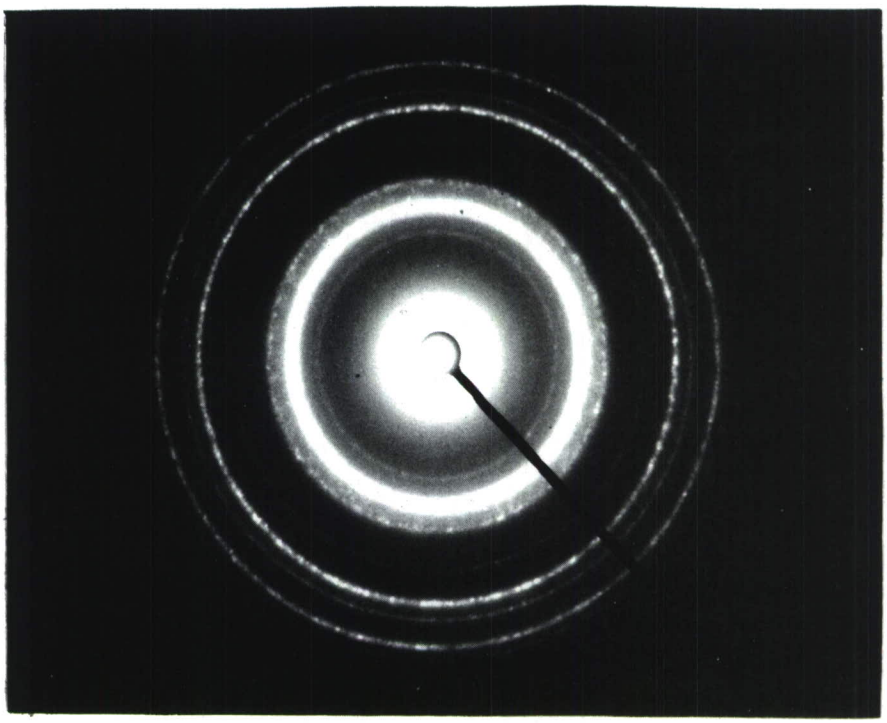

FIGURE 35. ELECTRON DIFFRACTION PATTERN OF THE VACUUM DEPOSITED CU-NI-ZN FILM

3.2.6 SENSOR CONFIGURATION

3.2.6.1 Influence of Sensor Configuration on Performance

The intended structural location of the sensor is one of the governing factors in determining sensor configuration for a practical application. The design of modern aircraft structure is such that it is difficult, if not impossible, to locate gages at points of known high stress concentration. The actual areas of high strains are usually faying surfaces such as under fastener heads or splice joints, resulting in limited accessibility. Previous experience with spiral grid configurations (Ref. 1) for use around fasteners or drain holes has left something to be desired. Since existing sensor capabilities are more favorable toward monitoring load exposure and then assessing damage, (rather than direct measurement of damage) it appears more feasible to locate in clean nominal areas of the structure. The direction of the principal cyclic strains can therefore be defined and the sensitive axis of the sensor oriented accordingly.

The feasibility of making sensor end loops responsive to transverse cyclic strains was analytically evaluated since any strain which contributes to damage is of interest rather than just principal axial strains. The conventional strain gage makes use of dimensional changes to produce a resistance change; therefore it seeks to minimize the effect of transverse strains upon resistance change of the end loops. A metallurgical change to produce resistance change is the area of interest in a sensor; therefore a resistance change of the complete grid was a consideration. Single strand construction, however, proved to offer increased fatigue life, simplicity of construction, and miniature size. It is believed these advantages offset any benefits to be gained by making the device sensitive to transverse strains; consequently single strand construction was the final configuration selected.

3.2.6.2 Fabrication of the Film Strip

The deposited metal film was formed by a flash evaporation process on a Kapton substrate approximately 1 mil thick, 7/8 inch wide and 4 inches long. A strip mask was placed over the Kapton substrate lengthwise so that a 1/8 inch edge of the substrate was exposed along the two longer sides. A pure copper underlay was then deposited on this restricted surface, forming the solder pad area for the sensors that were later fabricated from the strip. After deposition of the copper the mechanical fingers were used to remove the mask and then the Cu-Ni-Zn alloy was deposited, all without breaking the chamber vacuum. Each batch of material was given a sample number so that sensor response could be correlated with a material compositional analysis. The individual single strand sensors were then cut from the basic film strip. The basic film strip and the sensors used in the screening tests were configured similar to the following.

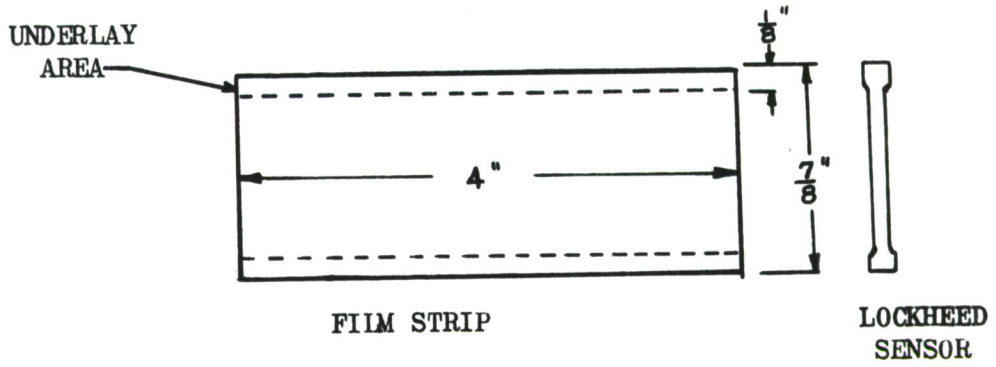

The copper underlay was deposited on the ends of the strand to facilitate the attachment of solder dots or the direct soldering of leads. The thickness of the copper underlay was not considered critical; consequently, it was allowed to vary over a range of 20 to 40 microinches in thickness. The fabricated sensors were then bonded to the specimen with an adhesive in a manner typical of other gages. To protect against stress corrosion, the thin film was either encapsulated or moistureproofed as soon as possible. The film was approximately 5 microinches thick as compared with conventional Constantan strain gage foil having a nominal thickness of approximately 200 microinches.

Fabrication of a metallic strip by deposition of a Cu-Ni-Zn alloy on Kapton film permitted the expeditious evaluation of different sensor configurations. The cost of precision masks made experimentation with different mask configurations economically unattractive at this stage of evaluation. The larger deposited area also allowed sampling of deposited film for compositional analyses. The individual sensors, as fabricated by the Lockheed-Georgia Company, were not encapsulated and varied over a resistance range of approximately 30 to 40 ohms.

3.2.6.3 Fabrication of Commercial Grade Sensors

The fabrication of "commercial grade" sensors from the basic strip material was subcontracted to Dentronics Inc. Although the nominal resistance was not critical, it was desired that an initial resistance within a 1% tolerance be maintained to simplify data measurements.

Several possible sensor designs were evaluated, with the preferable sensor having a die-cut single strand with copper underlay solder pads, a treated Kapton backing and a targeted resistance tolerance of 1%. The configuration, as fabricated by Dentronic Inc., is shown as follows:

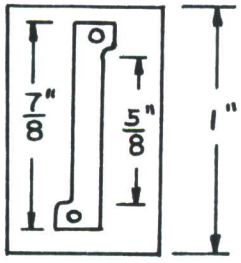

Encapsulation of the sensitive grid was accomplished using a 1 mil thickness of Kapton to encase the single strand grid. The total thickness of the composite was approximately 2.5 mil. The strand width was approximately 50 mil with the strand length adjusted to maintain a constant resistance from sensor to sensor. The vernier adjustment on the die allows a convenient method for resistance trimming and compensates for any nonuniformity of thickness.

Photographs of the critical areas of the single strand sensor are shown in Figures 36 through 39. The solder tab end radius was considered as a potential fatigue sensitive area; therefore, a special effort was directed toward a precise die-cut edge line. Since the solder dots were installed on a thin deposited film, their size appeared very critical to this application.

Two proprietary sizes of solder dots were given a cursory evaluation. Either size was acceptable for attaching lead wires and no handling or fatigue problems occurred with these solder dots.

During testing the commercially fabricated sensors produced no resistance increase at all for the required strain level of $\pm$ 500 $\mu\varepsilon$ and for a test duration of 10,000,000 cycles. Further evaluations of the same type sensors at strain levels of $\pm$ 700 $\mu\varepsilon$ and $\pm$ 1000 $\mu\varepsilon$ produced the same difficulties. Examinations of these commercially fabricated sensors indicated no fatigue cracks, electrical grounding, or loss of bond as a result of cycling. No data points were plotted or response curves shown for these sensors since their resistance change was zero. All the sensor response curves shown in the graphs of Phase II were of the Lockheed fabricated variety.

The construction, configuration, and general appearance of the commercial sensor was acceptable; however, its performance was not. It is believed that the sensitivity of the deposited film was severely attenuated by the fabrication process, possibly by the pressure required for bonding the backing and encapsulation. The deposited film in the ordered state is rather delicate in regard to pressures and although different types of epoxy adhesives were evaluated, all required some pressure to eliminate "bubbles" and produce a flat surface.

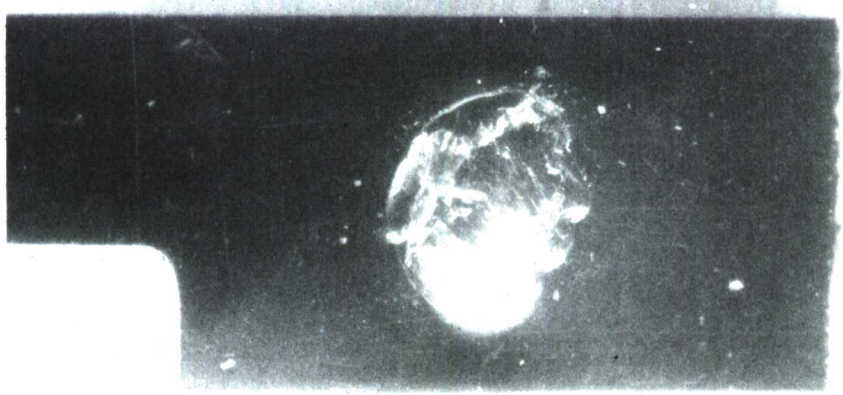

FIGURE 36. END TAB OF COMMERCIAL GRADE SENSOR SHOWING THE LARGER SOLDER DOT INSTALLATION (20X)

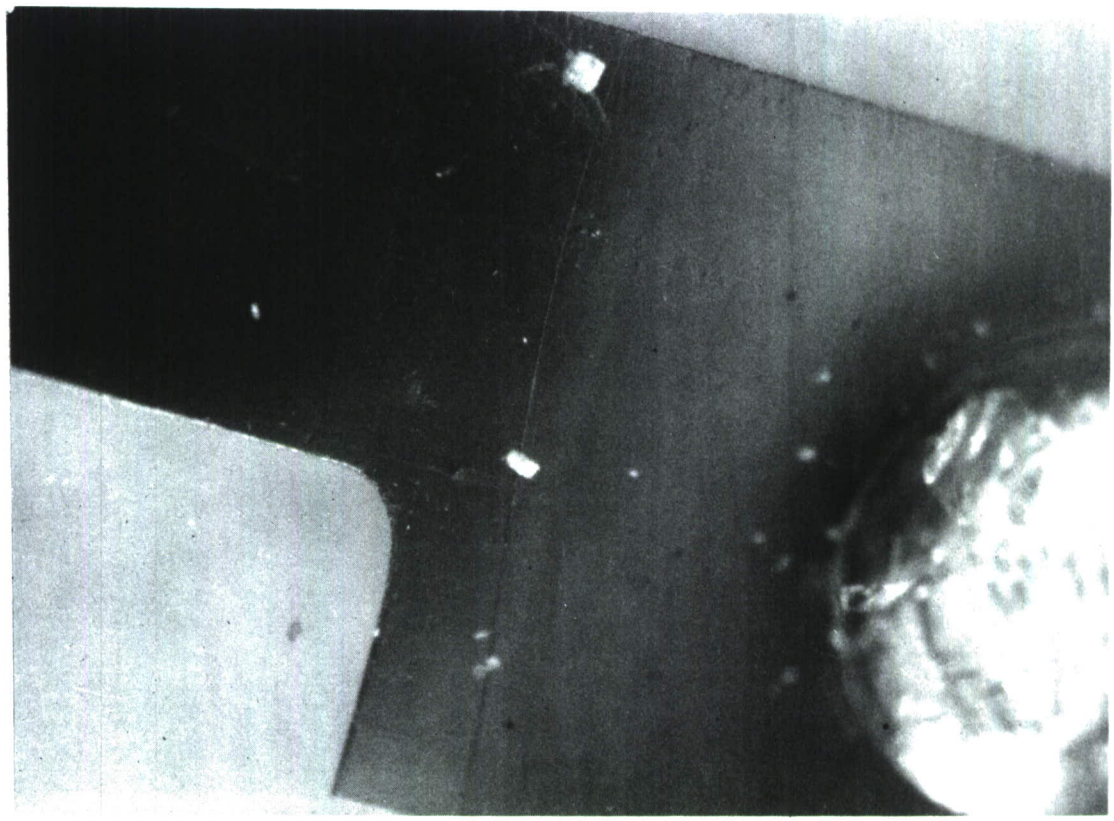

FIGURE 37. PHOTO OF END TAB SHOWING THE CRITICAL RADIUS SECTION (50X)

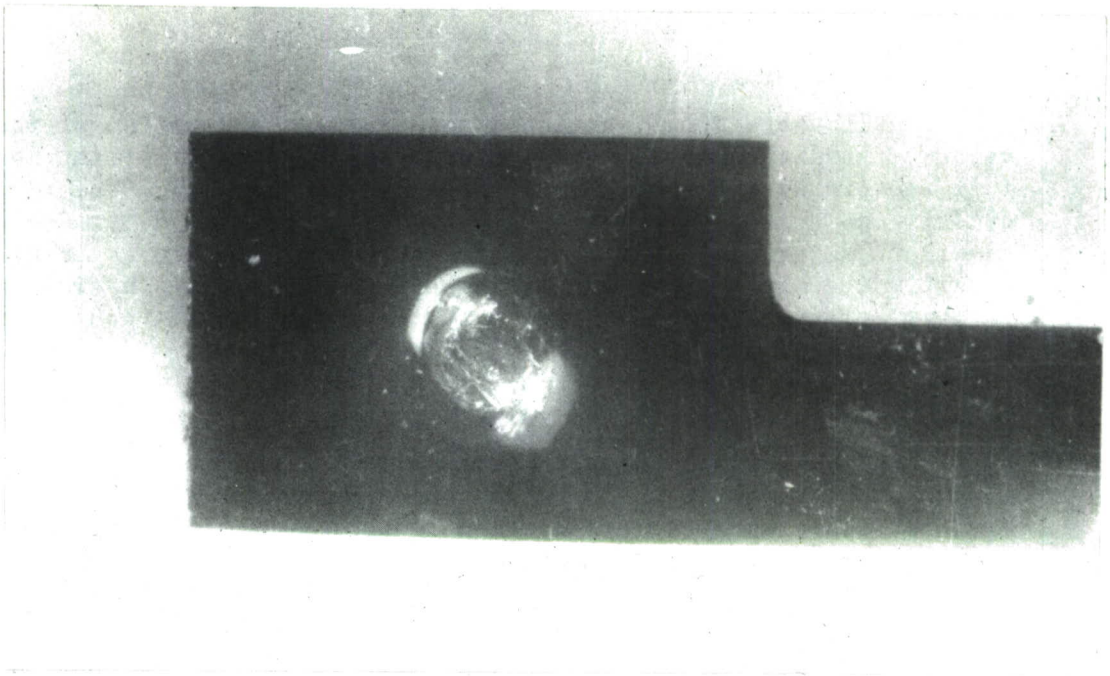

FIGURE 38. END TAB OF SINGLE STRAND SENSOR SHOWING THE SMALL SOLDER DOT (20X)

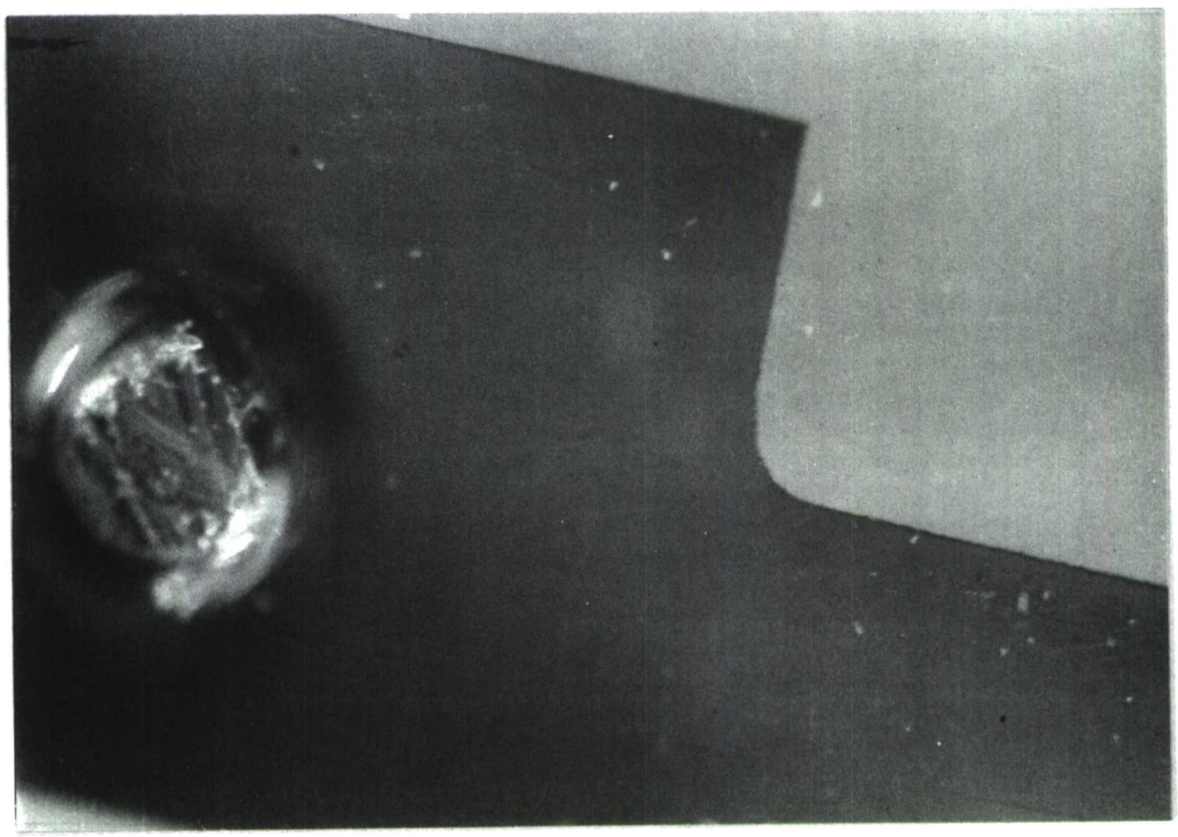

FIGURE 39. END TAB RADIUS (50X) (PHOTO TAKEN THROUGH KAPTON ENCAPSULATION.)

3.2.7 TEST PROCEDURES AND EQUIPMENT

3.2.7.1 Screening Tests

The screening techniques used for the evaluation of the vacuum deposited sensors were the same as those used for the annealed foil sensors as previously described in Section 3.1.4. The screening evaluations were simply meant to be a "first try" to determine if the candidate materials could meet the first priority, e.g., threshold sensitivity. If this requirement was satisfied, the sensor was further screened for compliance with the other target requirements (Section 1.1).

3.2.7.2 Axial Load Fatigue Tests

The sensor type which best satisfied the target requirements of the screening program was then evaluated in axial load fatigue. This mode of loading is more representative of the loading experienced by airframe structural elements than completely reversed bending. The purpose of these evaluations was to determine

- o sensor performance under axial load conditions as opposed to bending;
- o sensor performance at various strain levels and strain ratios;
- o sensor repeatability under axial load conditions at various strain ratios;
- o total sensor resistance change and life at various strain ratios.

3.2.7.3 Test Specimens

Sensors were applied to axial load fatigue specimens of the configuration shown in Figure 40. This specimen is somewhat different from those used for axial fatigue in the past (Ref. 1) but it has certain advantages. The long test section of constant area will allow several sensors to be evaluated at the same time and at the same peak-to-peak strain. Also, the strain will be constant along the sensor grid length. Two sensors were bonded to the center section of the specimen in a back-to-back arrangement. Although the sensors are suitable for bonding with either an epoxy or contact adhesive, the contact adhesive was selected to expedite the preparation of specimens. A commercially available adhesive (Eastman 910) with an elongation capability, specified by the strain gage industry as 6 to 10% strain, was utilized. It is recognized that the contact adhesive is not suitable for a long term installation.

3.2.7.4 Test Equipment

The axial fatigue evaluations encompassed strain ratios, R, of -1.0, -0.33, +0.10 and +0.33 where R is the ratio of minimum strain to maximum strain. For each strain ratio, four different dynamic strain ranges were used to define resistance change for each sensor. A minimum of two specimens was tested for each strain range and each specimen had a minimum of two sensors. A total of 80 sensors installed on 40 specimens were evaluated. Specific test conditions for the axial load fatigue evaluations are contained in Table II.

The low cycle testing was performed in electrohydraulic servo controlled testing machines similar to the setup shown in Figure 41. The load form was sinusoidal, and a fixed frequency was selected between the approximate limits of 5 and 30 cycles per second, depending upon the strain level required. The loading equipment as shown in Figure 41, is a direct force type machine having a full-scale fatigue load capacity of $\pm$ 100,000 pounds. The lowest load range is $\pm$ 10,000 pounds, and all ranges were calibrated to $\pm$ 0.5% of indicated load using standards certified by the National Bureau of Standards (Ref.10). The control console for the machine contained the necessary instrumentation properly integrated to provide complete control, monitor, and fail-safe functions for the test system. Monitoring of the applied loads was accomplished using the amplitude measuring unit which simultaneously displays both the maximum and minimum load in a null fashion on an oscilloscope. The signal monitored was produced by a load transducer which was in series with the test specimen. The axial loads required to produce the desired maximum and minimum strains were determined using standard stress-strain relationships for the 7075-T6 aluminum alloy sheet as published in Reference 11.

Teflon lined lateral support plates as shown in Figure 42 were used on all negative strain ratio tests to prevent specimen buckling during compressive loading. These plates contained windows to provide clearance for the sensor installations. Measurements of sensor resistance change were made in the same manner as described for the screening tests. Frequency of resistance measurement varied from test to test depending on the test strain level and associated test duration. In all cases sufficient data were collected to adequately define the resistance change versus cycles relationships.

All high cycle fatigue evaluations were performed in Lockheed designed fatigue (Fig. 43) machines which operate on the resonant principle. Each machine as illustrated in Figure 44 has a flat grip which will accept specimens up to three inches wide.

Maximum specimen length was 18 inches. One grip was attached to an electrical resistance type strain gage load transducer which was directed to a dynamic load analyzer comprised of calibrated potentiometers, a carrier amplifier, and an oscilloscope. In operation the carrier amplitude was set by the calibrated potentiometers to a value proportional to the desired load. The carrier was then amplitude modulated by the transducer signal until a null was achieved as indicated by the oscilloscope. Maximum, minimum, and mean loads were monitored in this manner. Each machine, as shown in Figure 45, was system calibrated to MIL-C-45662A (Ref. 10) to an accuracy of $\pm$ 0.5% of indicated load using standards certified by the National Bureau of Standards. A variety of transducers having different full-scale load capacities was available which allowed a high ratio of test load to transducer capacity to be maintained. Operating frequency range of the machine was 20 to 40 cycles per second, and the load form was sinusoidal. Operating frequency was established by speed of the variable speed motor, and dynamic load at a given frequency was a function of variable eccentric setting, variable mass of the machine, and position of the grips in the machine.

Mean load was applied by a hydraulic actuator on most machines; however some of the machines had a mechanical screw for application of mean load. Each machine had an automatic cutoff system which stopped the motor and cycle counter upon specimen failure. The cycle counter indicated a least count of one thousand cycles.

The resistance change of each sensor was periodically measured by a wheatstone bridge while the specimen was under a no-load condition. The variation in initial resistance from sensor to sensor was not a problem since percent resistance change was the parameter of interest. Lockheed fabricated sensor strips were connected in series as shown in Appendix II to provide initial sensor resistance values as low as 20 ohms and as high as 300 ohms to confirm that percent resistance change is not a function of initial resistance.

DIMENSIONS IN INCHES

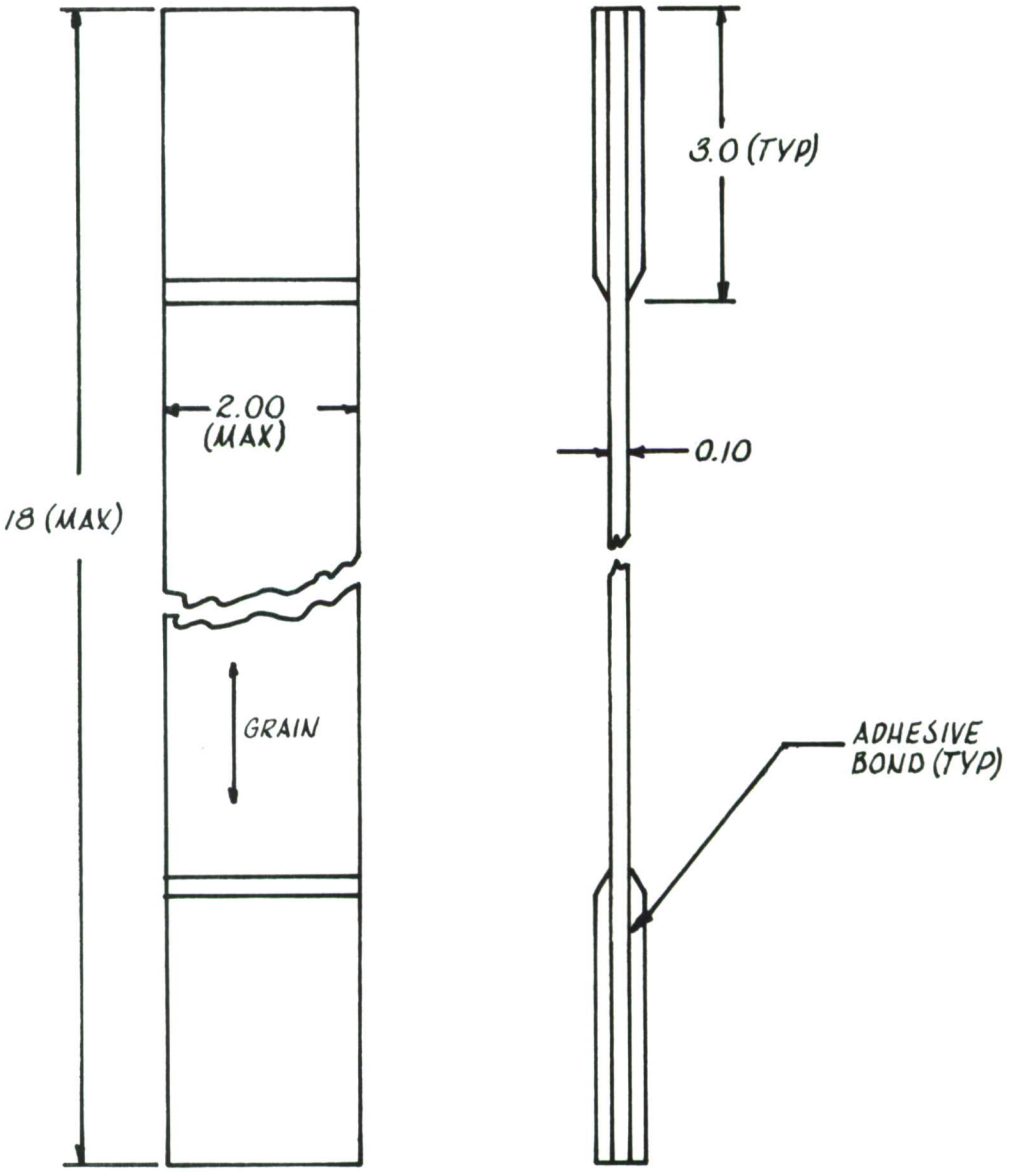

FIGURE 40. AXIAL FATIGUE SPECIMEN — BARE 7075—T6 ALUMINUM ALLOY SHEET

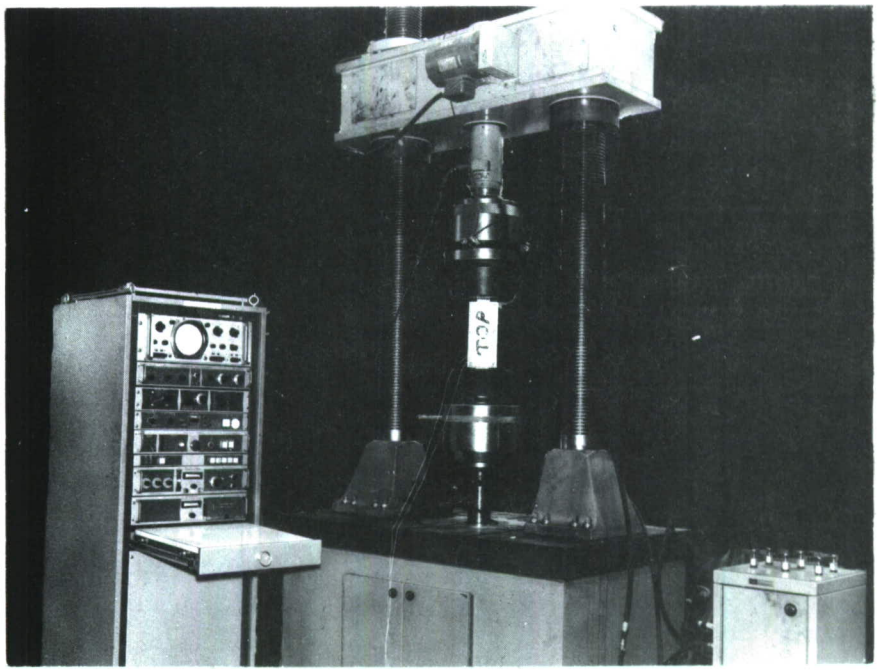

FIGURE 41. TEST SETUP FOR LOW CYCLE AXIAL STRAIN EVALUATIONS

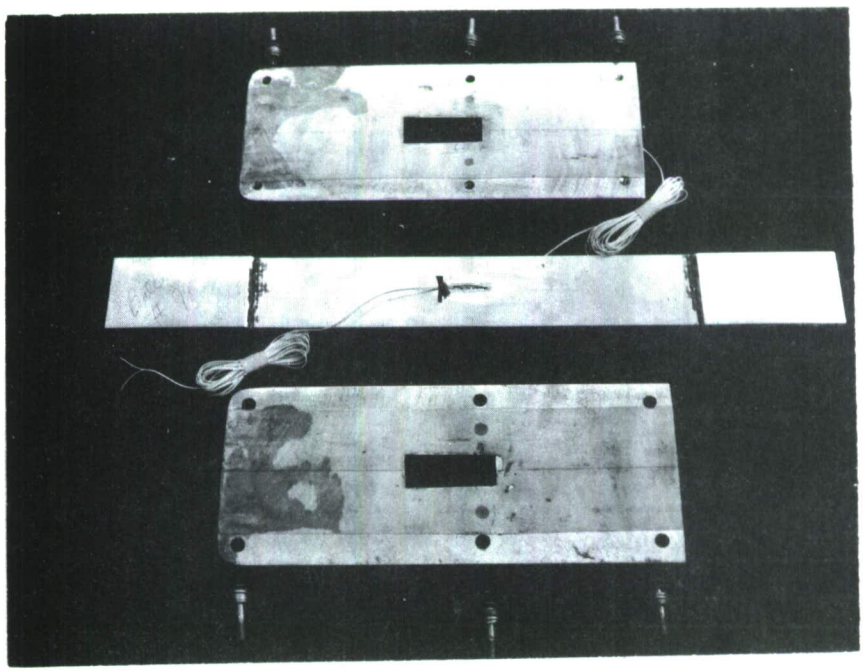

FIGURE 42. TEST SPECIMEN SHOWING INSTALLED SENSOR AND TEFLON-LINED LATERAL SUPPORT PLATES

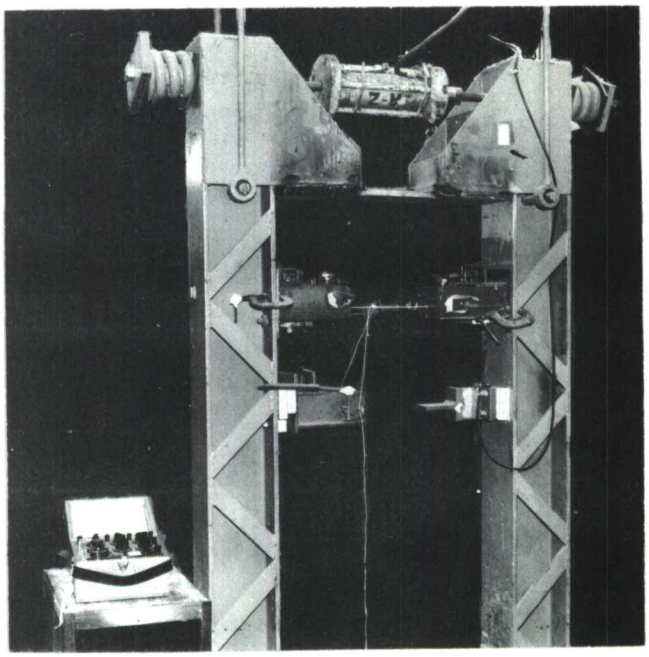

FIGURE 43. TEST SETUP FOR EVALUATING THE SENSOR IN A HIGH CYCLE FATIGUE ENVIRONMENT

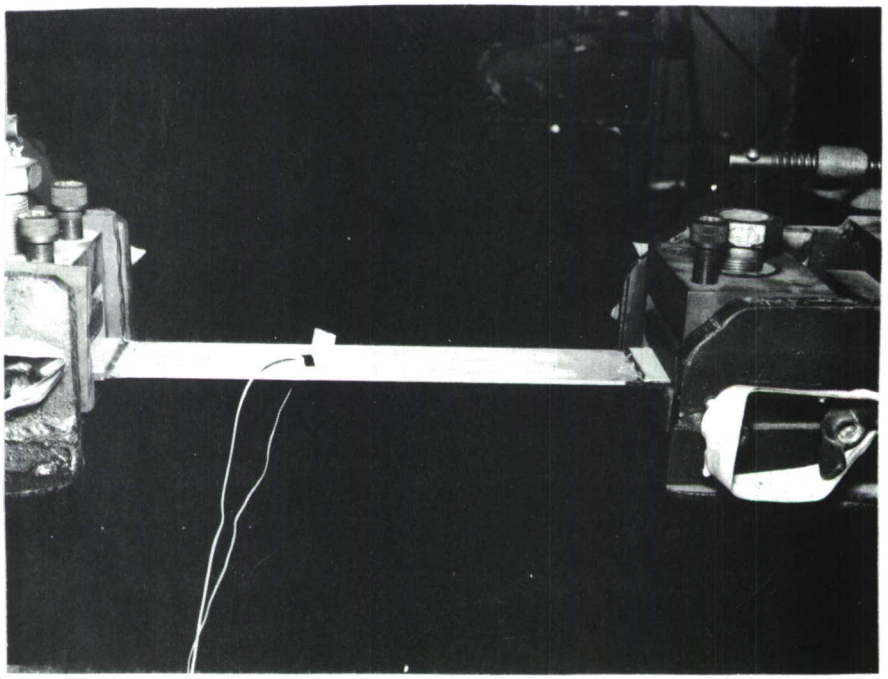

FIGURE 44. INSTRUMENTED AXIAL SPECIMEN MOUNTED IN FATIGUE TEST EQUIPMENT

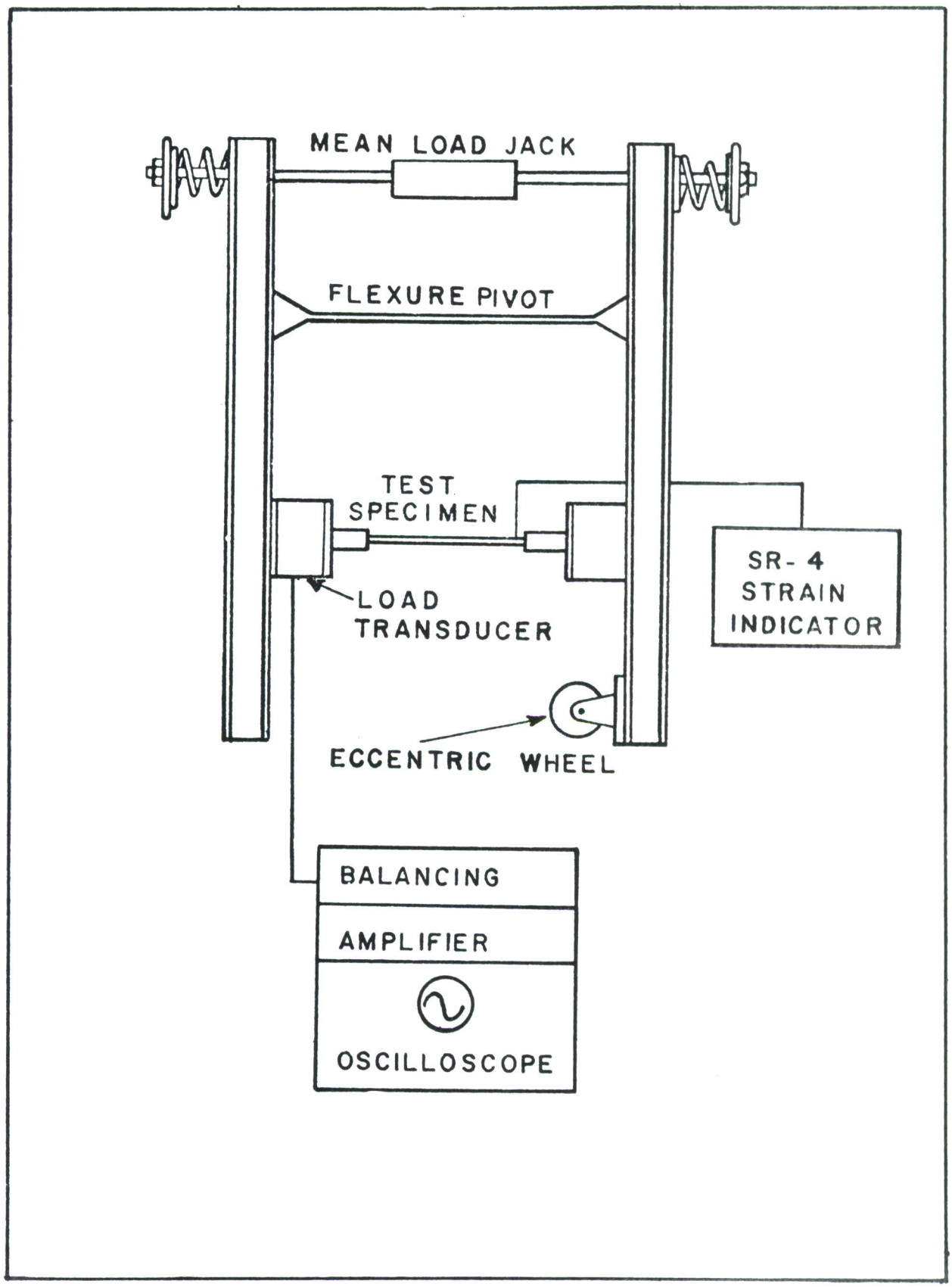

FIGURE 45. SCHEMATIC DIAGRAM OF AXIAL LOAD TUNING FORK TYPE FATIGUE MACHINES

3.2.8 TEST RESULTS - VACUUM DEPOSITED SENSORS

3.2.8.1 Screening Tests

The decision to evaluate vacuum deposited sensors possessing an ordered atomic structure prompted a slight departure from the original test plan. Initially it was felt that disordering the sensor material at a high cyclic strain level might possibly prevent any further disordering at a lower cyclic strain level. For a practical application to service aircraft, this kind of behavior could not be tolerated. The response curves shown in Figures 46 and 47, indicate that disordering continues regardless of the sequence of strain and the resistance change is also directly responsive to the amplitude of cyclic strain. Figures 46 and 47 represent typical sensor sensitivities to a block loading sequence composed of two different cyclic strain levels. Although there were some inconsistencies in sensor slope when related to order of loading, it was not precisely determined if the sensor truly responded to order of loading. The significant development was the confirmation that the destruction of atomic order continued despite previous higher strain levels.

The screening tests of the vacuum deposited sensors mounted on the cantilever flexure beams were tested to the envelope shown in Figure 20 and to the specific test conditions noted in Table II. All sensors were identified by batch number so as to assist in a correlation of sensor response with material composition and degree of atomic order. Sensors designated with the same batch number were all fabricated from the same "run" of deposited material.

The ordinates used in Figures 48 and 49 are representative of possible scale alternates, so the selection becomes a choice between sacrificing range or resolution. All the curves of sensor response could have been displayed in either semilog or log-log form; however the wide range of sensor resistance change and variation in number of test cycles make the choice of a two cycle log-log presentation appear more appropriate. This procedure necessitates the deletion of a portion of the sensor response curves which, in this case, was selected as the initial cycles. The SF-2 test equipment used during screening had a mechanical counter which displayed a least cycle count of 1000 cycles; therefore, it was only logical to record data for increments of 1000 cycles or larger. In practice the high cyclic rate (30 cps) made the choice of 10,000 cycles as the first data point a very reasonable one. In retrospect, this practice makes it difficult to analyze sensor behavior for the initial cycles; however, defining the parameters of threshold sensitivity and percent resistance change was considered the most important at this stage of evaluation.

The determination of sensor temperature sensitivity was not a requirement of this program; however, temperature excursions of approximately 10°F occurred during cyclic tests of the sensors on flexure beams. Although the temperature coefficient of resistance for the Nickel-Silver (Cu-Ni-Zn) is slightly higher than that of Constantan, the variations were not detectable on a four decade wheatstone bridge. The wheatstone bridge was used for measuring the sensor output because the wide variation in initial sensor resistance was not compatible with the SR-4 strain indicator and standard completion resistors. The higher strain levels also produced resistance changes on the order of 18 to 80% which exceeded the 12% operating range of the SR-4 indicator. The instrumentation setup used for the screening tests was the same as illustrated in Figure 22.

A continuation of testing and evaluation of the vacuum deposited Cu-Ni-Zn alloy on the flexure beams (Figs. 50 through 53) has indicated that it actually exceeds some of the target requirements. A target requirement not satisfied was the one regarding repeatability. The bandwidth of 5% on repeatability of sensor resistance change is a direct function of quality control during fabrication. The criteria for improving repeatability are primarily control of film composition and degree of atomic order. The customary analytical instrumentation (Appendix I) for determining film composition was utilized and experience in analyzing various material batches has improved the confidence level for accurately defining composition. Once the composition of the deposited film can be defined, corrective measures to control the composition can be implemented. The question of degree of atomic order, however, is much more elusive. The standard methods for determining order were used with little success.

Scatter in sensor response and other irregularities in the data have been observed. Eliminating these irregularities depends on the ability to isolate and correct the causes. Preliminary evaluations presented in Figures 49 through 51 show considerable variation in percent resistance change during initial fatigue exposure. There seems to be some initial "shake-out" during the first few thousand cycles in which there was a large variation in resistance change for sensors mounted on the same specimen and subjected to the same strain level. This variation is partially due to the variation in resistance change during the first few initial cycles, after which the rate of change becomes more uniform for both sensors. Figure 52 represents a typical sensor response (ΔR) to the higher strain level of $\pm$ 3000 $\mu\varepsilon$. Resistance changes (ΔR) of up to 80% were typical of sensors exposed to the higher strain levels and to fatigue life cycles of 30,000 or more. The programmed specimen test cycles as shown in Table II were selected to allow termination of cycling prior to a specimen failure. The unusually low amplitude of resistance change (ΔR) experienced at a strain level of $\pm$ 5000 $\mu\varepsilon$ (Fig. 53) may have been due to a deterioration of the sensor bond.

Although strain gage suppliers claim an elongation capability of 6 to 10% strain for Eastman 910 contact adhesive, a visual inspection of the sensor indicated possible bond deterioration.

Screening evaluations were confined to tests of sensors fabricated only from material batches three and four. Although the screening tests were not planned to provide extensive statistical data, it appeared that batch three material showed a higher sensitivity than that of batch four. Reference to Section 3.2.5, "Quality Analysis," shows that batch three material was composed of 57% Cu, 21% Ni, 22% Zn which was much closer to the desired 60% Cu, 20% Ni, 20% Zn composition than batch four.

Even with the minor inconsistencies that developed during the screening tests, performance of the deposited sensor was very encouraging and revealed no real barriers to further testing. An analysis of the screening tests and the behavior of the sensor subjected to completely reversed bending strains indicated that more extensive sensor evaluations on axial specimens were in order. The axial fatigue tests conducted at various strain ratios and strain levels were more representative of loading experienced by airframe structural elements than the reversed bending tests.

TABLE II

SENSOR EVALUATION FATIGUE TESTS (1)

FLEXURE FATIGUE TESTS R=−1.0				AXIAL LOAD FATIGUE TESTS						
MICROSTRAIN (PEAK-TO-PEAK)	TOTAL CYCLES	REQ'D NO. (2) TESTS	TESTS COMPLETED	STRAIN RATIO	MICROSTRAIN (PEAK-TO-PEAK)	MAXIMUM MICROSTRAIN	MINIMUM MICROSTRAIN	TOTAL CYCLES	REQ'D NO. (2) TESTS	TESTS COMPLETED
1000	10^7	2	2	−1.0	1000	500	−500	10^7	3	3
2000	10^6	2	2	−1.0	2000	1000	−1000	10^6	3	3
3000	4×10^5	2	2	−1.0	4000	2000	−2000	10^5	2	2
4000	10^5	2	2	−1.0	6000	3000	−3000	3×10^4	2	2
				−0.33	1000	750	−250	10^7	3	3
6000	3×10^4	2	2	−0.33	2000	1500	−500	10^6	3	3
				−0.33	4000	3000	−1000	10^5	2	2
10,000	9×10^3	2	2	−0.33	6000	4500	−1500	3×10^4	2	2
				+0.10	1000	1110	110	10^7	2	2
				+0.10	2000	2225	225	10^6	3	3
				+0.10	3000	3340	340	3×10^5	3	3
				+0.10	4000	4450	450	10^5	2	2
				+0.33	1000	1490	490	10^7	2	2
				+0.33	2000	2980	980	10^6	3	3
				+0.33	3000	4480	1480	3×10^5	3	3
				+0.33	3350	5000	1650	1.5×10^5	2	2

TOTAL — 40 BEAMS, 80 SENSORS

(1) THIS TABLE INCLUDES ONLY THOSE TESTS RUN ON THE VACUUM DEPOSITED OPTIMIZED SENSOR. IT DOES NOT INCLUDE PRELIMINARY TESTS CONDUCTED ON THE DIE-CUT SENSOR.

(2) THESE TESTS REQUIRED AS SPECIFIED BY TABLE I OF THE TEST PLAN. TWO SENSORS PER TEST BEAM.

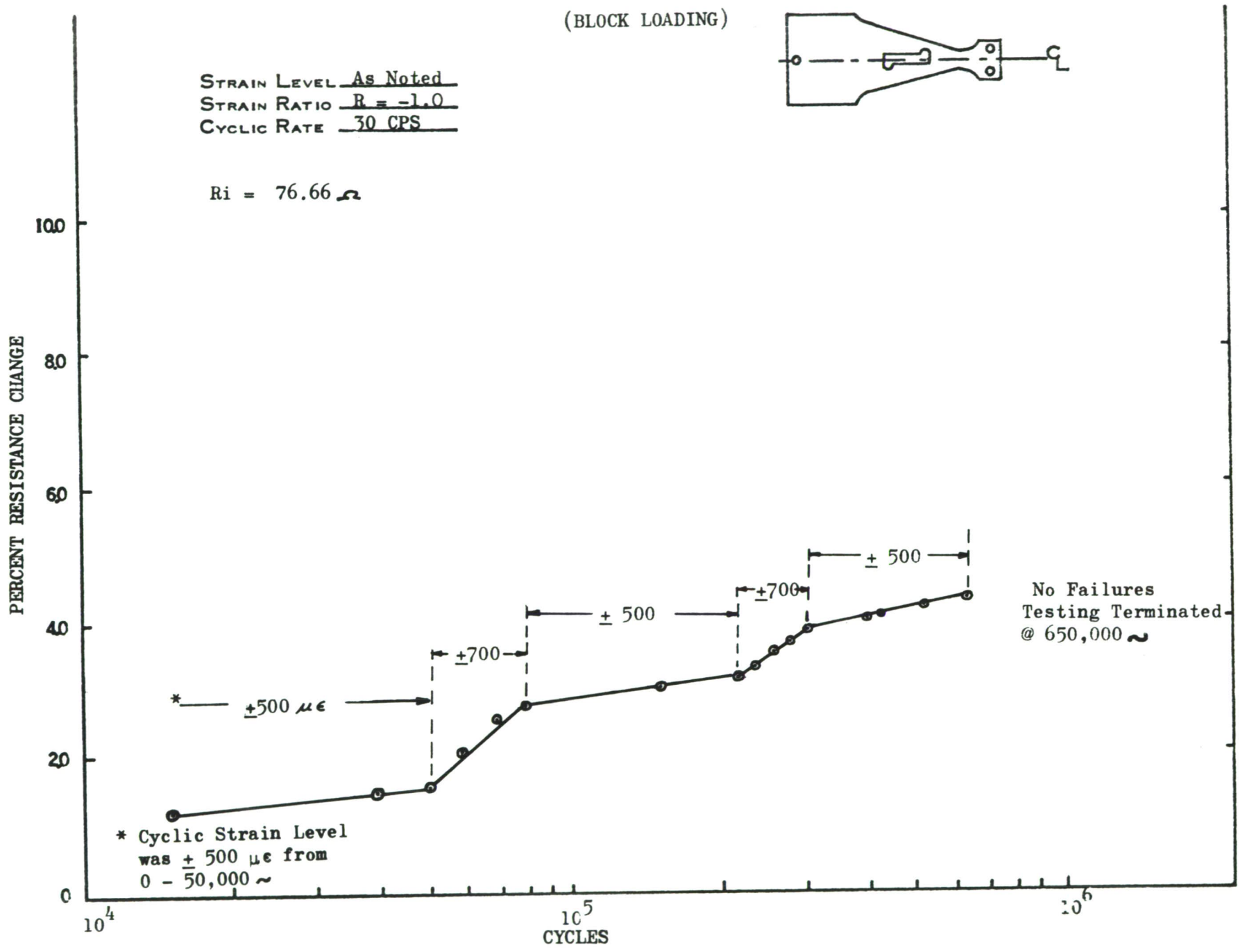

FIGURE 46. FATIGUE SENSOR RESPONSE FOR VACUUM DEPOSITED CU-NI-ZN, SPECIMEN 29, BATCH 3

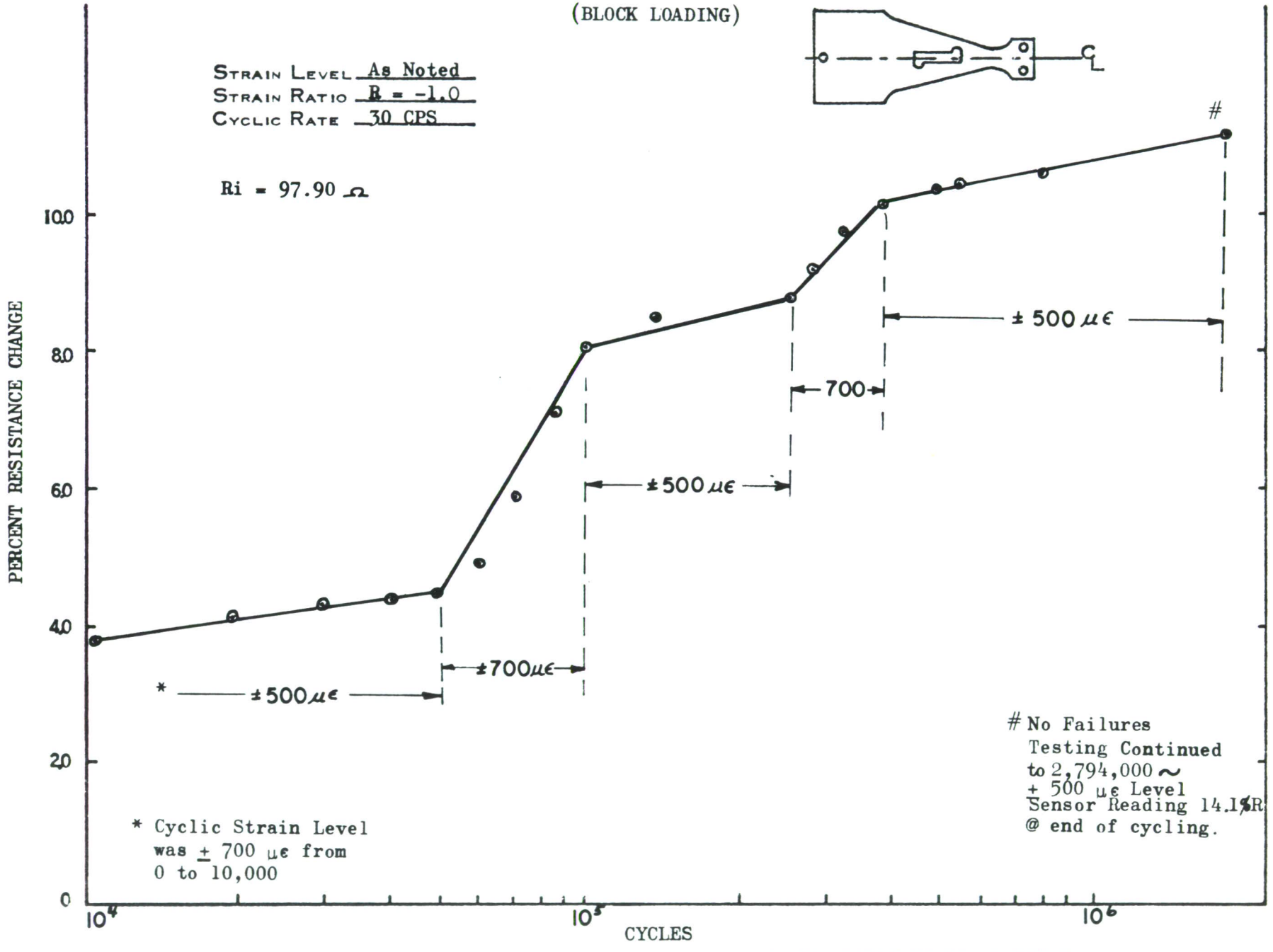

FIGURE 47. FATIGUE SENSOR RESPONSE FOR VACUUM DEPOSITED CU-NI-ZN, SPECIMEN 35, BATCH 3

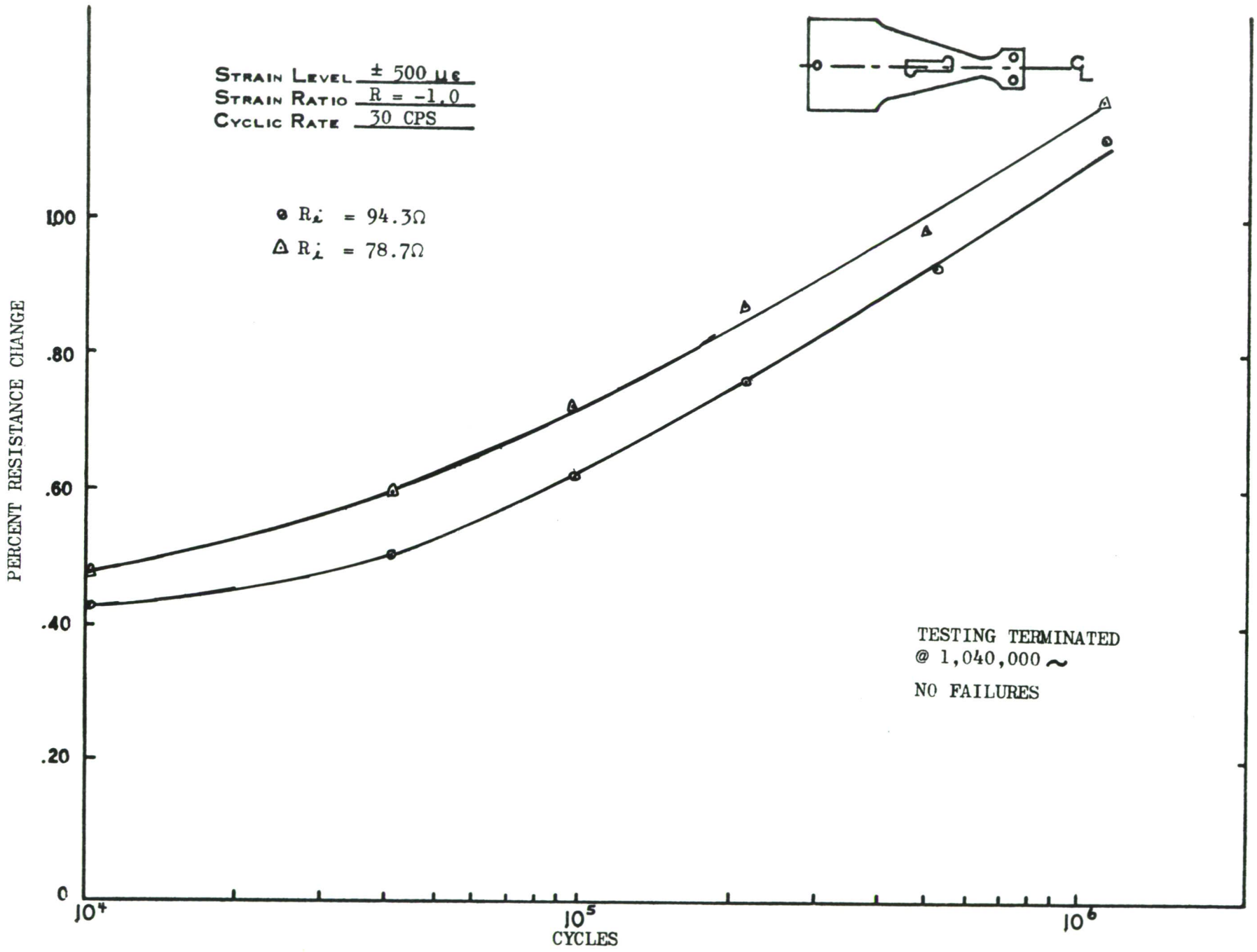

FIGURE 48. FATIGUE SENSOR RESPONSE FOR VACUUM DEPOSITED CU-NI-ZN, SPECIMEN 31, BATCH 3

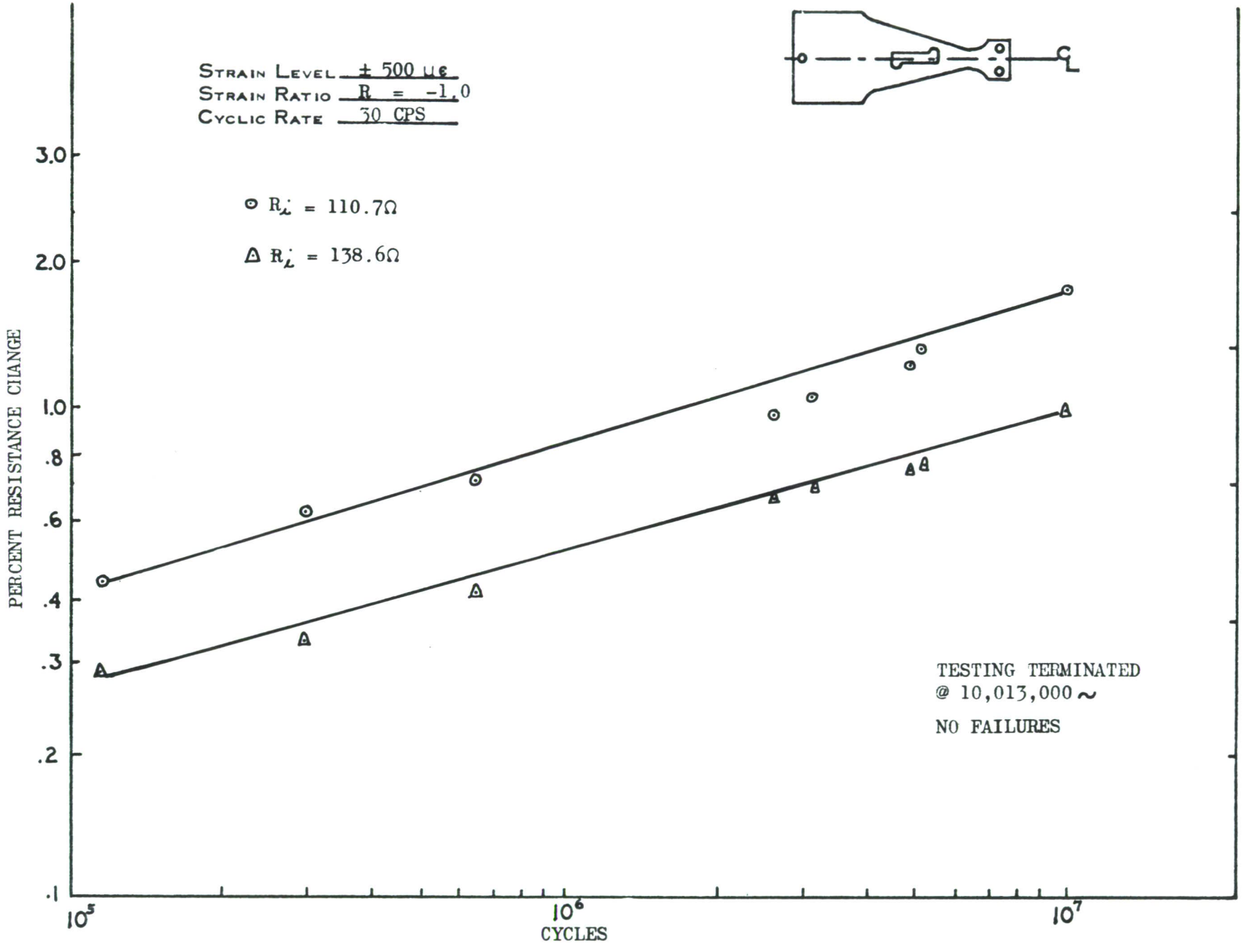

FIGURE 49. FATIGUE SENSOR RESPONSE FOR VACUUM DEPOSITED CU-NI-ZN, SPECIMEN 41, BATCH 4

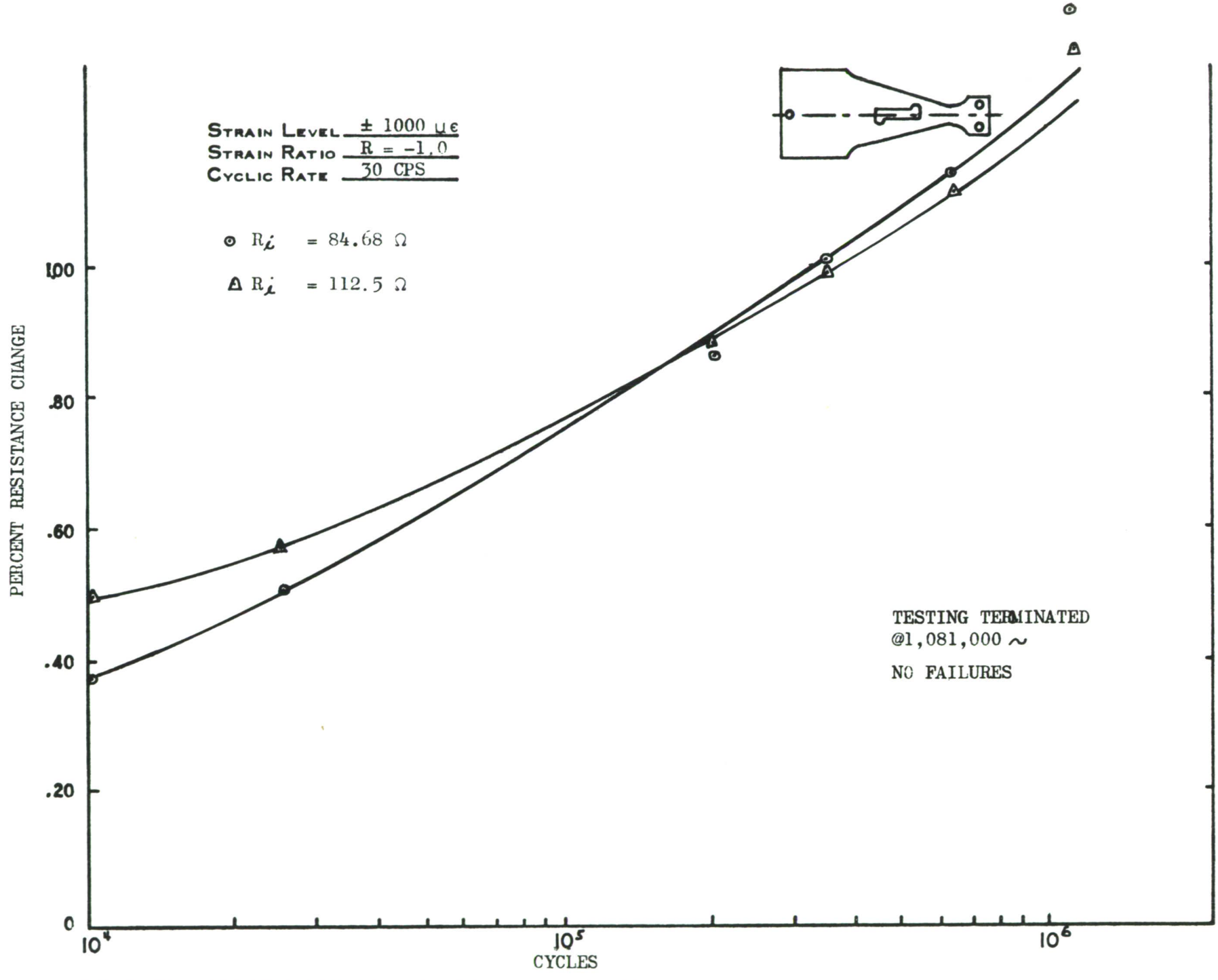

FIGURE 50. FATIGUE SENSOR RESPONSE FOR VACUUM DEPOSTED CU-NI-ZN, SPECIMEN 38, BATCH 4

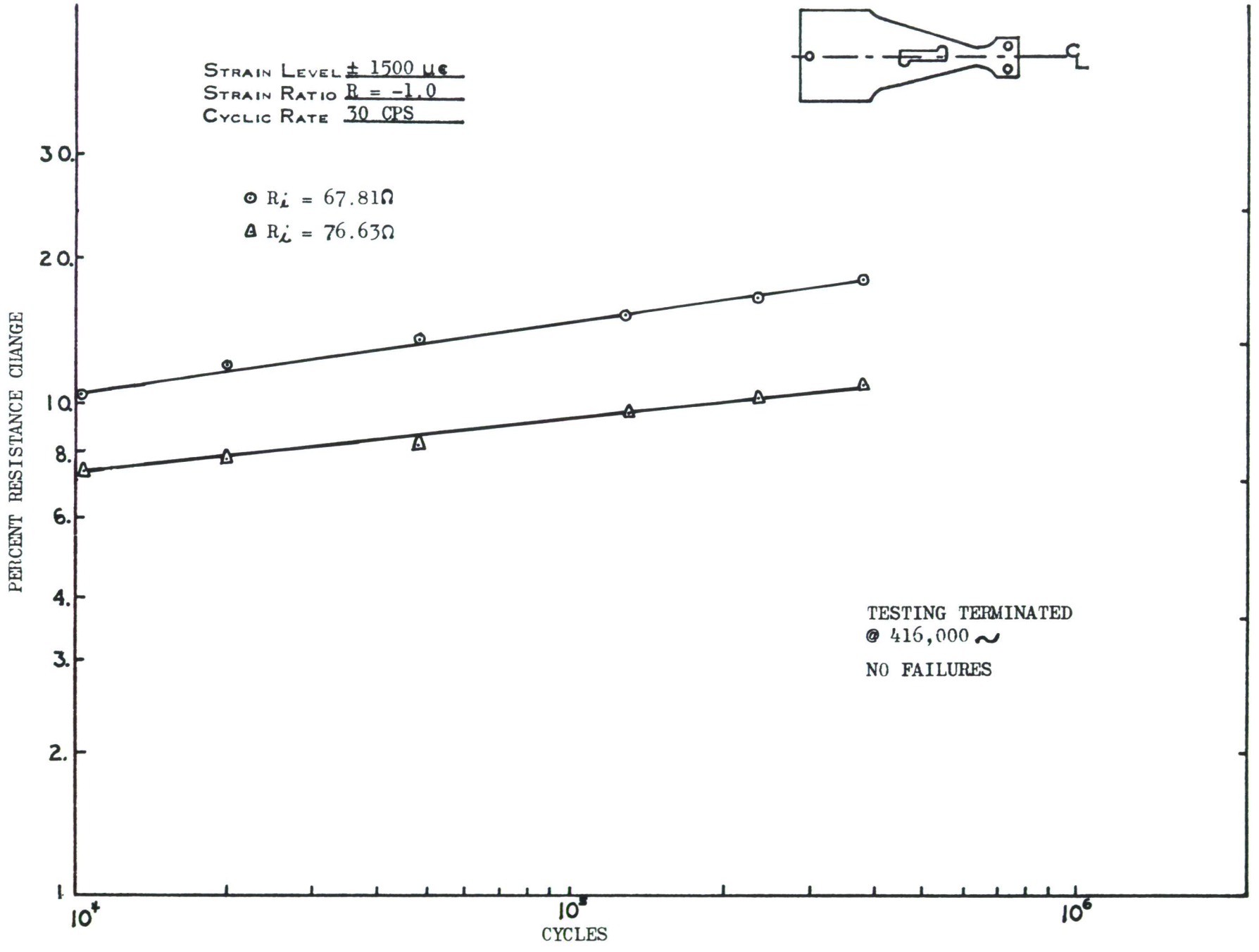

FIGURE 51. FATIGUE SENSOR RESPONSE FOR VACUUM DEPOSITED CU-NI-ZN, SPECIMEN 39, BATCH 4

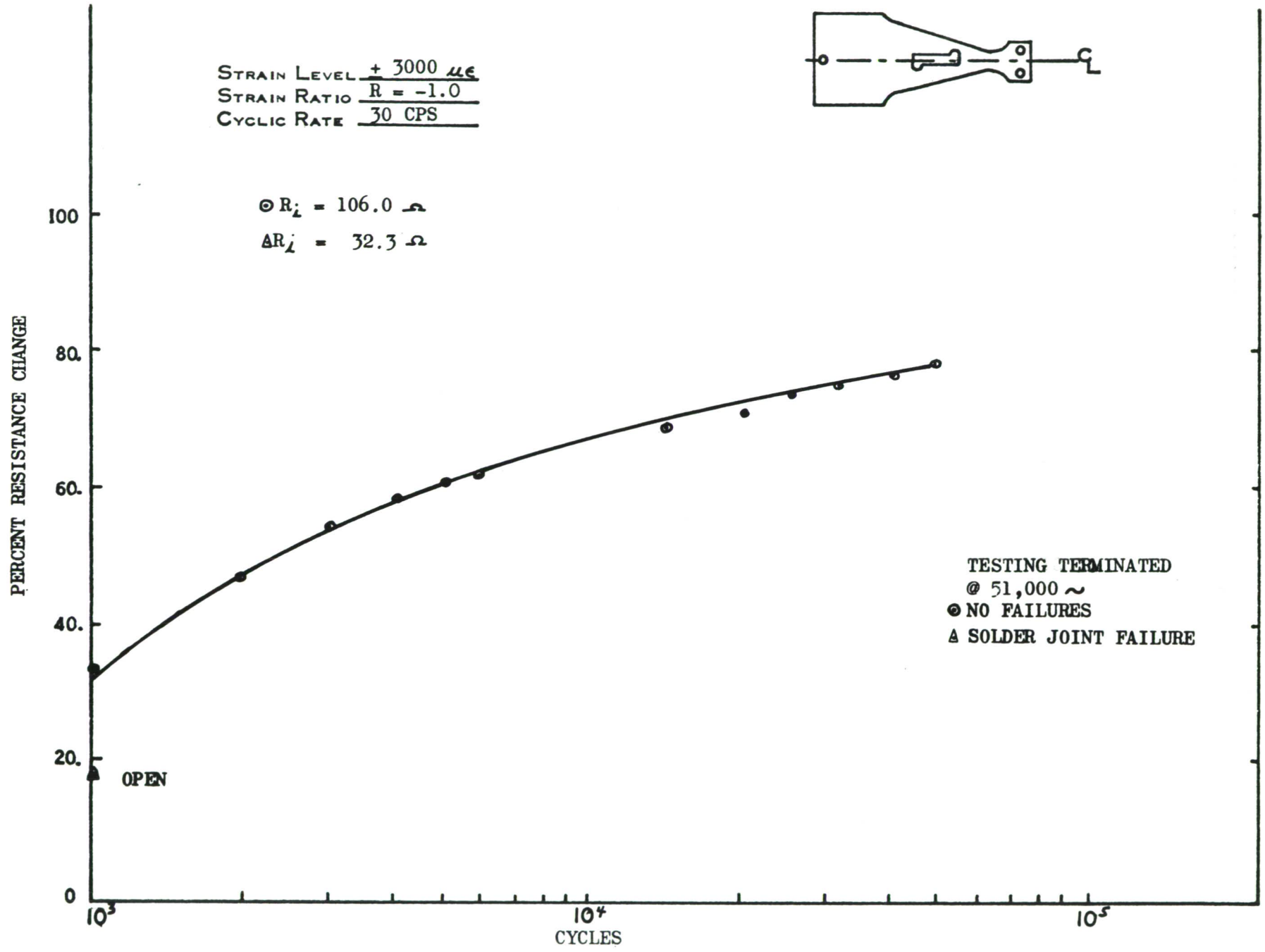

FIGURE 52. FATIGUE SENSOR RESPONSE FOR VACUUM DEPOSITED CU-NI-ZN, SPECIMEN 48, BATCH 4

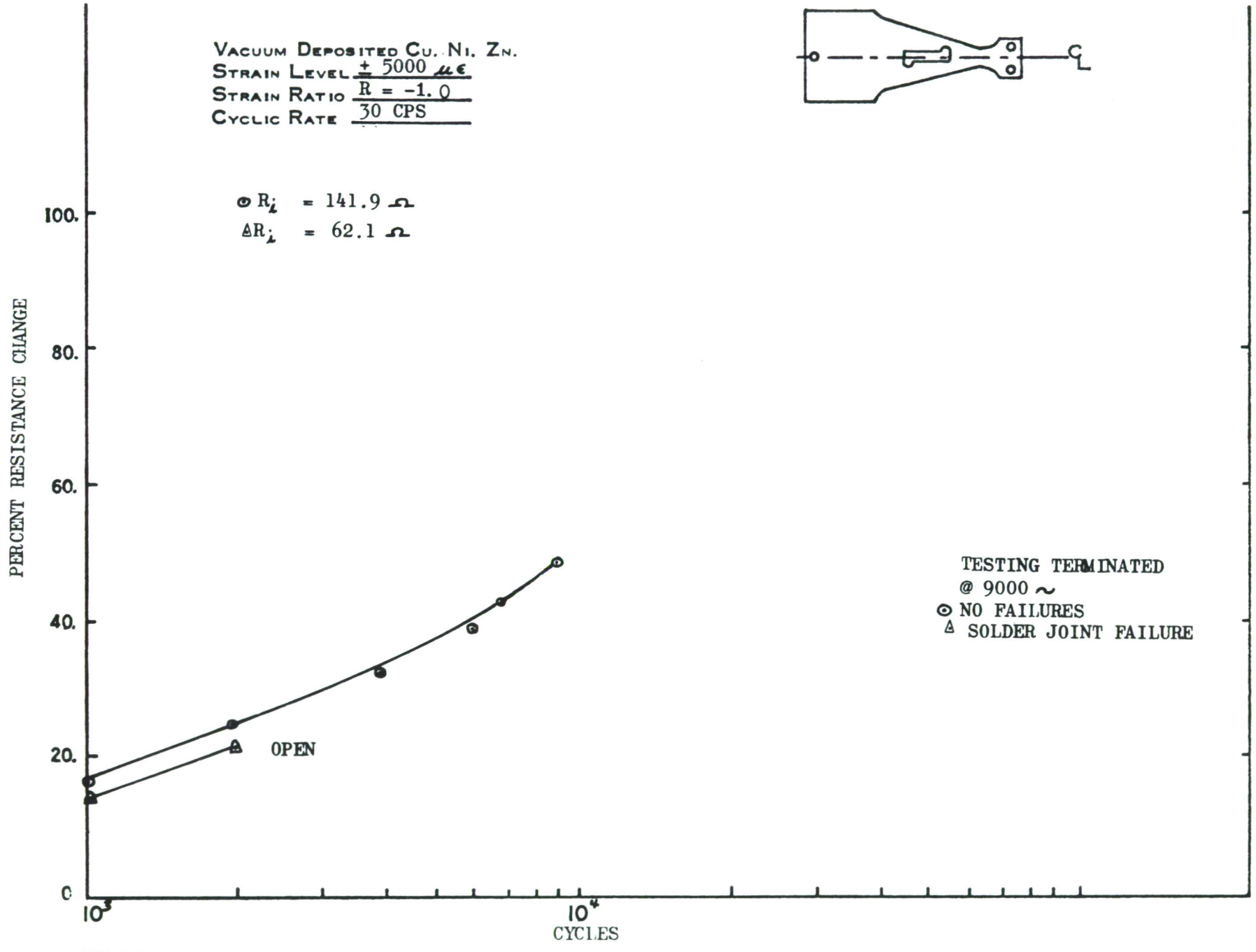

FIGURE 53. FATIGUE SENSOR RESPONSE FOR VACUUM DEPOSITED CU-NI-ZN, SPECIMEN 49, BATCH 4

3.2.8.2 Axial Tests

The evaluation of the sensor under axial loading conditions was designed to obtain more extensive data on sensor behavior over a wider range of strain ratios. A total of 40 axial specimens were instrumented with vacuum deposited sensors and tested according to the values shown in Table II. Figures 54 through 62 represent a point-by-point sensor response on the particular specimen shown, and Figures 63 through 78 constitute a boundary of the sensor response curves.

The sensors were installed in a back-to-back arrangement, two to each test specimen. Thus, each sensor was subjected to the same loading condition at any given time, permitting a comparison of sensor performance repeatability. No attempt was made to select sensors of the same initial resistance since the data were plotted in terms of percent resistance change rather than absolute resistance. Figures 54 and 55 show the response of back-to-back sensors on an axial specimen for a strain level of $\pm$ 500 $\mu\varepsilon$. Figures 56 and 57 show sensor response for the same strain range (1000 $\mu\varepsilon$ peak-to-peak) and the same strain ratio, but for different material batches. These curves compare reasonably well with sensor sensitivity outputs on the bending beams (see Figure 49) even for different material batches. If one considers slope only and not end resistance they appear even more repeatable. An overall review of performance repeatability indicates that the sensor response curves would more nearly coincide if the sensors were "exercised" prior to recording the initial zero. The effects of this procedure can be noted if the zero resistance measurements are made after about 1000 cycles and then data points plotted.

The data obtained on the axial specimens were consistent with previous data from the screening tests and the trends noted earlier continued during axial tests. Even when there was considerable scatter in the output of back-to-back sensors (Fig. 49), the threshold sensitivity level of either sensor exceeded the target requirements. Since the sensor threshold sensitivity exceeded the AFFDL requirement of 0.05% ΔR within 50,000 cycles @ $\pm$ 500 $\mu\varepsilon$, it was not necessary to determine the precise level of threshold sensitivity.

It has been noticed that a rest period will produce a slight decrease in resistance (Fig. 57) very similar to that experienced with the Constantan sensor during the feasibility study (Ref. 1). Although the variation is very small, it will be detected with sensitive resistance measuring instruments. It appears to be a function of the cyclic test frequency rather than variations in ambient temperature; however, the magnitude of change was insignificant so it was not pursued further. This behavior was not noted on sensors exposed to the lower frequencies (5 cps or lower).

Figures 63 through 78 represent a boundary of curves at a particular strain level and strain ratio which have been consolidated into one graphic presentation. The dotted boundary lines represent the sensor response from as many as three specimens (six sensors) at each test condition. The total number of sensors tested at each strain level are detailed in Table II.

The dotted boundary lines show the maximum deviation of sensor output for each specific test condition. Although this variation does not comply with the target requirement of repeatability within 5%, it was noted that the major portion of this variation always occurs during the initial cycles. The sensor response curves could have been displayed either as linear, semilog or log-log plots; however, to display the required wide range of resistance change and test cycles in detail, the log-log presentation appears as the logical choice. This procedure necessitates the deletion of the sensor response curves for the initial cycles. The major inconsistencies regarding sensor rate of change occurs during the initial cycles, after which a more uniform rate of change can be noted. Even though there was considerable difference in total resistance change for sensors installed as "mirror images" of each other, the slope of the curves did remain consistent, indicating a uniform sensitivity or a uniform ohms/ohm change.

Figure 78 represents a consolidation of the statistical average of the response curves for vacuum deposited Cu-Ni-Zn versus Constantan at the mutual strain level of $\pm$ 2000 $\mu\varepsilon$. The Constantan response curve was constructed from data obtained from References 1 and 2 and then superimposed upon the graph of a typical response curve for the deposited sensor. The data in Figure 78 reflect at least a factor of four gain in sensitivity of the deposited material over that of annealed Constantan.

All the sensor curves for the specified load condition (Figs. 63 through 77) fell between the dotted boundary lines, and although this represents an undesirable "scatter," the statistical average of test data did indicate specific trends. These trends are itemized as follows:

1. The sensor did respond to the mean load level, i.e., the sensor output increased for an increase in mean strain level (cyclic amplitude constant) as shown in Figure 79.

2. The effects of repeated load occurrences were stored as a resistance change in the sensor. This change was permanent and did not drift with time.

3. The sensor response was insensitive to cyclic rate over the frequency test range of 5 to 30 cps.

4. Loading cycles in the compressive sense did promote a continued resistance increase, i.e., the cumulative resistance change produced by cycles in the tension direction was not "erased" by compression cycles.

A summary of test results is shown in Figures 79 through 81. Figures 79 and 80 indicate that the sensor has a mild response to the mean load level, i.e., the strain ratio producing the higher peak tensile strains actually promoted the larger resistance increase in the sensor. Figure 81 shows a family of curves for an averaged value of sensor output over a range of strain levels from $\pm$ 500 to $\pm$ 3000 $\mu\varepsilon$. When the overall performance of this material is evaluated in view of potential application to service aircraft, the test results justify further sensor development and evaluation in a practical application.

3.2.8.3 Sensor Installation Reliability

The miniature size and delicate appearance of the vacuum deposited sensor actually belies its installation simplicity. In fact, when consideration is given to prescribed precautionary measures (see Appendix II) the ease of sensor installation is comparable to that of a conventional strain gage. Probably the most critical step is the attachment of lead wires; however, with reasonable care and practice reliable attachments can be made. Once the sensor is bonded to the structure or other heat sink material, lead wires (34 gage or smaller) may be soldered directly to the solder pad of the sensor. Continuity checks or other resistance measurements of the sensor should not be attempted until the sensor is bonded to a heat sink because the current output of an ohmmeter, or conventional multimeters, will produce artificial aging of the unbonded thin film. The bonded thin film if not encapsulated, should be moistureproofed at once to prevent corrosion with time or stress. Additional installation details and precautionary measures are described in Appendix II of this document.

A relatively large number of tests over a wide variety of strain levels produced no bond failures or fatigue cracks in the single strand deposited film sensor. There was never any indication of the "supersensitivity" that was so pronounced in previous evaluations (Ref. 1) of the annealed Constantan type sensor. The response curve "hookup" behavior so familiar with annealed Constantan just prior to complete failure of the gage never occurred with the deposited Cu-Ni-Zn alloy. Although the fatigue life of the optimized sensor exceeded the fatigue life requirements shown by the lifeline of Figure 20, the sensor was never deliberately cycled to a fatigue failure. It was anticipated, however, that the sensor fatigue life would exceed that of the aluminum specimen. A solder connection failure did occur as evidenced by the erratic behavior shown in Figure 58. The sensor solder joints were visually examined after the completion of 10^6 cycles and confirmed as a fatigue fracture of the joint.

The only other sensor damage that occurred resulted from installing the specimen in the test equipment. Sensor evaluation at negative strain ratios required the use of lateral support plates to prevent specimen bending. Sensor lead wire required an exit through a window cutout of the support plates, as shown in Figure 42. Interferences occasionally produced damage to the lead wire or solder joint.

Since most of the sensor testing occurred within a three months time span the long term (10 - 15 years) stability of the sensor was not established. The sensor resistance was periodically sampled over this period for drift, however, none was noted. It was generally concluded that the installation reliability of the sensor is comparable to that of a strain gage installation.

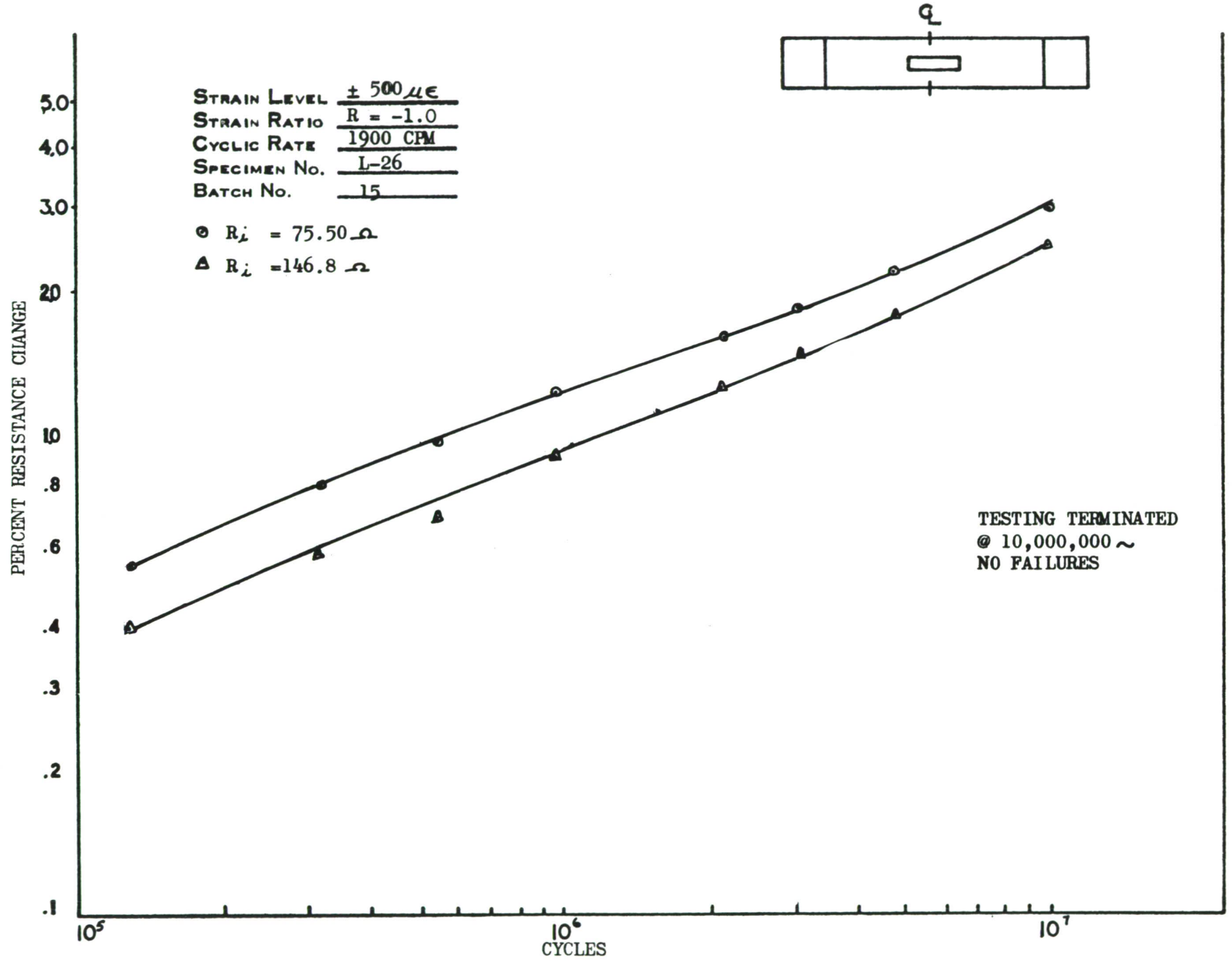

FIGURE 54. FATIGUE SENSOR RESPONSE FOR VACUUM DEPOSITED CU-NI-ZN. SPECIMEN L-26, BATCH 15

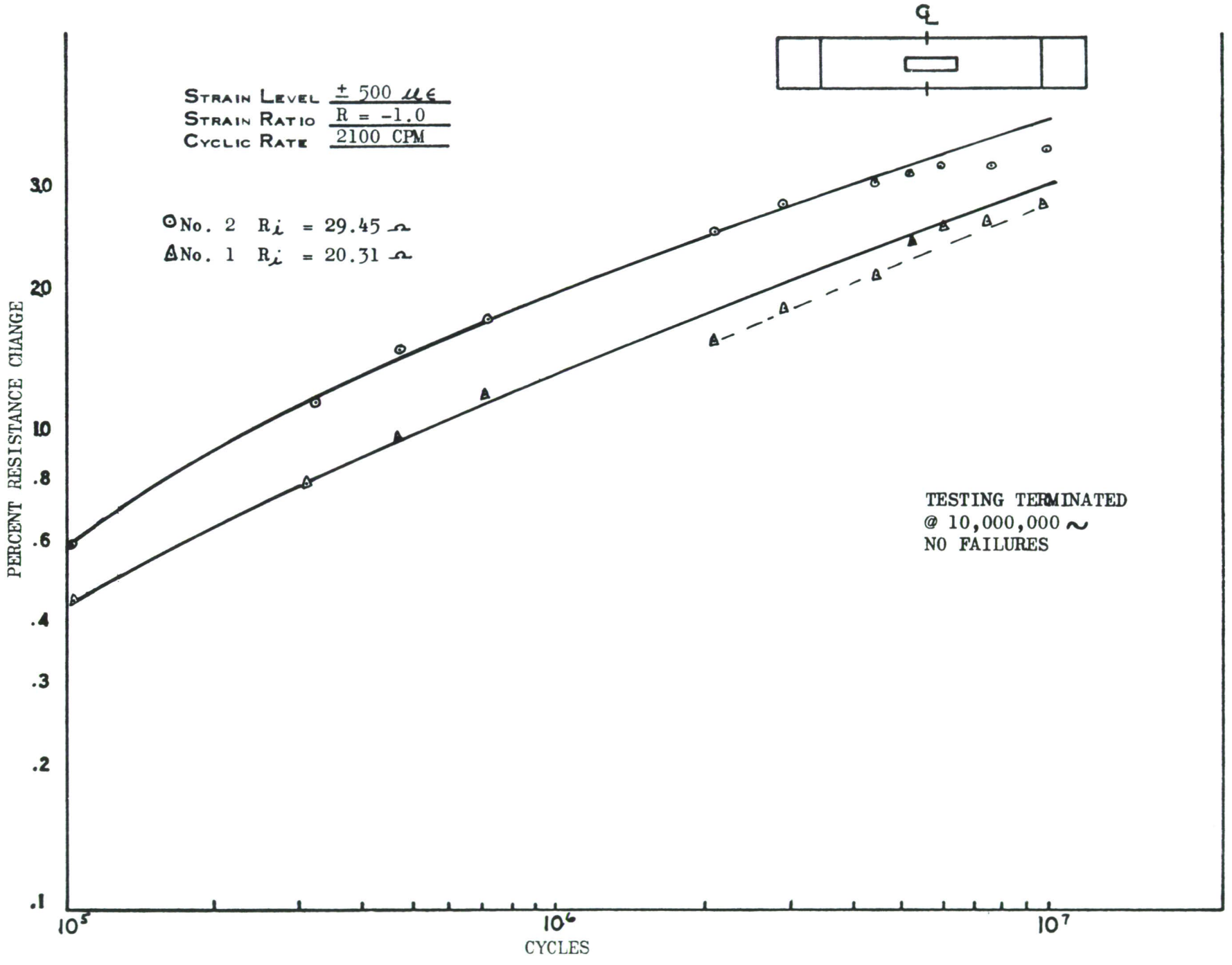

FIGURE 55. FATIGUE SENSOR RESPONSE FOR VACUUM DEPOSITED CU-NI-ZN, SPECIMEN L-14, BATCH 10

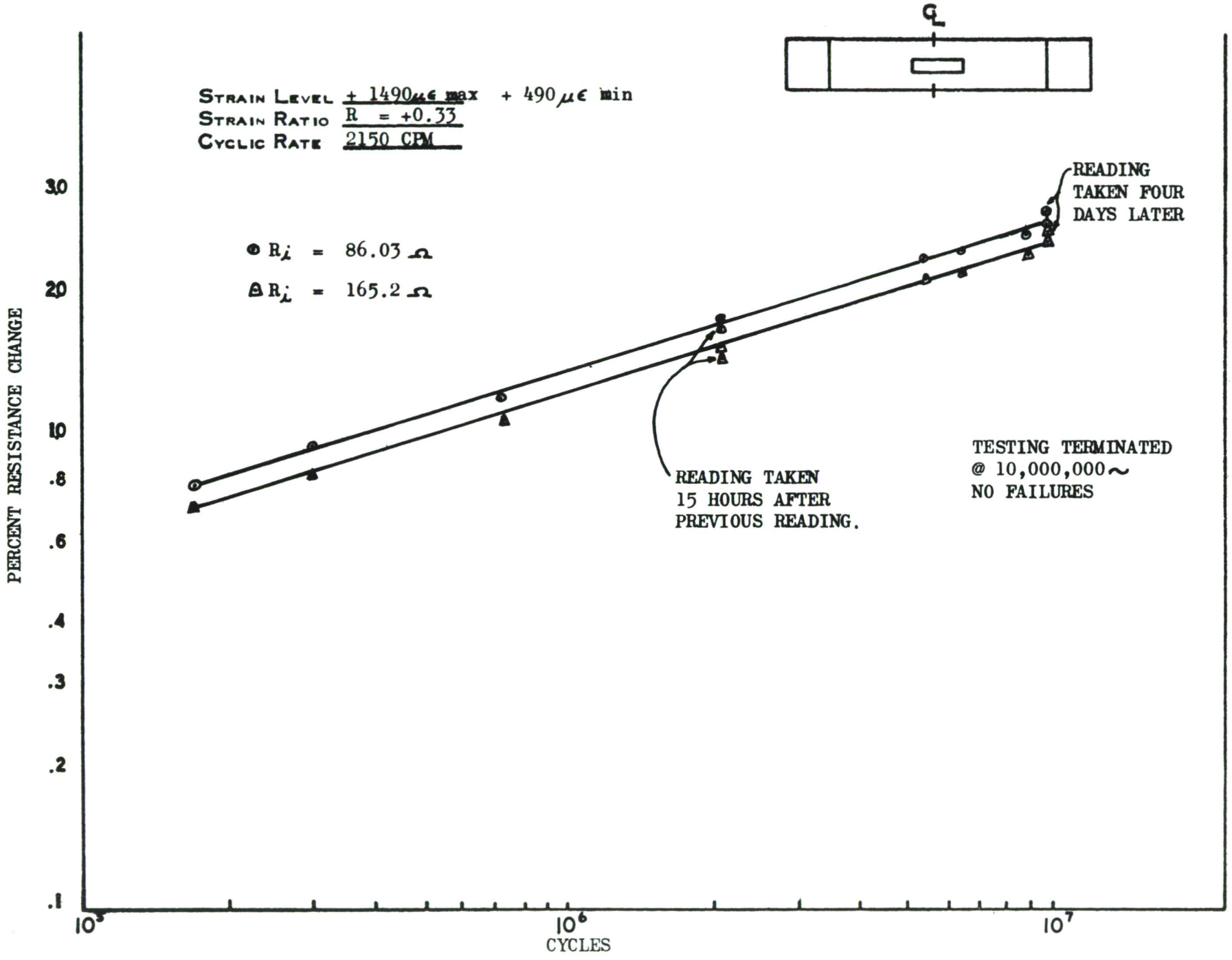

FIGURE 56. FATIGUE SENSOR RESPONSE FOR VACUUM DEPOSITED CU-NI-ZN, SPECIMEN L-34, BATCH 15

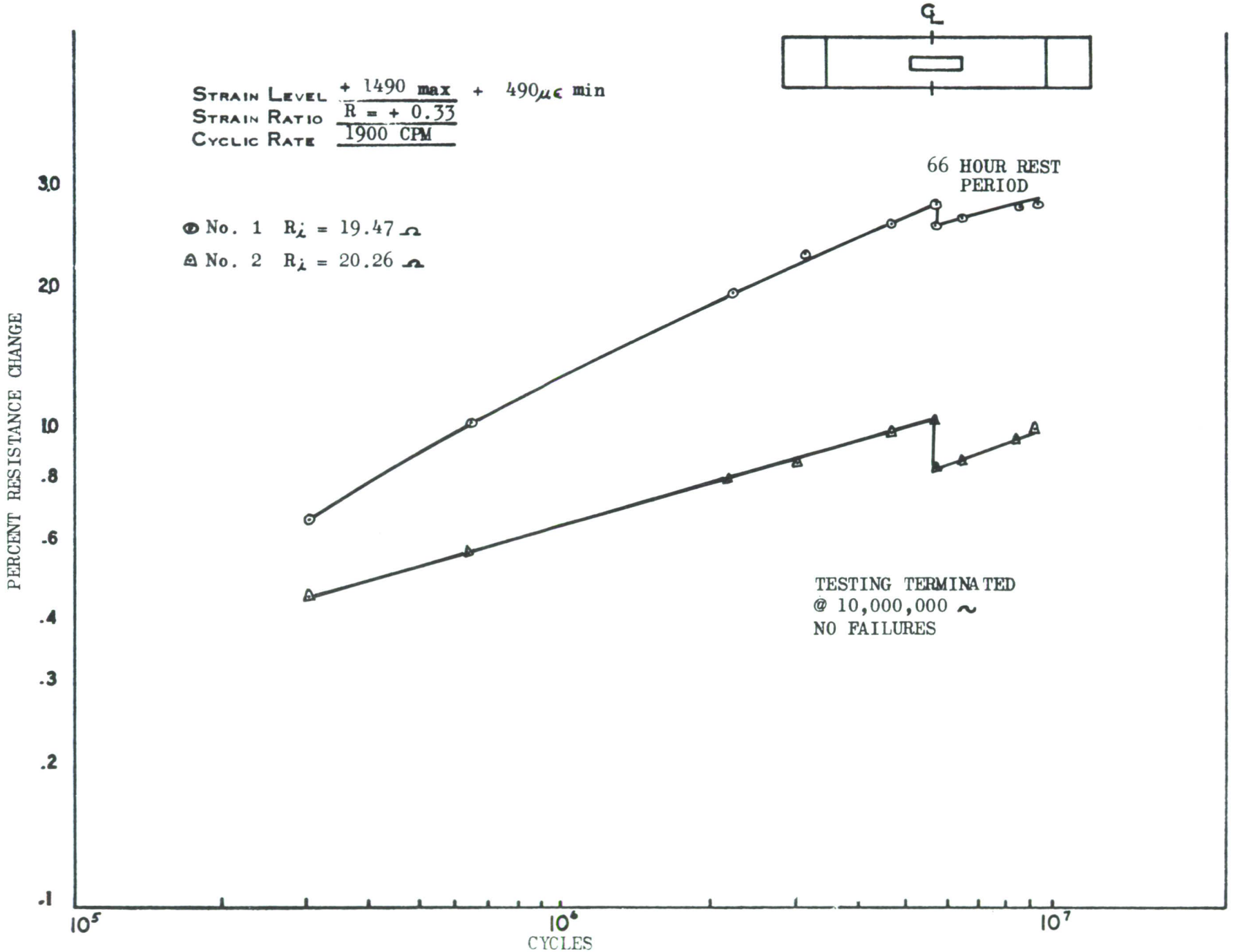

FIGURE 57. FATIGUE SENSOR RESPONSE OF VACUUM DEPOSITED CU-NI-ZN, SPECIMEN L-13, BATCH 10

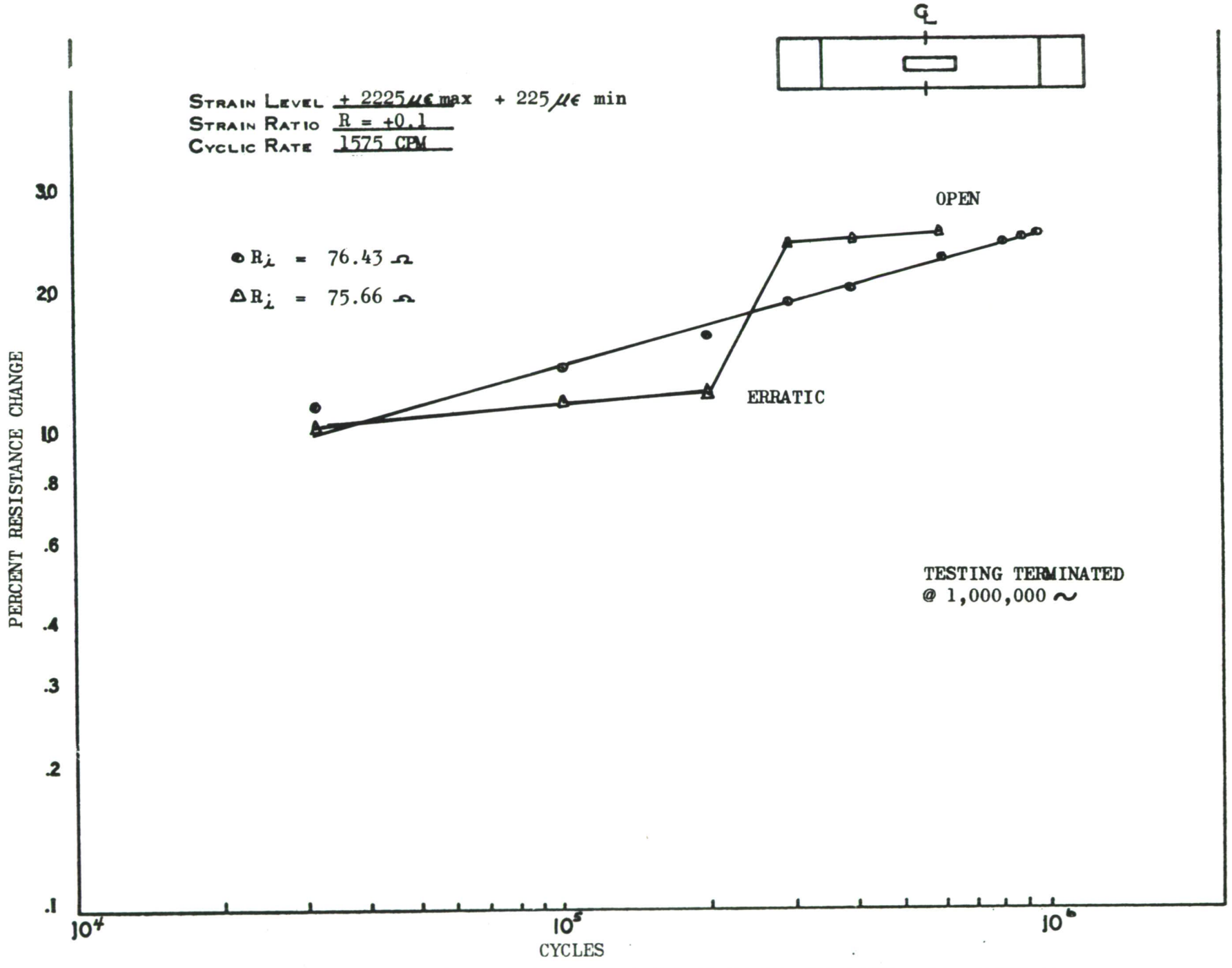

FIGURE 58. FATIGUE SENSOR RESPONSE OF VACUUM DEPOSITED CU-NI-ZN, SPECIMEN L-29, BATCH 17

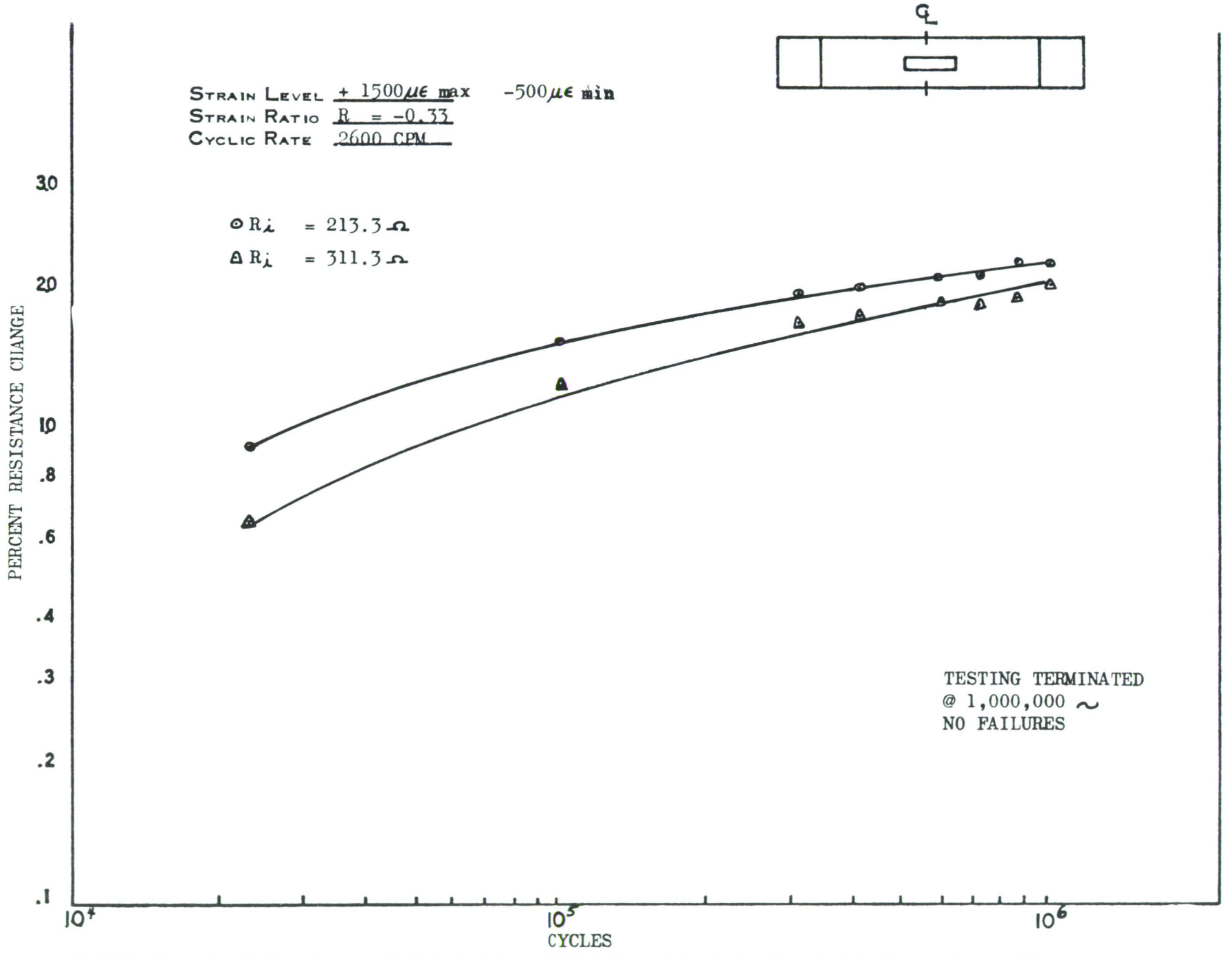

FIGURE 59. FATIGUE SENSOR RESPONSE FOR VACUUM DEPOSITED CU-NI-ZN, SPECIMEN L-25, BATCH 17

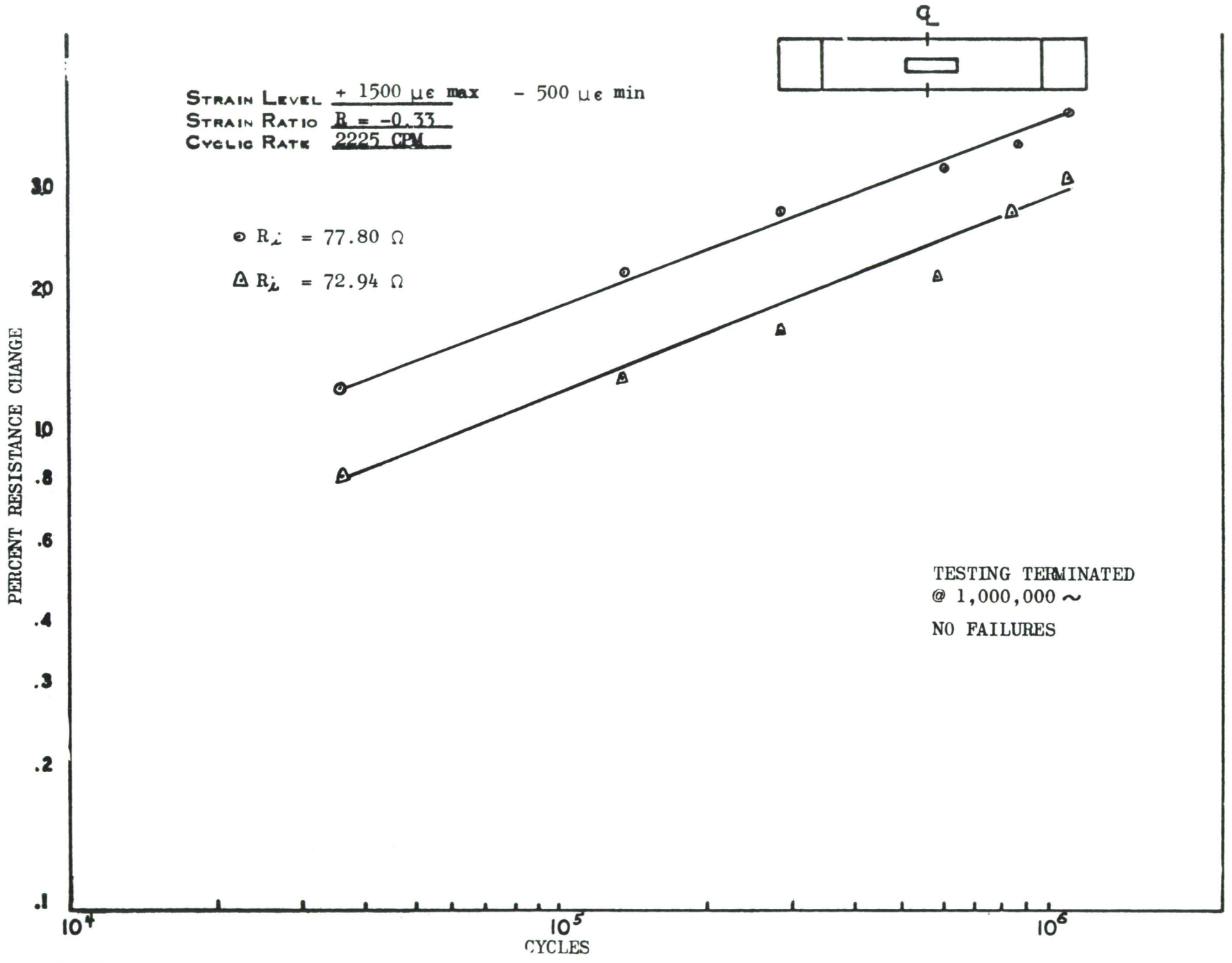

FIGURE 60. FATIGUE SENSOR RESPONSE FOR VACUUM DEPOSITED CU-NI-ZN, SPECIMEN L-14, BATCH 19

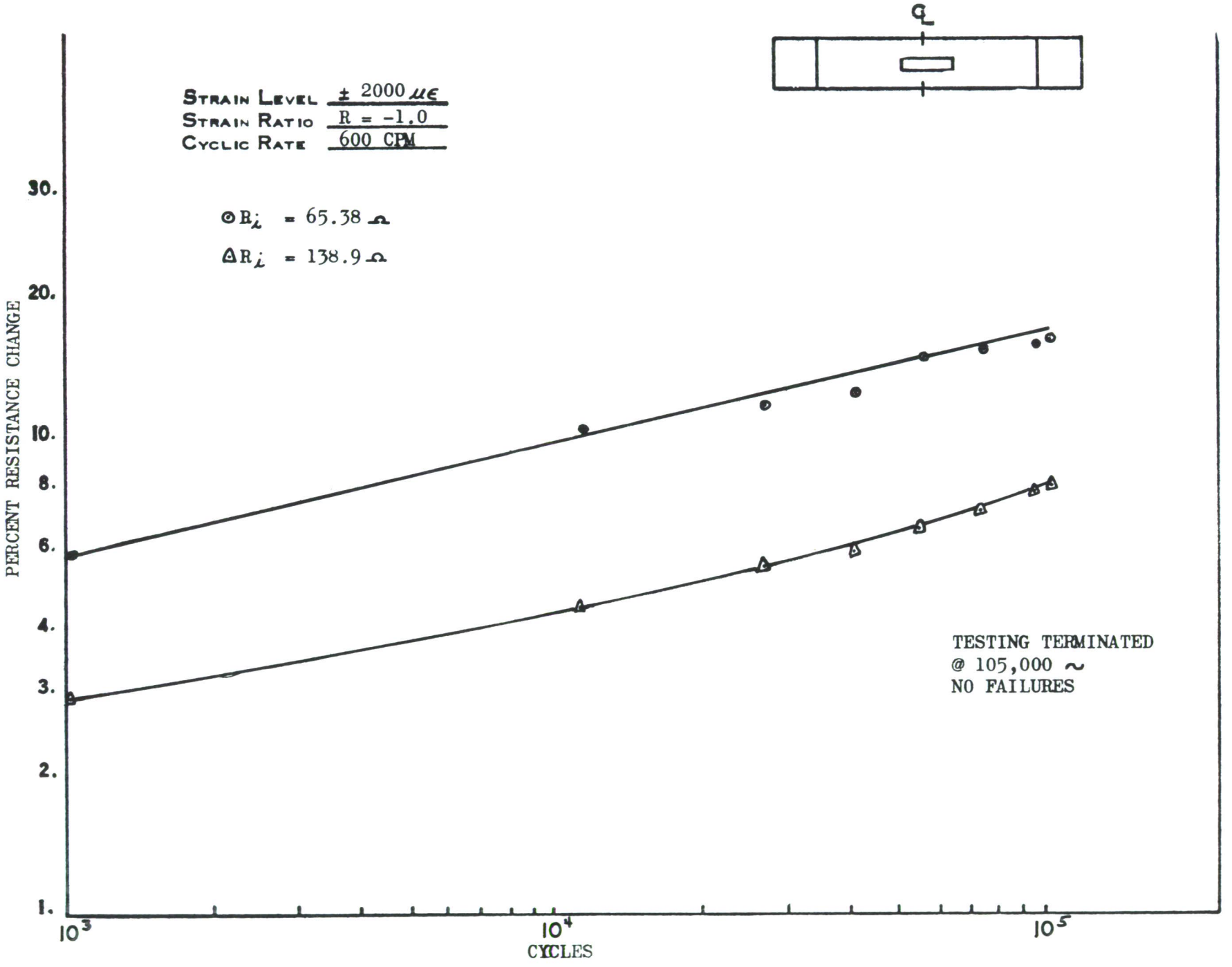

FIGURE 61 FATIGUE SENSOR RESPONSE FOR VACUUM DEPOSITED CU-NI-ZN, SPECIMEN L-31, BATCH 17

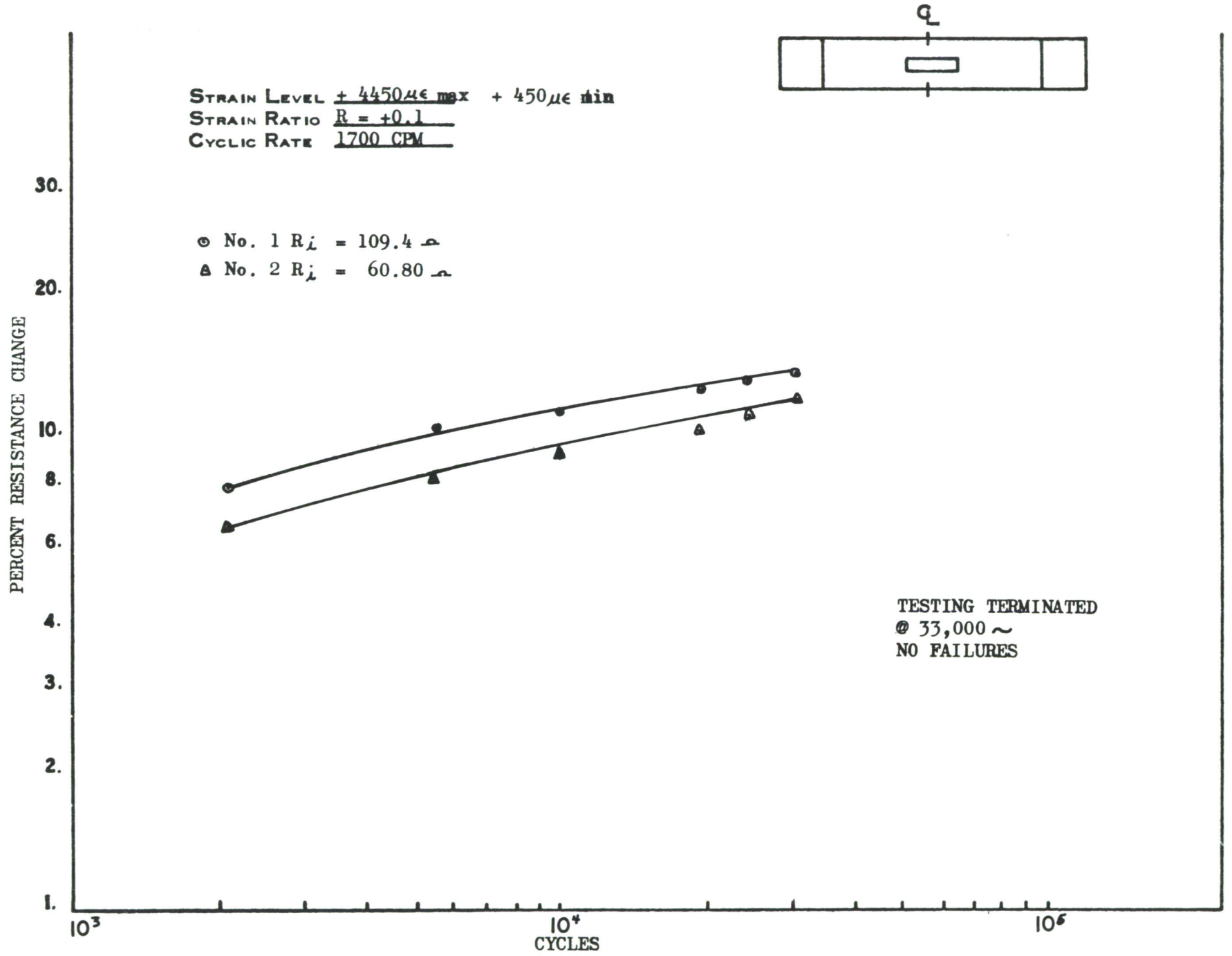

FIGURE 62. FATIGUE SENSOR RESPONSE FOR VACUUM DEPOSITED CU-NI-ZN, SPECIMEN L-43, BATCH 17

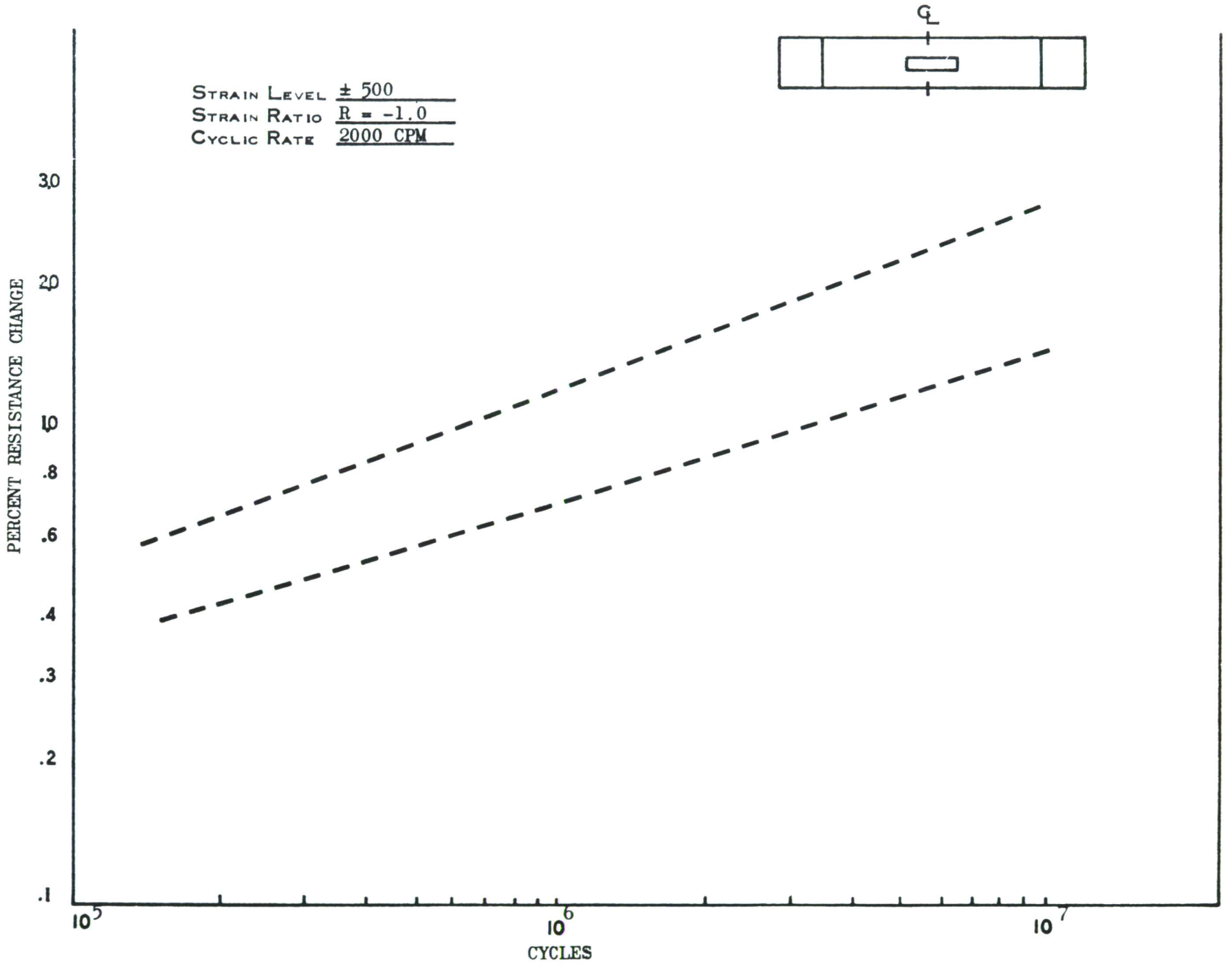

FIGURE 63. FATIGUE SENSOR RESPONSE FOR VACUUM DEPOSITED CU-NI-ZN SPECIMENS L-26 AND L-14 CONSOLIDATED CURVES.

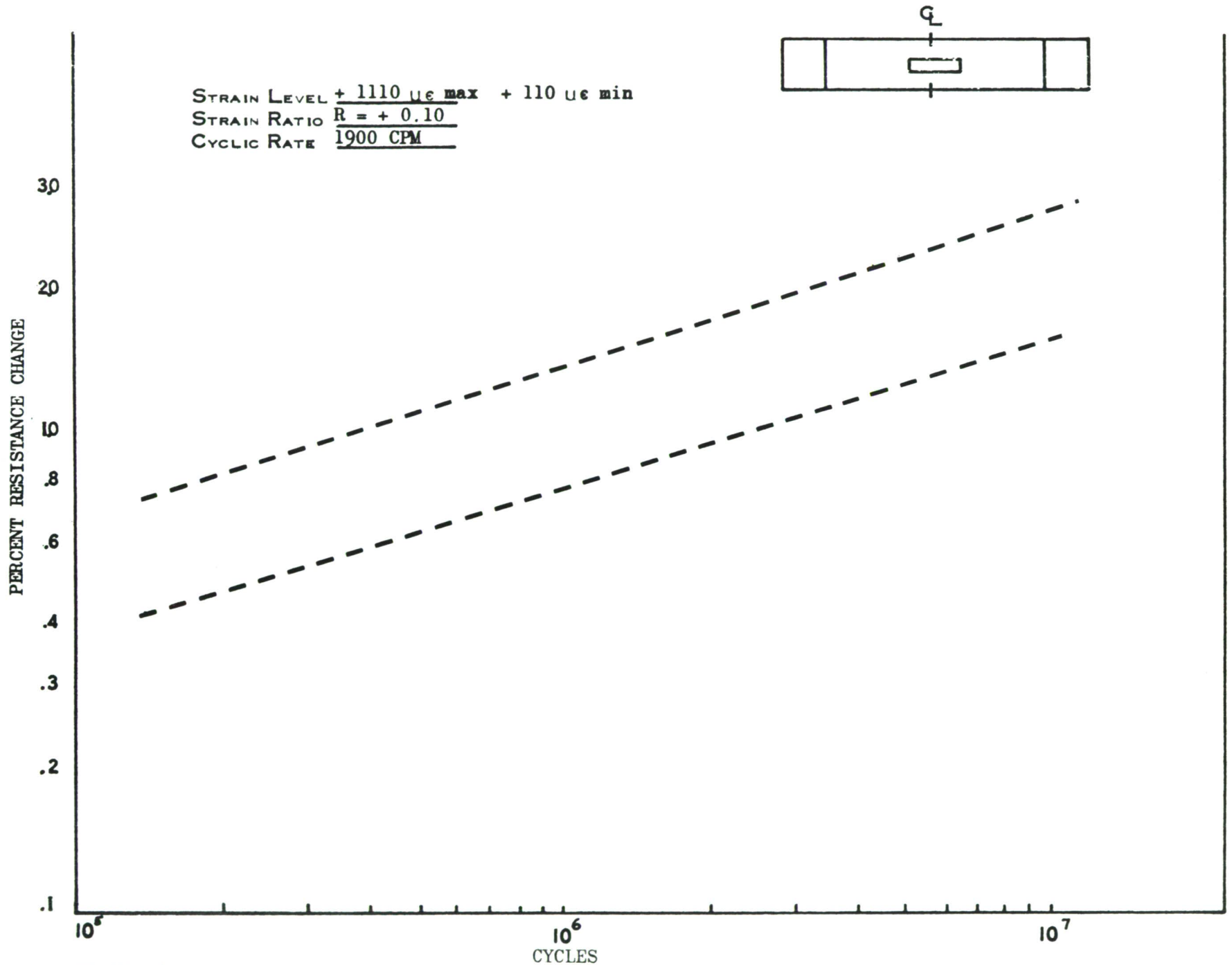

FIGURE 64. FATIGUE SENSOR RESPONSE OF VACUUM DEPOSITED CU-NI-ZN, CONSOLIDATED CURVES

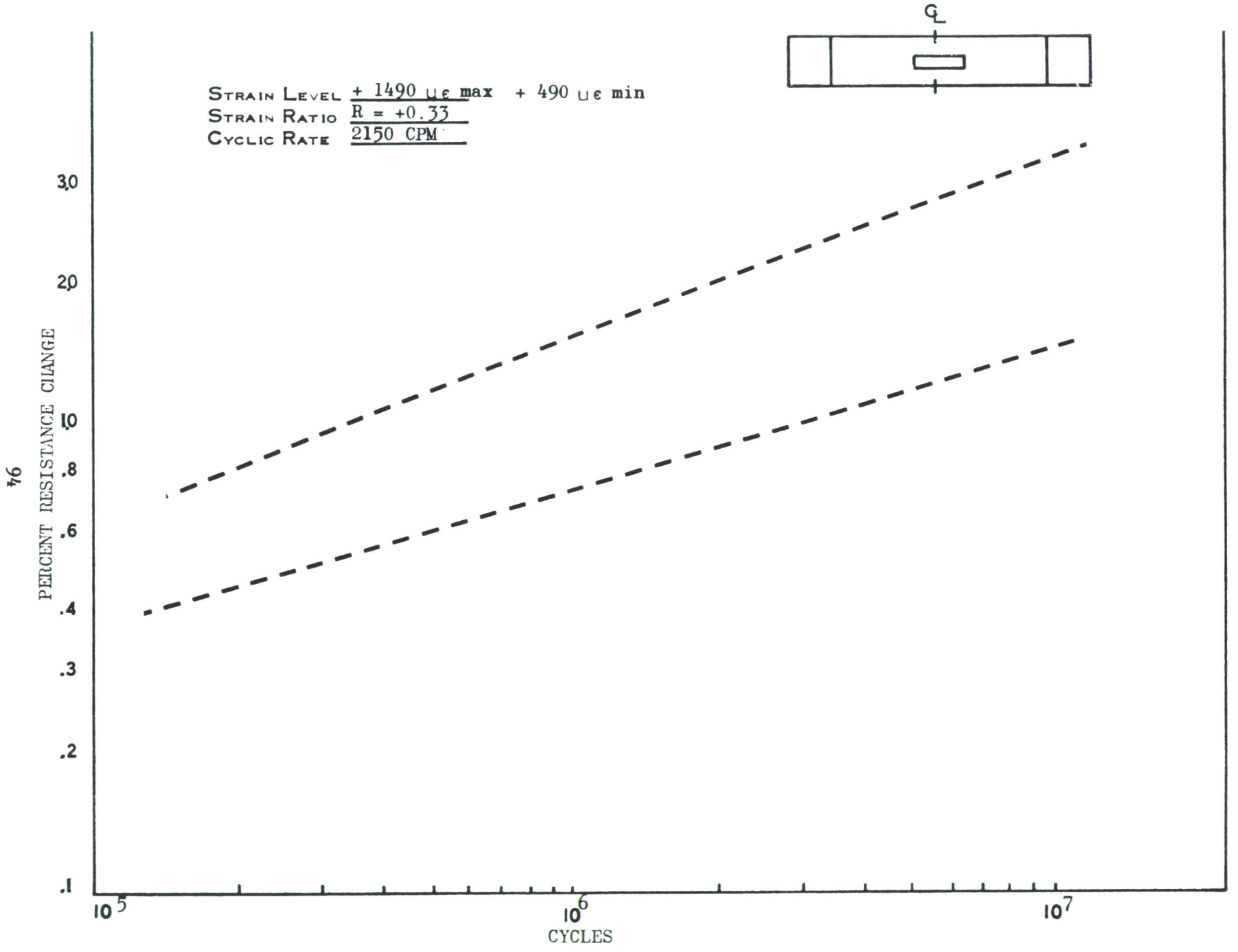

FIGURE 65. FATIGUE SENSOR RESPONSE FOR VACUUM DEPOSITED CU-NI-ZN, CONSOLIDATED CURVES

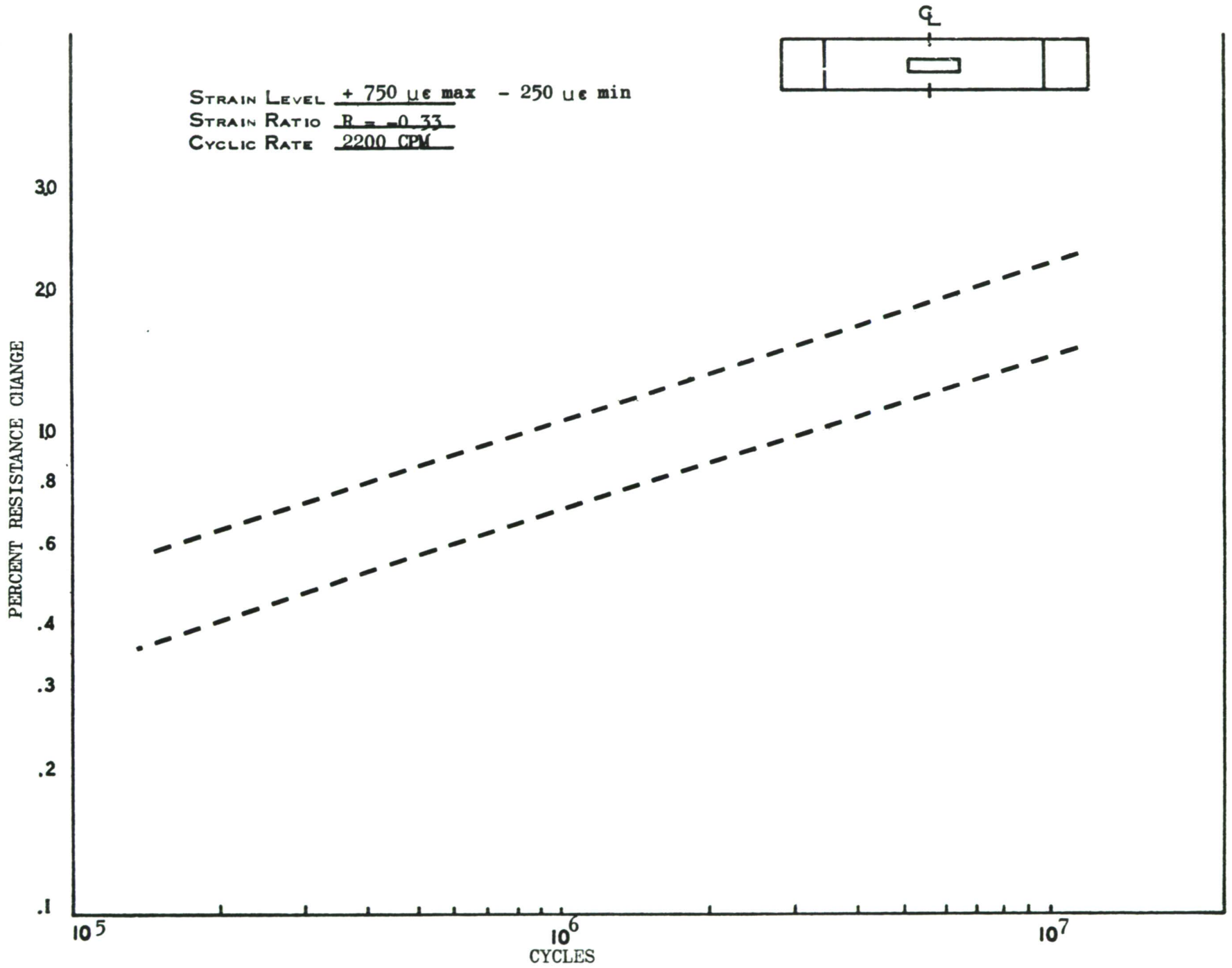

FIGURE 66. FATIGUE SENSOR RESPONSE FOR VACUUM DEPOSITED CU-NI-ZN, CONSOLIDATED CURVES

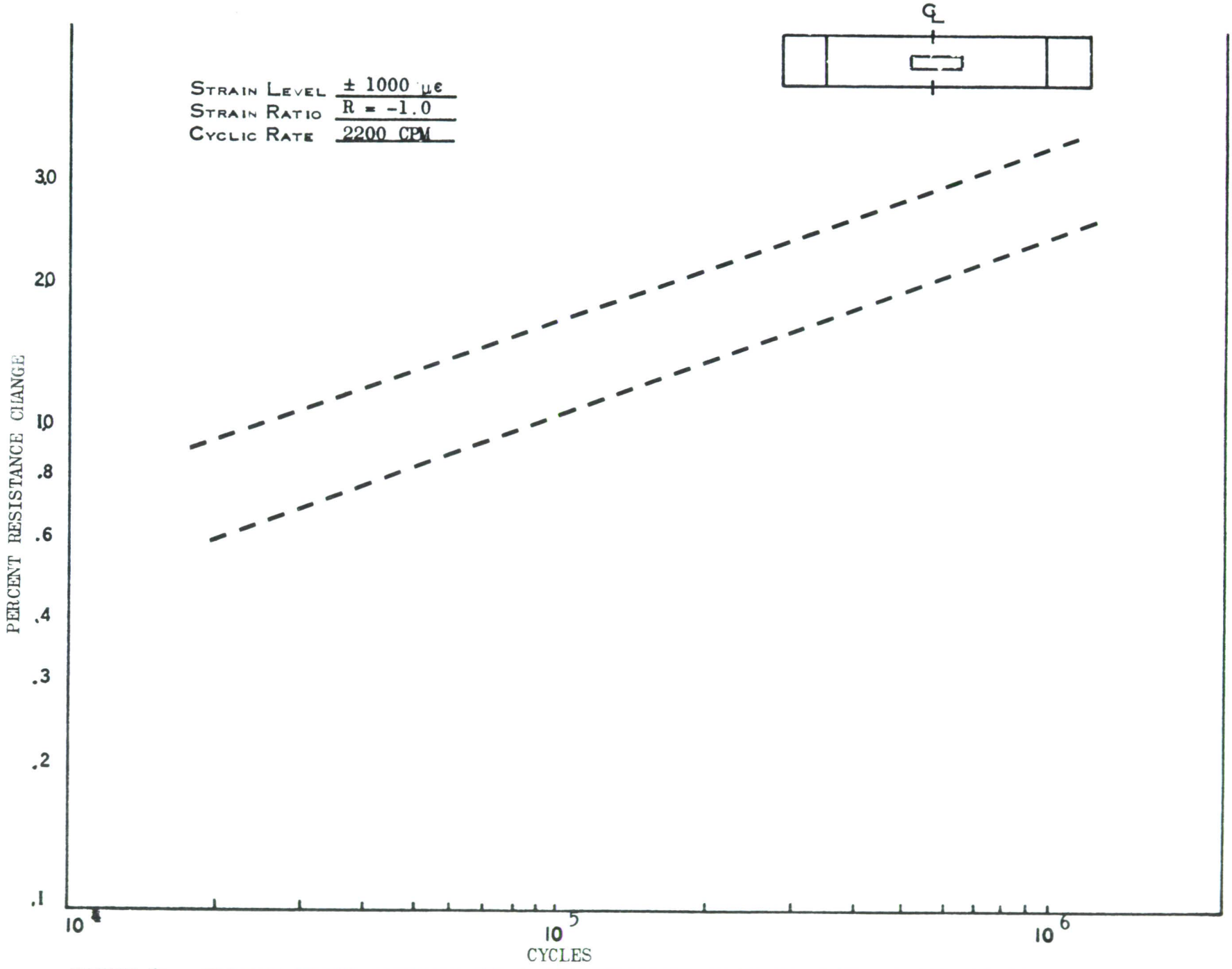

FIGURE 67. FATIGUE SENSOR RESPONSE FOR VACUUM DEPOSITED CU-NI-ZN, CONSOLIDATED CURVES

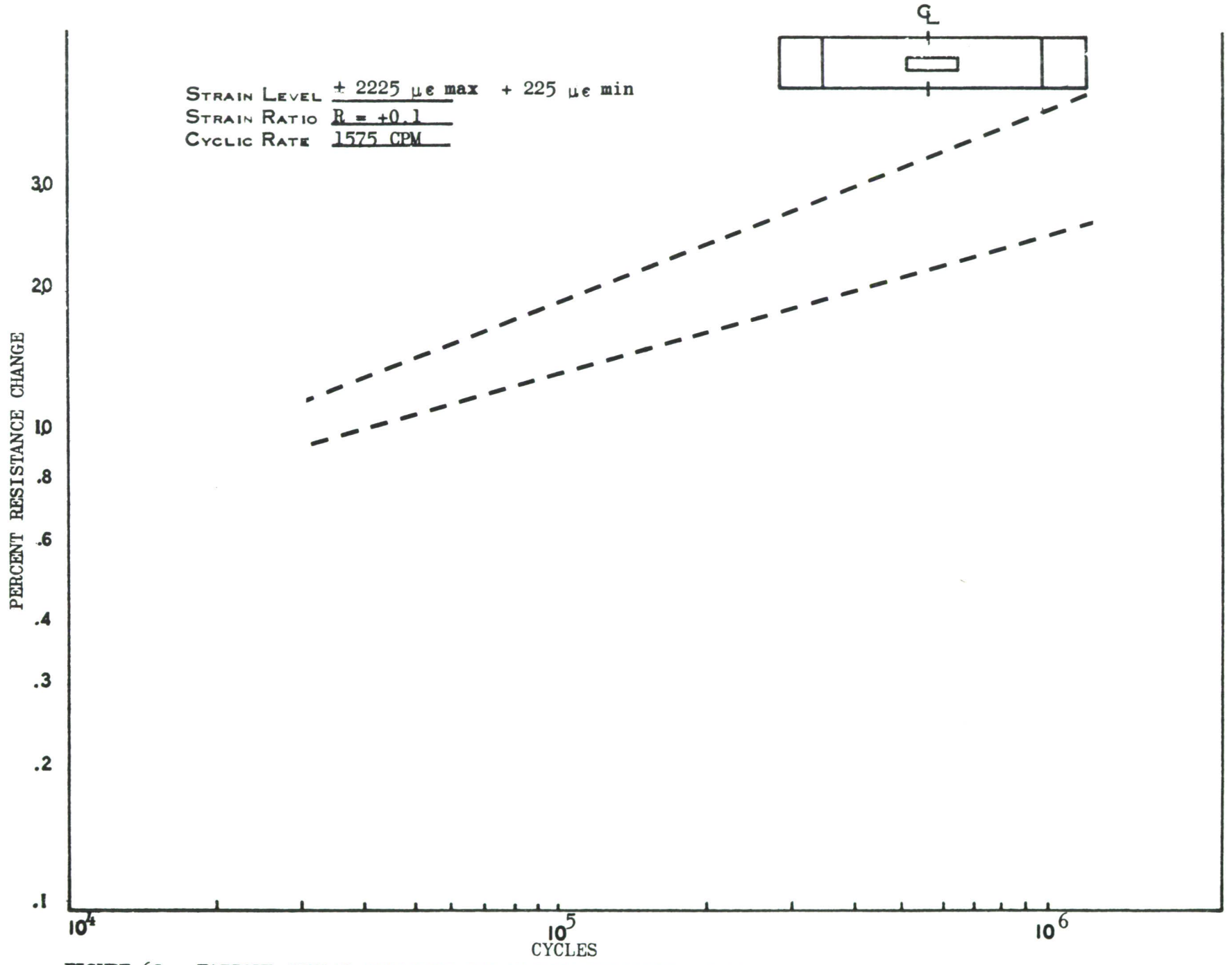

FIGURE 68. FATIGUE SENSOR RESPONSE FOR VACUUM DEPOSITED CU-NI-ZN, CONSOLIDATED CURVES

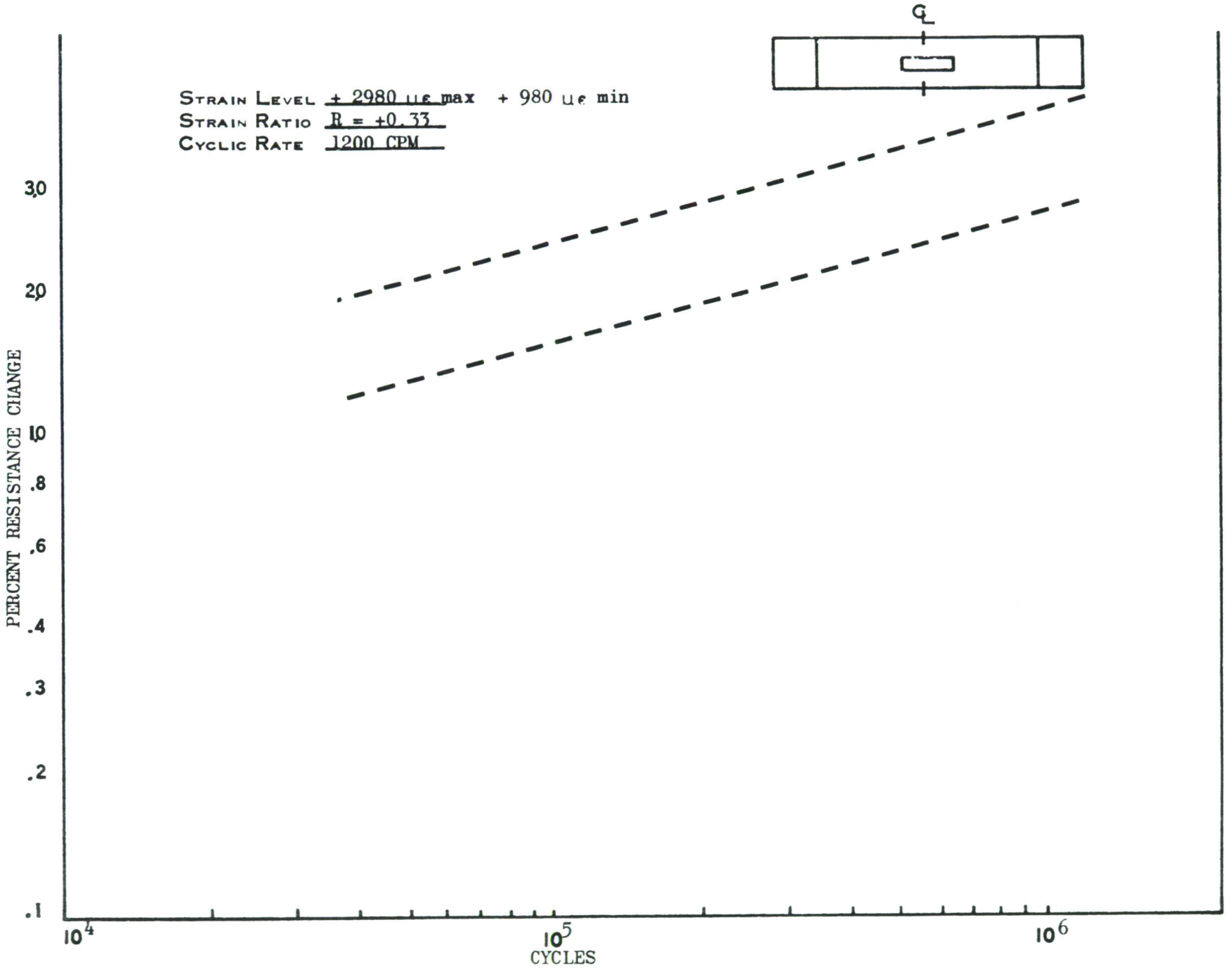

FIGURE 69. FATIGUE SENSOR RESPONSE FOR VACUUM DEPOSITED CU-NI-ZN, CONSOLIDATED CURVES

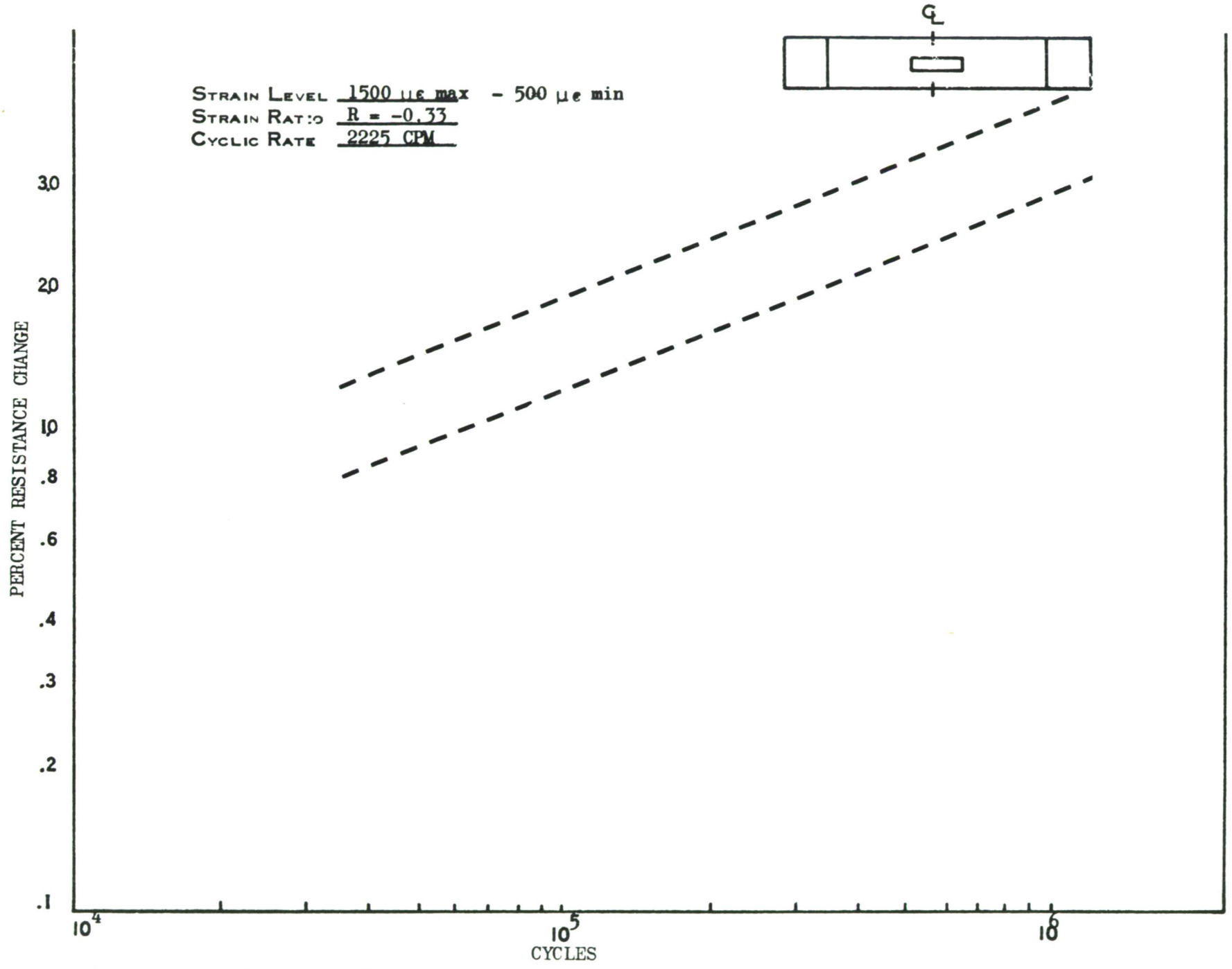

FIGURE 70. FATIGUE SENSOR RESPONSE FOR VACUUM DEPOSITED CU-NI-ZN, CONSOLIDATED CURVES

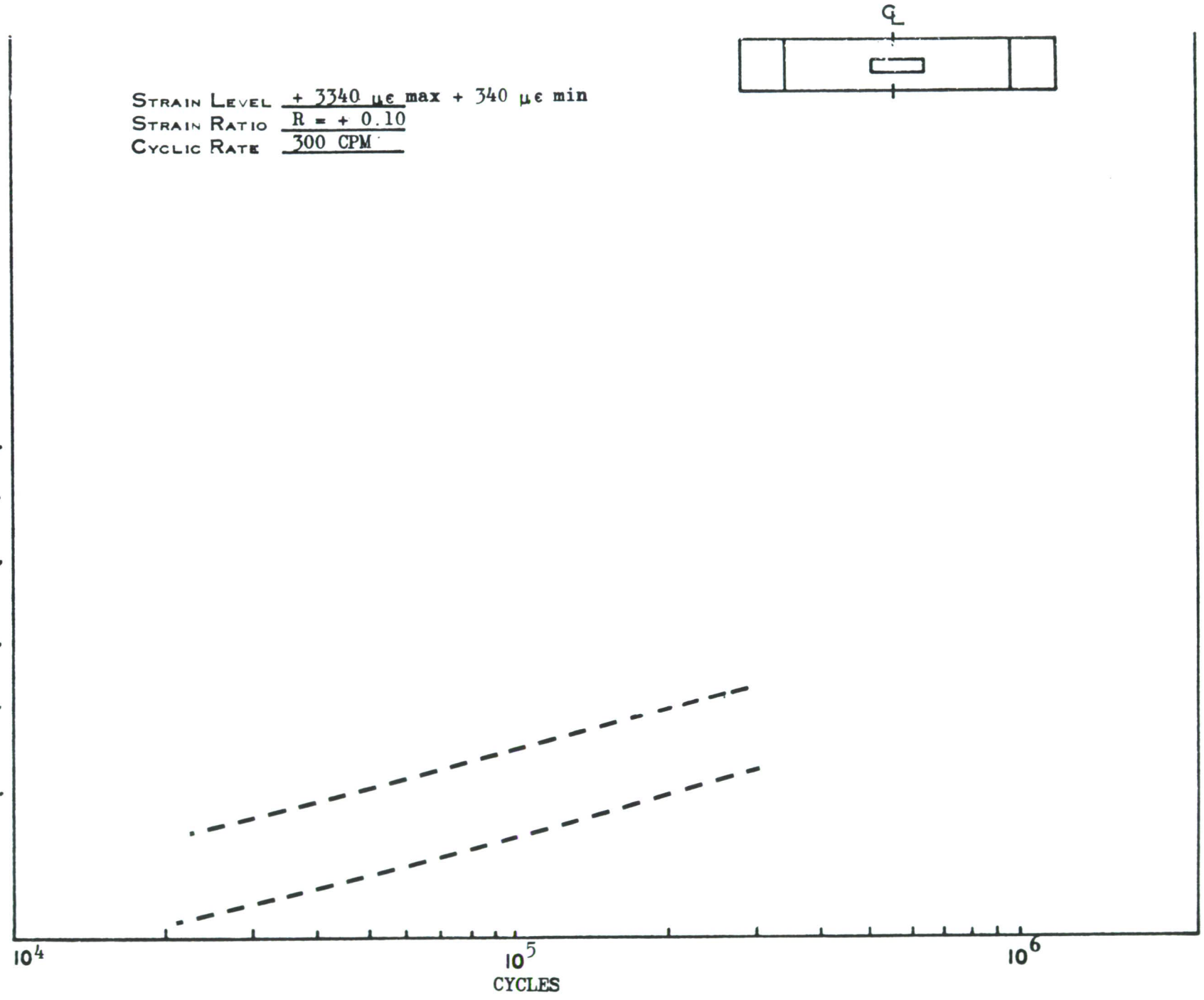

FIGURE 71. FATIGUE SENSOR RESPONSE FOR VACUUM DEPOSITED CU-NI-ZN, CONSOLIDATED CURVES

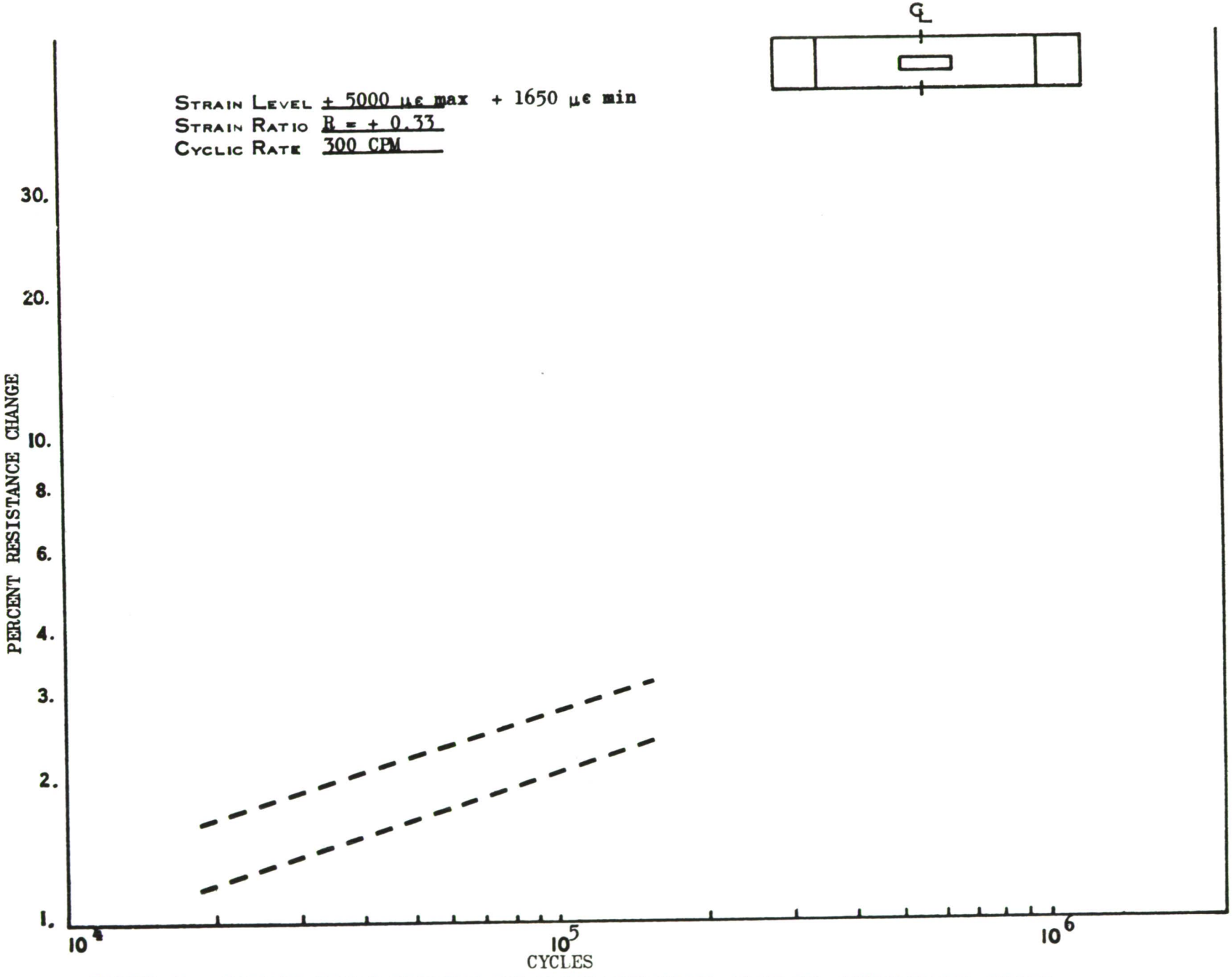

FIGURE 72. FATIGUE SENSOR RESPONSE FOR VACUUM DEPOSITED CU-NI-ZN, CONSOLIDATED CURVES

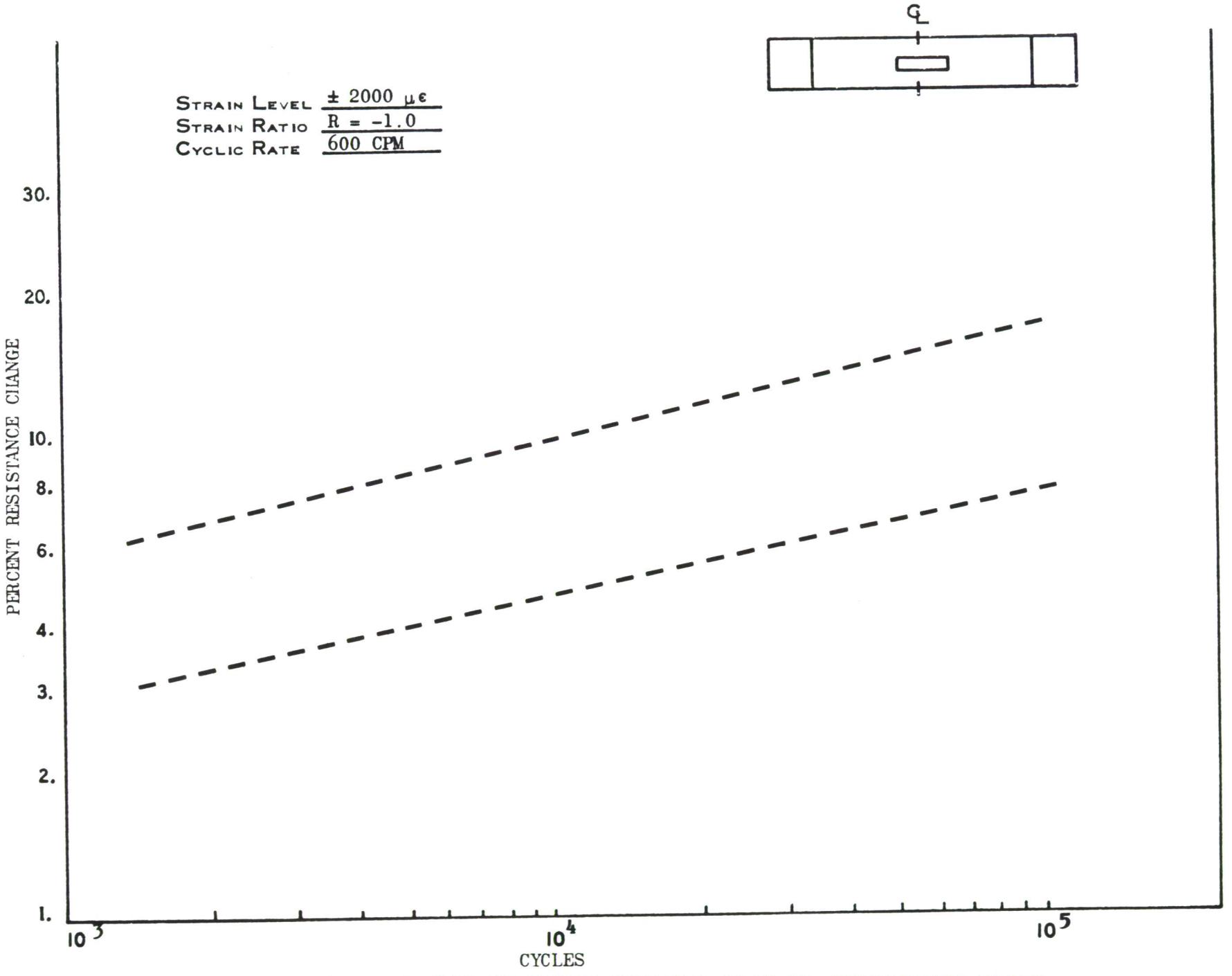

FIGURE 73. FATIGUE SENSOR RESPONSE FOR VACUUM DEPOSITED CU-NI-ZN, CONSOLIDATED CURVES

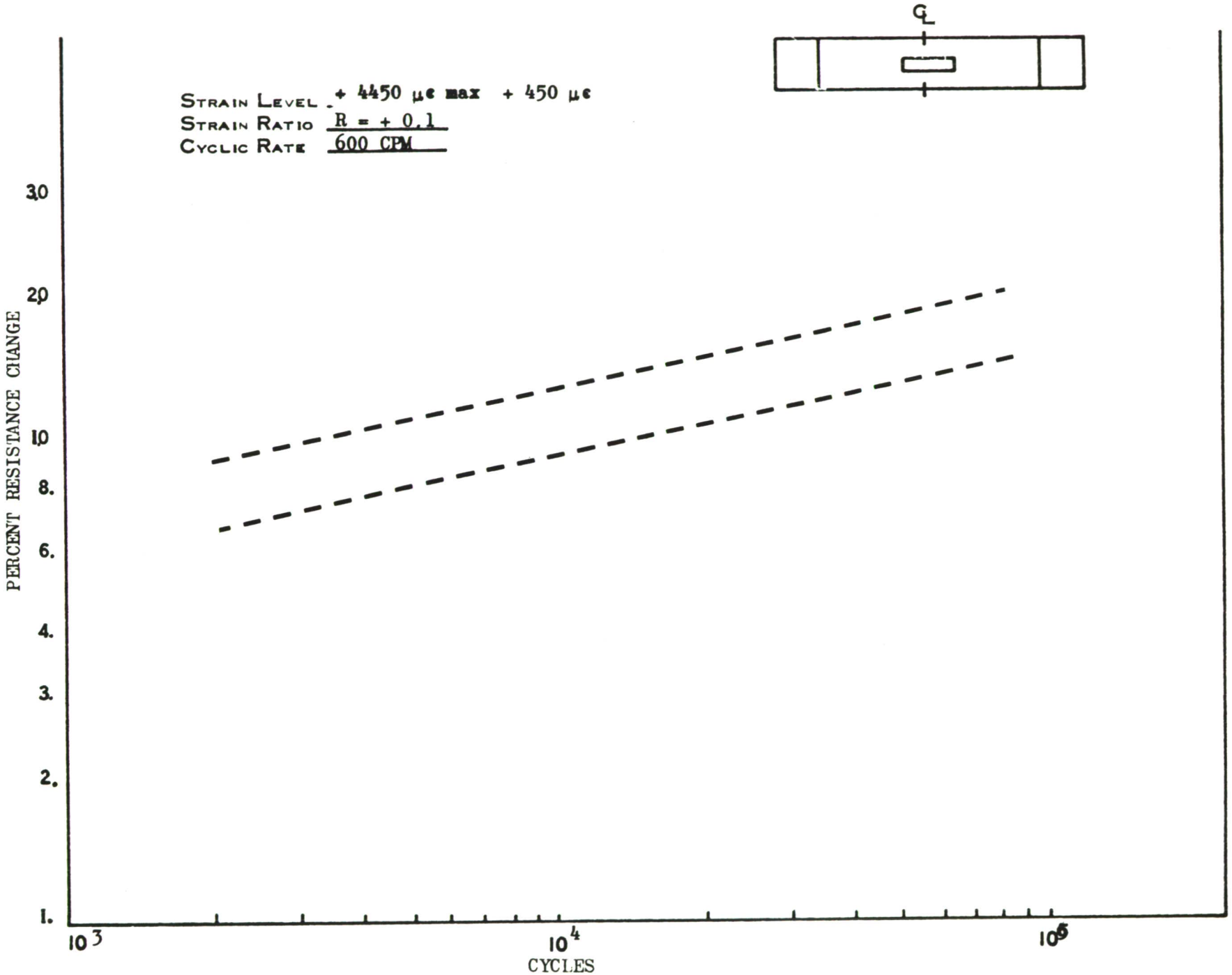

FIGURE 74. FATIGUE SENSOR RESPONSE FOR VACUUM DEPOSITED CU-NI-ZN, CONSOLIDATED CURVES

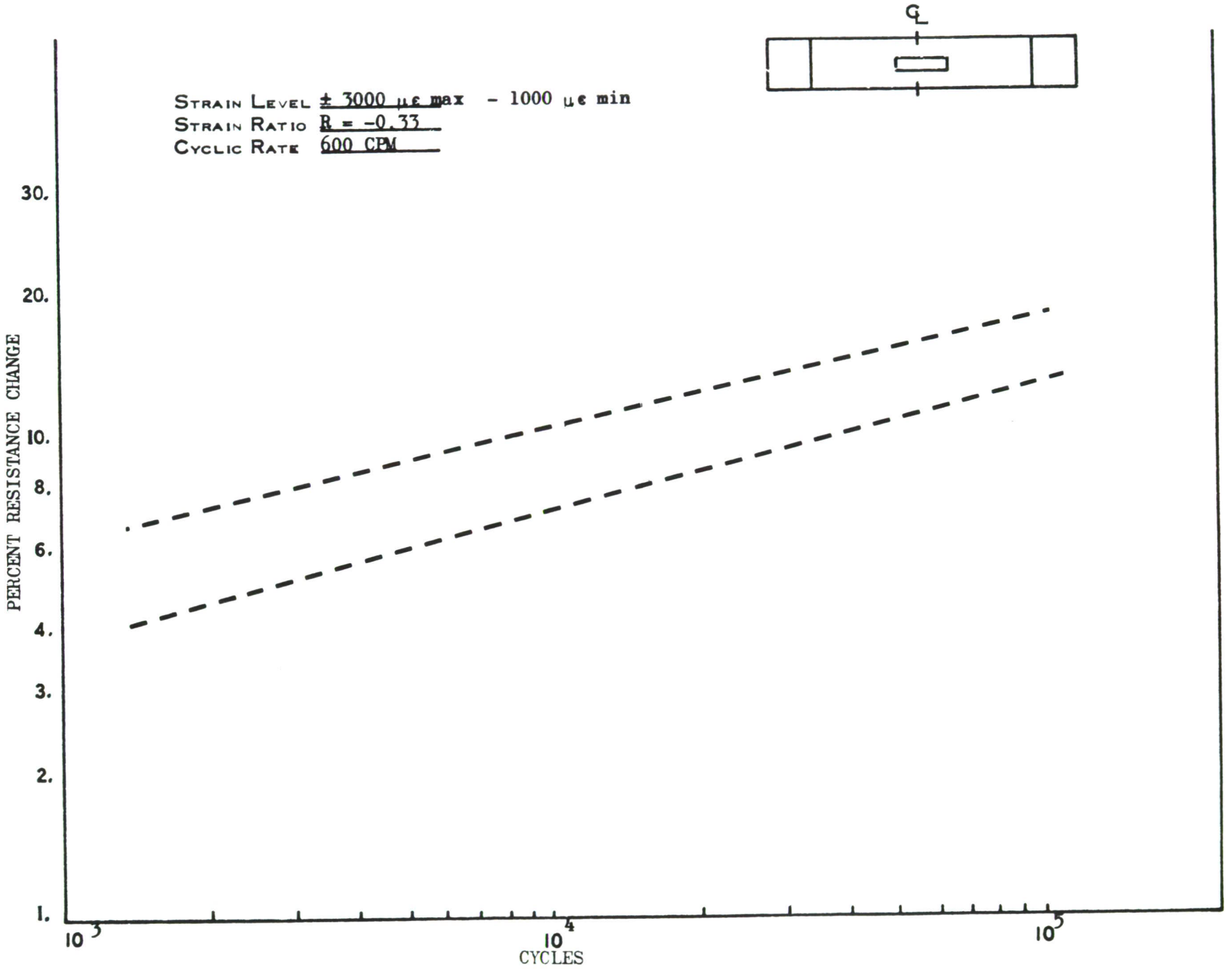

FIGURE 75. FATIGUE SENSOR RESPONSE FOR VACUUM DEPOSITED CU-NI-ZN, CONSOLIDATED CURVES

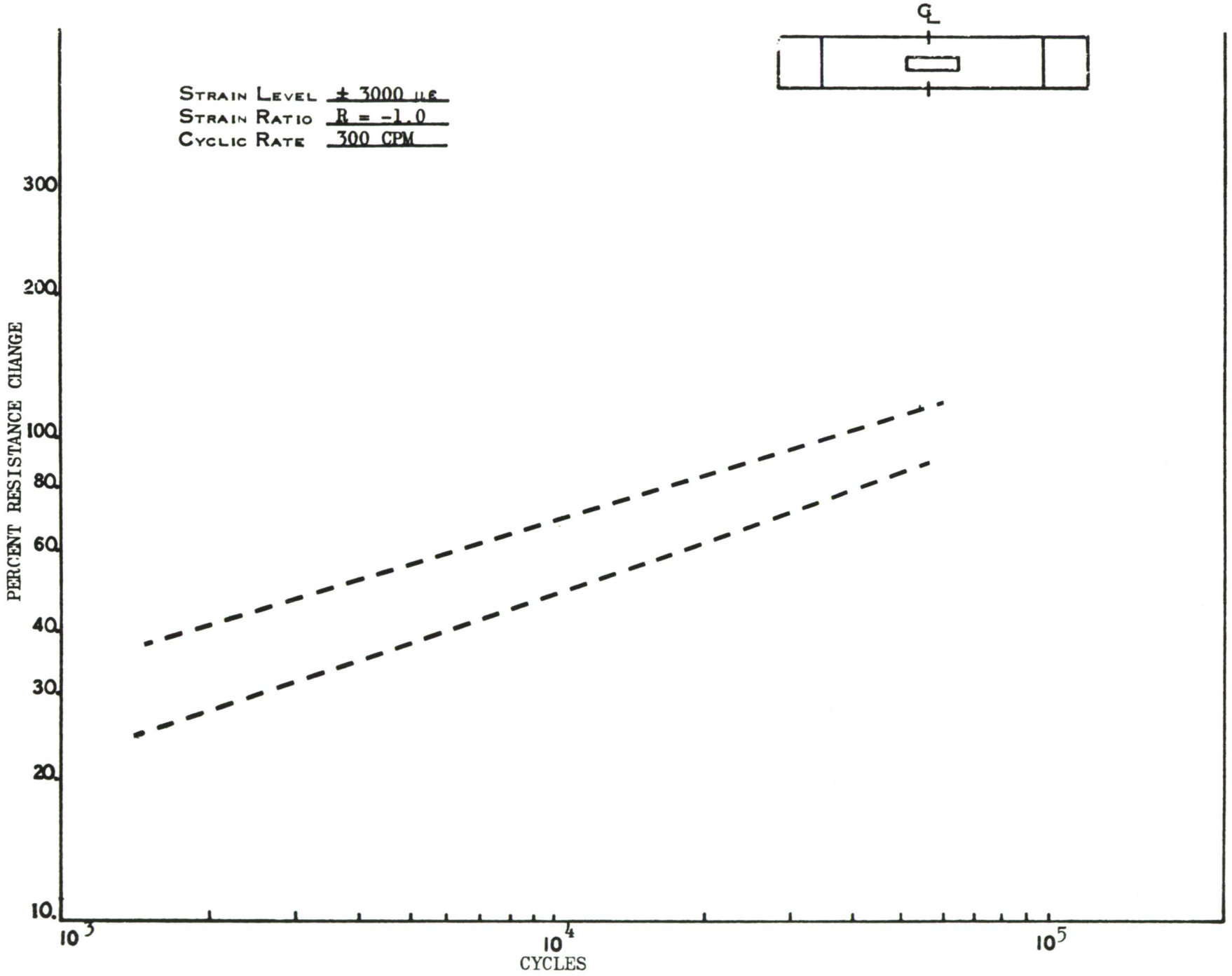

FIGURE 76. FATIGUE SENSOR RESPONSE FOR VACUUM DEPOSITED CU-NI-ZN, CONSOLIDATED CURVES

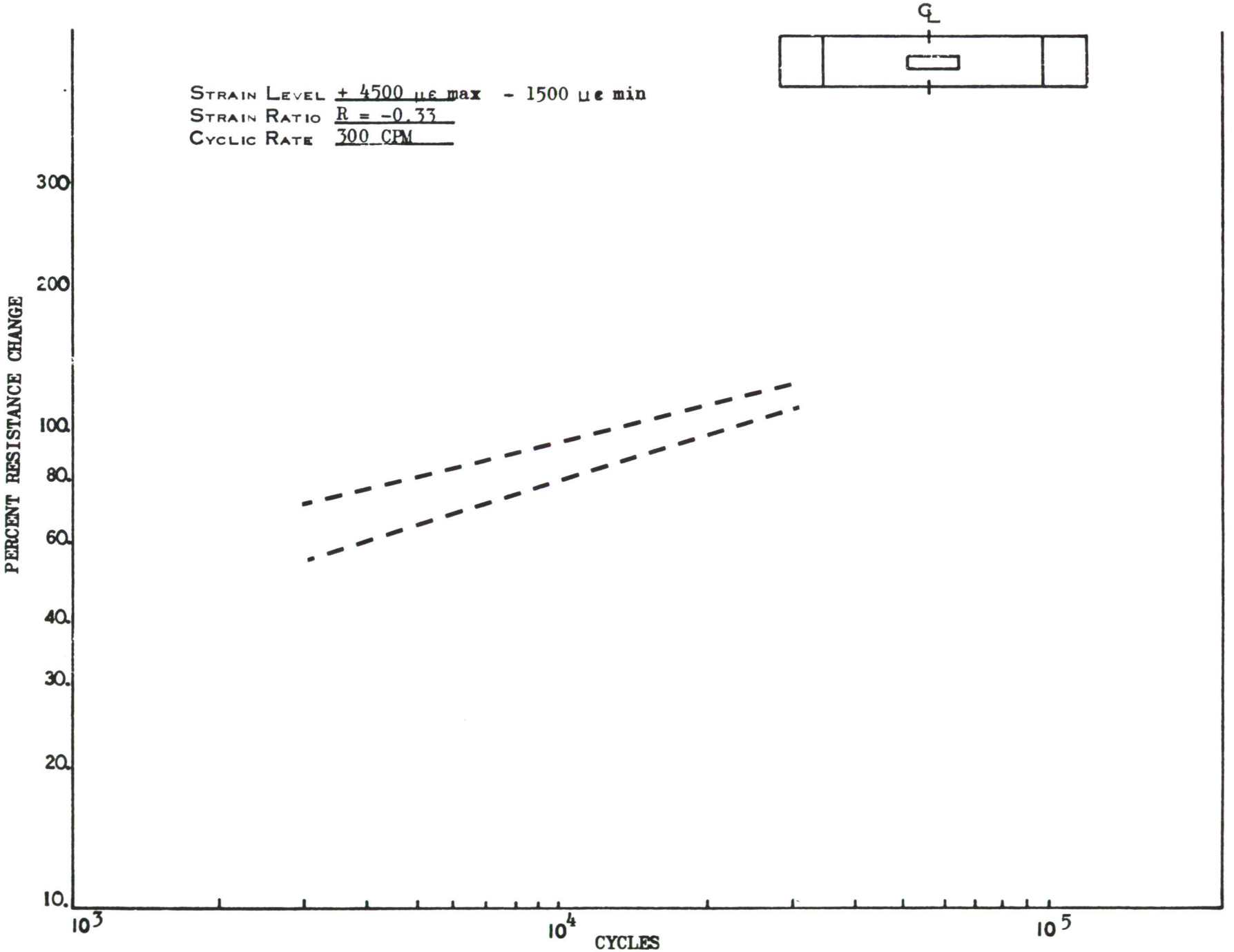

FIGURE 77. FATIGUE SENSOR RESPONSE FOR VACUUM DEPOSITED CU-NI-ZN, CONSOLIDATED CURVES

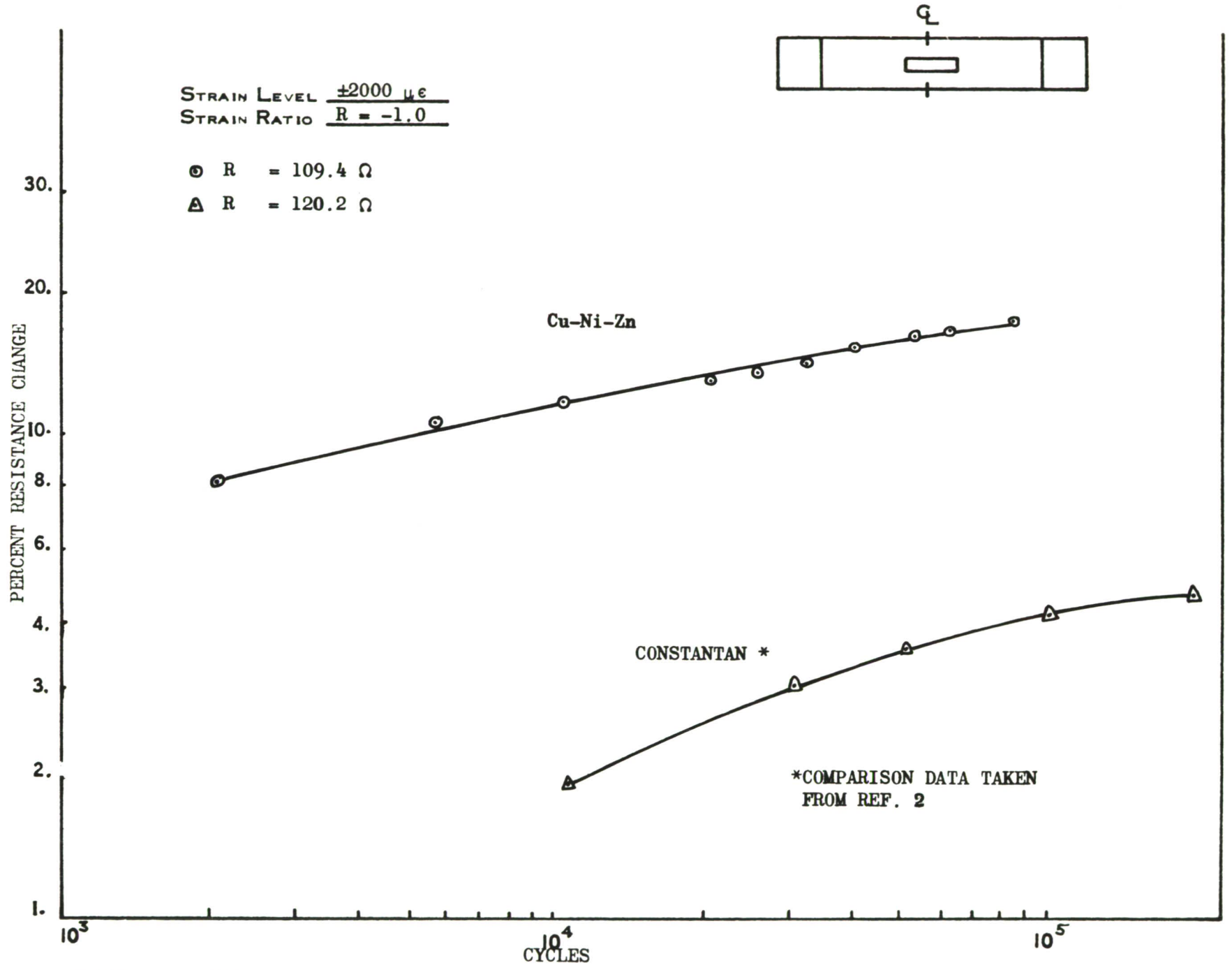

FIGURE 78. FATIGUE SENSOR RESPONSE FOR VACUUM DEPOSITED CU-NI-ZN VS ANNEALED CONSTANTAN, CONSOLIDATED

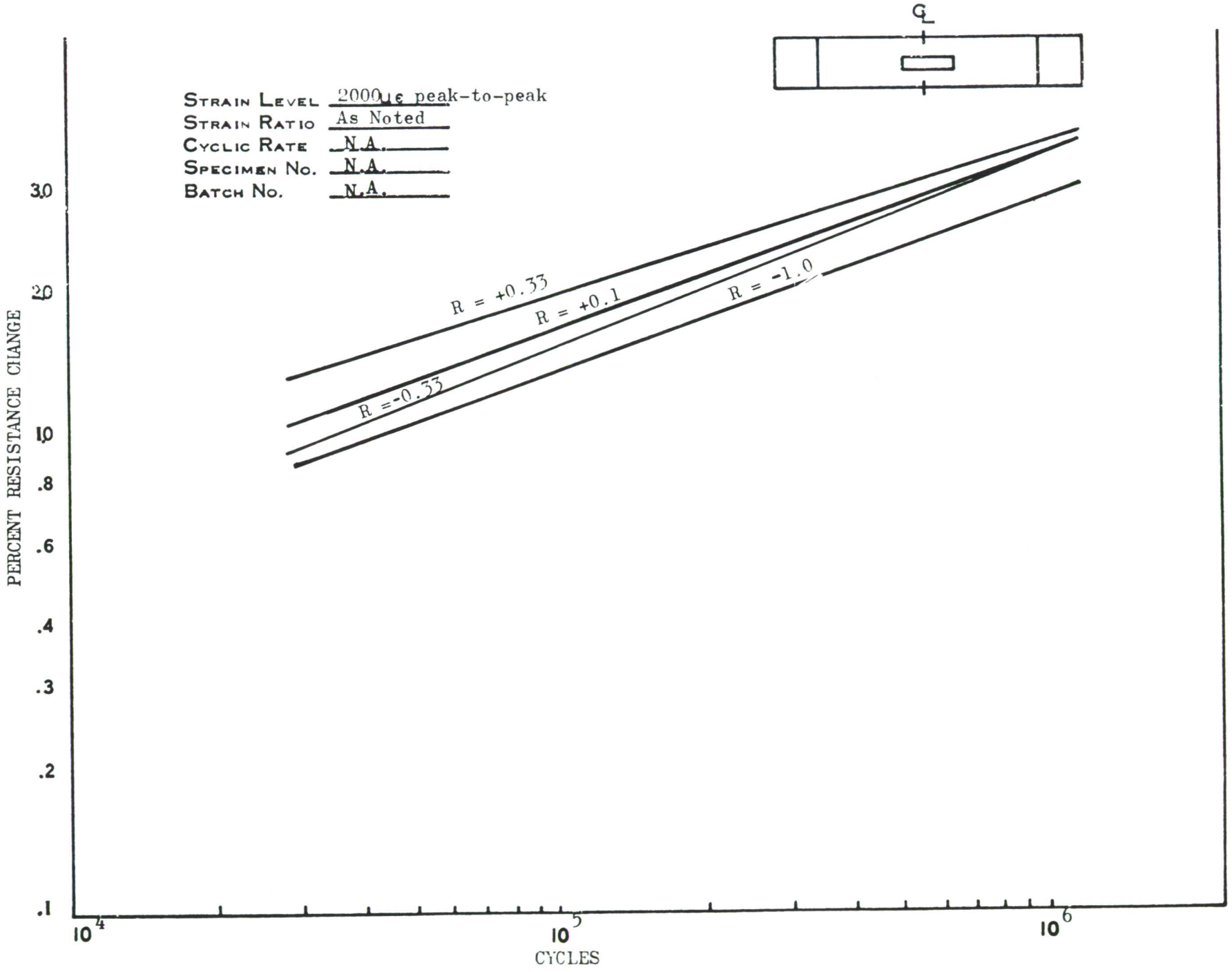

FIGURE 79. FATIGUE SENSOR RESPONSE FOR VACUUM DEPOSITED CU-NI-ZN SHOWING EFFECT OF VARIOUS STRAIN RATIOS, CONSOLIDATED CURVES

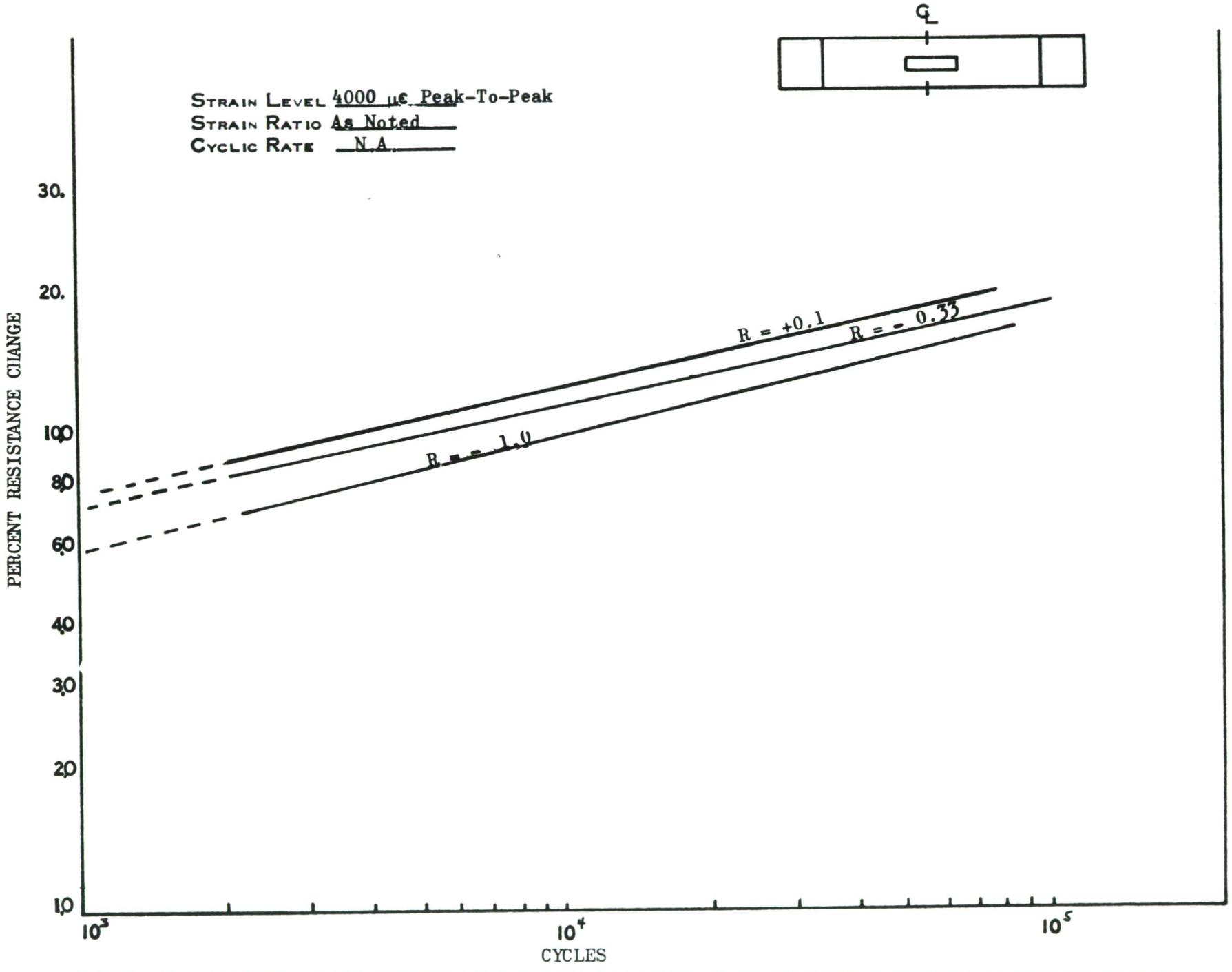

FIGURE 80. FATIGUE SENSOR RESPONSE FOR VACUUM DEPOSITED CU-NI-ZN SHOWING EFFECTS OF VARIOUS STRAIN RATIOS, CONSOLIDATED CURVES

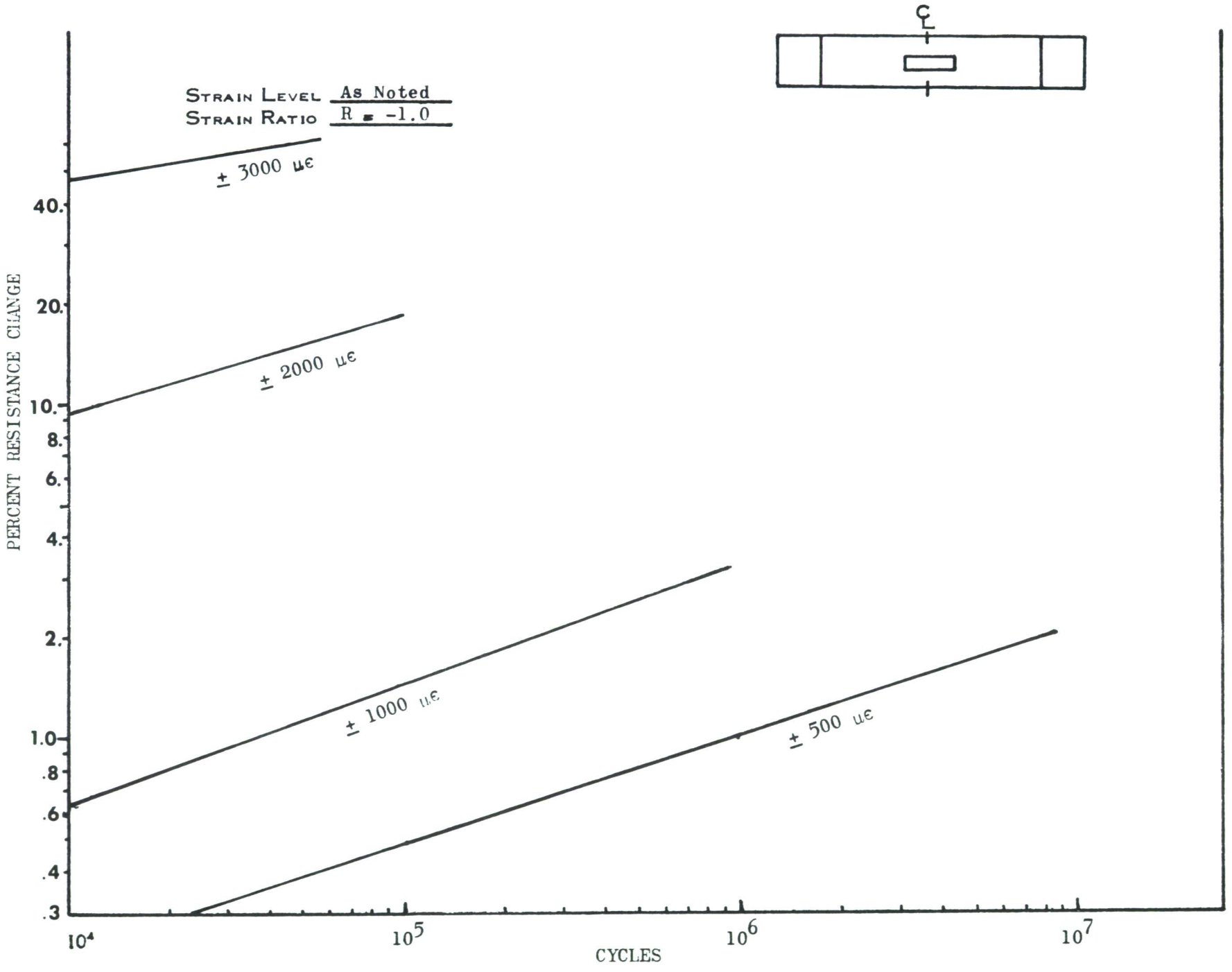

FIGURE 81. FATIGUE SENSOR RESPONSE FOR VACUUM DEPOSITED CU-NI-ZN, SUMMARY

SECTION IV

SUMMARY AND CONCLUSIONS

Previous investigations and development of foil type fatigue sensing devices have been centered around strain gage technology and the use of strain gage materials, i.e., Constantan foil, epoxy backings, strain gage configurations, etc. Considerable efforts were concentrated on working around the limitations of Constantan rather than developing new materials with more desirable operating characteristics.

Results of the AFFDL initiated effort toward the search for an improved resistive material, the testing and evaluation of prospective material candidates, and the optimization of grid configurations and fabrication techniques indicate that the vacuum deposition of ordered metallic films offers the greatest improvements. To go this route, however, one is required to develop techniques in two areas, namely (1) the development of an ordered resistive material by means of a vapor deposition technique and (2) the vapor deposition of an alloy on a flexible substrate. It was initially planned by the Lockheed-Georgia Co. to concentrate only on developing suitable resistive materials and to minimize any development of new fabrication methods. It soon became apparent that just varying the composition of the alloy and then annealing offered only a modest improvement over Constantan. Work hardening of other types of copper-nickel alloys did not offer the significant improvement desired so a new approach, the investigation of order-disorder phenomena, was undertaken. The work hardening process of annealed foils is dependent upon a plastic yielding mechanism which means that only cyclic strains above a specific threshold produce a measurable resistance change. By comparison the vacuum deposited fine grain Cu-Ni-Zn film produces a relatively large resistance change by a disordering process which is not related to any yield point or strength of the material. Generally a material which can be vacuum deposited as a fine grain sensitive metallic film will possess a much higher tensile yield strengh than any of the larger grained annealed foil materials. The use of an ordered material for fabrication of a sensor apparently improved the sensitivity and fatigue life to a degree not possible with the larger grained foils.

The deposited Cu-Ni-Zn resistive material produced a more favorable response to those parameters which cause structural fatigue damage than the currently used Constantan material. The primary sensor requirements for use in subsonic aircraft operational parameters are recognized as (1) long fatigue life, (2) sensitivity to low amplitude strain levels, and (3) uniform resistance change upon exposure to repeated loads. It should be noted, however, that like Constantan foil, correlation factors between sensor thin film information and structural material fatigue damage must still be defined.

The recognized improvements obtained by the use of a Cu-Ni-Zn deposited film when compared to annealed Constantan foil are noted as follows.

(1) Lower threshold sensitivity

(2) Higher resistance change

(3) Longer fatigue life

(4) Removal of material contaminants

(5) Single strand construction

(6) Reduced number and severity of stress concentrators

The vacuum deposition technique results in mechanical and electrical improvements that have contributed significantly to the overall performance of the sensing device when employed in a practical situation. The more desirable sensor operating characteristic, and the one given top priority, i.e., threshold sensitivity, actually exceeded target requirements. The long fatigue life (over 10^7 cycles @ $\pm$ 500 $\mu\epsilon$) exceeded the AFFDL requirement as established by the lifeline of Figure 20. This improvement in fatigue life is attributed to single strand construction, higher tensile strength, refined grain structure, reduced contaminants, and absence of severe stress concentrators. A summary of the basic behavior characteristics of the materials evaluated in Phase I and Phase II of this program are compared as follows.

COMPARISON SUMMARY OF BASIC CHARACTERISTICS

APPLICABLE PROPERTY	ANNEALED METALS (CU-NI FOILS)	VACUUM DEPOSITED (CU-NI-ZN FILM)
Metallurgical	Large, equiaxed grain. Soft annealed. Atomically disordered	Very small grain. Ordered atomic structure. Not annealed.
Mechanical	Low yield strength. Low tensile strength. Short fatigue life.	Moderate tensile strength. Long fatigue life.
Electrical	Electrical resistance change is dependent upon plastic yielding mechanisms to produce metal defects.	Electrical resistance change produced by metal defects, independent of the material yield point. Defects produced by disorder phenomenon.
Temperature	Reannealing occurs. Defects are recovered. Fatigue induced resistance change retroacts.	Disordered condition cannot be recovered below recrystalization temperatures.

Although elevated temperature tests were not a part of this program, the behavior of the ordered Cu-Ni-Zn film sensor does show the potential for utilization at elevated temperatures. The manufacturer of the Kapton backing (E. I. DuPont Co.) indicates an operational limit of 400°C. The other materials selected for evaluation and development were also analyzed with a view toward elevated temperature conditions. The Cu-Ni-Zn alloy used in the sensor does not recrystallize until reaching temperatures of approximately 1110°C. Thus, the sensor has the potential for operating at elevated temperatures (300°C or more) providing suitable attachment materials (adhesives, solder, etc.) are available. Present industry trends toward supersonic operation of aircraft and the related higher temperatures on structural surfaces, necessitate fatigue sensing devices suitable for elevated temperatures.

The most promising application of a bonded fatigue sensing device is considered by the Lockheed-Georgia Company to be a comparison method using a full-scale fatigue test article for calibration and then correlating with damage on a flight vehicle. A system of sensing devices on fleet aircraft could also be used to determine relative usage rates occurring on operational airplanes and thus allow aircraft rotation with respect to missions for the purpose of normalizing fatigue damage. Therefore, a basic requirement for successful utilization is sensor-to-sensor repeatability. The test results have shown that the major deficiency of the vacuum deposited sensor is in performance repeatability which is governed by film deposition uniformity. Exacting quality control measures are necessary to assure uniformity of:

(1) Degree of atomic order;

(2) Material composition;

(3) Grid thickness.

The contribution each of the above factors makes to performance repeatability was not precisely determined and guidelines were not established for correlating each parameter to sensor operating behavior. For instance the sensor deposition procedures can be varied to influence the degree of atomic order i.e., the cool-down rate of the deposited material can be controlled to allow more time for each atom to seek its own energy level. When the contribution each factor makes to performance can be isolated, more positive corrective action can be taken. The ambitious program scope and the limited time allocated did not permit sufficient refinements in the sensor quality control procedures to produce desired repeatable results. Efforts were concentrated on completing the test commitments as previously established by the test plan and in defining operational characteristics rather than investigating fabrication refinement techniques.

It is believed that the apparent nonrepeatability deficiency (controlled by deposition uniformity) of the deposited sensor actually stems from the multistep fabrication techniques employed to obtain experimental sensor quantities. If larger sensor quantities are needed, it may be economically feasible to simplify this technique by depositing the grid element in its final configuration rather than die-cutting the element from a deposited film strip. The additional handling that was required for attaching backings, pressure cures, etc., could also be eliminated. A single step operation using a protective mask would allow the deposition of many sensors simultaneously upon a flexible substrate. The vapor deposition process used in this program was experimental in nature; however, commercial facilities, as used by concerns normally engaged in the vapor deposition of metals, could reduce the procedure to a single step operation.

In conclusion, the results of this program have confirmed several new and pertinent concepts. Program accomplishments have demonstrated that an atomically ordered metal film can be produced by the vapor deposition of a selected Cu-Ni-Zn alloy. The feasibility of producing a fatigue sensing device from a material vacuum deposited in an atomically ordered configuration has been established and indicates a significant improvement in the state of the art. The performance of the vacuum deposited sensor as applied and evaluated in this program exceeds that of the annealed Constantan sensor. A breakthrough in fatigue sensor technology is evident and the sensor performance obtained indicates the potential for a practical application to fleet aircraft.

REFERENCES

1. Horne, R. S., A Feasibility Study for the Development of a Fatigue Damage Indicator, Lockheed-Georgia Company, AFFDL-TR-66-113, Air Force Flight Dynamics Laboratory, Wright-Patterson Air Force Base, Ohio, January 1967.

2. Horne, R. S., "Annealed Foil Fatigue Sensor Development", Interim Report, Lockheed-Georgia Company, AFFDL-TM-70-2-FDTT, Air Force Flight Dynamics Laboratory, Wright-Patterson Air Force Base, Ohio, May 1970.

3. Menden, George T., Electrical Resistance of Metals, Plenum Press, New York, 1965.

4. Broom, T., Lattice Defects and the Electrical Resistivity of Metals, Dept. of Ind. Metallurgy, University of Birmingham, 1958.

5. Wong, Kubilins and Starr, C. D. "Metallurgical Aspect of Resistance," Electronic Industries (1957) 16 Pages 52 - 54, 120 - 122, 124.

6. Taylor, Lyman, Metals Handbook 8th Edition Vol 1, "Properties and Selection of Metals" American Society for Metals, Metal Park, Ohio 1961.

7. Belfour Stulen, Inc., Aero Space Structural Metals Handbook, Vol II and Vol IIA, AFML TR-68-115, Air Force Materials Laboratory, Wright-Patterson Air Force Base, Ohio, January 1968.

8. Sessler, Weiss, Aero Space Structural Metals Handbook Vol IIA, ASD-TDR 63-741 Aeronautical Systems Division, Wright-Patterson Air Force Base, Ohio, March 1967.

9. Stanley, J. K., "Electrical and Magnetic Properties of Metals," American Society for Metals, Metal Park, Ohio, Pages 68 - 70, 1959.

10. "Calibration System Requirements," MIL-C-45662A, dated 9 February 1962.

11. Metallic Materials and Elements for Aerospace Vehicle Structures, MIL-HDBK-5A, Department of Defense, Washington 25, D. C., February 1966.

12. Perino, P. R., "Characteristics of Thin Film Strain Gage Transducers," Statham Instruments, Inc. Paper presented at ISA Conference, New York, 1966.

13. Seamans, R., Singdale, F., Research in the Field of Deposited Strain Gages and Development of Miniature Gage Deposition, Lockheed Aircraft Corporation, AD 253,535, WADD 60-712, Wright Air Development Division, Wright-Patterson Air Force Base, Ohio, July 1960.

BIBLIOGRAPHY

Belser, R. B., "Aging Study of Metal Plating on Quartz Crystals," Report No. 7, Engineering Experiment Station, Georgia Institute of Technology Project 163-176 (Resistors), October 1956.

Belser, R. B., "Electrical Resistance of Thin Metal Films Before and After Artificial Aging by Heating, " Jnl. of Apply. Phys. 28/1, January 1957.

Belser, R. B. Hicklin, W. H., "The Electrical Conductivity of Metallic Films in the Temperature Range 25 to 600 C," Reprint 133 Georgia Institute of Technology, (Resistors), November 1957.

Caldwell, F. R., Thermocouple Materials, National Bureau of Standards Monograph 40, March 1962.

Crampton, D. K., Stacy, G. T., Burghoff, H. L., "Effect of Cold Work Upon the Electrical Resistance of Copper Alloys," Transaction AIME Vol 143, Pages 228 to 245, Pub. 1941.

Crewe, A. V., "A Microscope that sees Atoms", New Scientist, 9 July 1970.

Darken, Gurry, Bover, Physical Chemistry of Metals, McGraw-Hill Co. Chapter 4, Pages 92 - 102, 1953.

Dean, R. S., Electrolytic Manganese and its Alloys, Plenum Press, New York, 1952 .

Feltman, P., "The Electrical Resistivity of Metals due to Plastic Deformation," Metalurgia, Brunel College of Advanced Technology, London W.3, August 1964.

Hirth, J. P., "Work Hardening," Metallurgical Society Conference, Vol 46, Chicago, November 1966.

Holland, L., Thin Film Microelectronics, John Wiley and Sons, Inc., 1965, Chapter 4.

Holland, L., Vacuum Deposition of Thin Films, John Wiley and Sons, Inc. 1958.

Kailash, Joshi, "High Frequency Fatigue of Copper and Aluminum: Cyclic Plastic Strain Response and Electrical Resistivity Studies," Cornell Univ., PH.D., 1968.

Kushner, J. B., "Factors Affecting Residual Stress in Electro-deposited Metals," Metal Finishing, April, May, June, July, 1958.

Material Research Corp., "School and Conference Transactions on the Elements, Techniques and Applications of Sputtering," Pebble Beach, California, 1969.

Moore, D. W., Study of Physical Characteristics of Thin Film Resistance Elements, WADC TR 57-371, ASTIA AD 142324, PB 131703, (Resistors), Wright Air Development Center, Wright-Patterson Air Force Base, Ohio, December 1957.

Rider, J. G., "The Relationship Between Hardness and Electrical Resistivity Changes Induced by Cold Work in Aluminum," Applied Materials Research Journal, January 1963.

Schule, W., Colella, R., "Increase in Electrical Resistivity due to Long Range Order in Cu_3, Ni_3, Zn_2," Journal of the Institute of Metals, Vol 97, 1969.

Sully, A. H., Metallurgy of the Rarer Metals - Manganese, Butterworths Scientific Publications, 1955.

Turk, C., Scala, E., "Microplasticity in Ductile and Brittle Molybdenum and Molybdenum alloys," Symposium Metallurgical Society of AIME Chicago, November 1966.

Van Bueren, "Electrical Resistance and Plastic Deformation of Metals," Z Metallk 46, No. 4, April 1955

Wise, E. M., "Copper Nickel Alloys," Metals Handbook, The American Society for Metals, Cleveland, Ohio 1413, 1939 Ed.

Yves, Morchoisne, "Work-Hardening of Metallic Materials" (Sur L'Ecrouis-Sage des Materiaux Metalliques) 1965.

APPENDIX I

ANALYTICAL INSTRUMENTATION

The following constitutes a general description of the analytical instrumentation and techniques used in the analysis of the resistive materials evaluated during this program. Some peripheral equipment such as photomicroscopes and Polaroid industrial cameras were also used.

X-Ray Diffraction

Crystals are symmetrical arrays of atoms arranged in rows and planes of high atomic density which are able to act as three dimensional diffraction gratings. The atoms, separated by only a few angstroms distance, will diffract short wavelength radiation, termed **X rays,** when certain geometrical conditions are satisfied. Analysis of diffracted x-ray beams, in terms of the laws governing diffraction, gives the size, shape and orientation of the unit cell of the crystal, and analysis of the relative intensities of the diffracted beams determines the position of atoms within the cell. Therefore, x-ray diffraction provides a method for structural analysis of crystals.

X-Ray Spectroscopy

X-ray spectroscopy is the technique for analyzing the wavelengths of radiation from an element bombarded by electrons or **X rays of high energy.** Since every element emits its own characteristic wavelength spectrum, x-ray spectroscopy is the basis for a method of chemical analysis. Fluorescent x-ray spectroscopy is the most common form of this analytical method.

Atomic Absorption

An atom will absorb only highly specific wavelengths of radiation. This atomic absorption of characteristic radiation is the basis of a quantitative technique for analysis of metals in solution. Metal ions of the sample are introduced into a flame. Concurrently, light from a lamp in which the same metal is used as an emission source is transmitted through the flame. The metal ions of the sample, vaporized in the flame, selectively absorb the light from the emission source. The amount of absorption is a function of the concentration of metal atoms in the sample.

Metallograph

The metallograph is an optical instrument designed for both visual observation and photomicrography of prepared surfaces of opaque materials at magnifications up to about 1500 diameters.

Electron Microscope

The electron microscope used was a Japan Electron Optic Co. (JEM-7) high resolution microscope (approximately 4.5Å in transmission) with direct magnification ranges from 600X to 250,000X with no change in optical system. Gun voltages operate at 50, 80, and 100 KV. The photographic chamber accepts $3\frac{1}{4}$ inch x 4 inch plates. Accessories include tilting and rotating stages, tensile deformation and fatigue stage, heating stage, and simultaneous heating and deformation stages.

APPENDIX II

VACUUM DEPOSITED

SENSOR INSTALLATION PROCEDURES

INTRODUCTION

This procedure covers the installation, wiring, and check-out that is necessary for the fatigue sensor installation of the vacuum deposited Cu-Ni-Zn type sensor. Although many of the techniques applicable to a quality strain gage installation are also necessary for a quality fatigue sensor installation, additional care must be taken during certain critical steps. The fact that the sensor is composed of a metal film, approximately four microinches thick, deposited on a Kapton substrate requires a departure from standard strain gaging procedures. The delicate nature of the ordered atomic structure of the thin deposited film makes it rather sensitive to conventional strain gage clamping pressures. The thin film is also sensitive to overheating during the soldering of lead wire.

CLEANING AND SURFACE PREPARATION

The specimen surface preparation requires that an area about twice that of the sensor be thoroughly cleaned. Basically the area to be cleaned should be large enough to accommodate the sensor and moistureproofing. After the removal of oxides and grease by sanding and solvents (MEK) the surface is then scrubbed with Alconox and Scotch Brite pads. The surface is then rinsed with distilled water and air dried.

BONDING

After one or more bonding areas have been prepared, the sensors are carefully removed from the package and visually checked for damage. Cellophane tape placed across the top of the sensor crosswise as shown below will facilitate handling of the sensor.

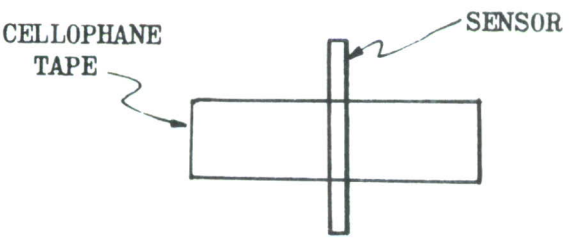

The cellophane carrier tape is used to accurately align the sensor and to position the sensor while applying the adhesive and (catalyst) accelerator. The contact adhesive (Eastman 910)[1] and accelerator is applied according to the manufacturer's specifications. The tape with the sensor adhering to it is now accurately positioned on the mounting area and the tape pressed down to hold the sensor in position. The excess adhesive is gently pressed from the center out to each end of the sensor. Avoid excessive pressure and rubbing of the sensor area as this will induce disorder in the metal film. Anchor terminals are optional; however, they are recommended and may be bonded in place at this time. Oxides may be cleaned from the terminals with a fiber glass brush or pencil eraser. Check the sensor with an ohmmeter at this stage to see if the sensor strand has been opened or grounded.

IV. LEAD ATTACHMENT

The lead attachment can best be made by connecting a small jumper wire to the anchor terminal and then to the bonded sensor strip. The # 34 Soldereze insulated wire is cut to a length of approximately 1/2 inch and 1/8 inch of the insulation removed from each end of the wire either by enamel stripper or heating with a soldering iron. The ends of the wire are now tinned, preferably using Kester Number 44 solder and flux. Excessive heat should be avoided when soldering the jumper wire to the sensor strip. The soldering iron should be limited to 25 watts or less with a 1/8 inch pencil tip.

The lead should be soldered to the outer portion of the sensor solder pad so that if burning occurs on the first attempt, sufficient area will remain for a second try. Moistureproofing may be accomplished with any of the room temperature cured strain gage coatings. The sensor may be made into a dual strand configuration with a proportional increase in resistivity by the arrangement diagrammed below.

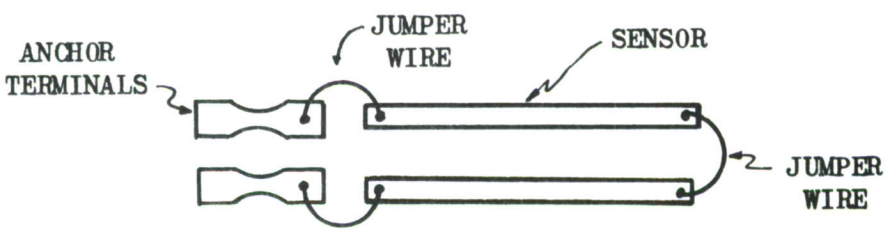

NOTE 1. To expedite the test specimen preparation for this program a pressure sensitive adhesive was normally used. For long term application an epoxy adhesive should be used.

NOTE 2. Sensor initial resistivity can be increased by connecting additional strands in series.

UNCLASSIFIED
Security Classification

DOCUMENT CONTROL DATA - R&D

(Security classification of title, body of abstract and indexing annotation must be entered when the overall report is classified)

1. ORIGINATING ACTIVITY *(Corporate author)*
LOCKHEED-GEORGIA COMPANY
86 S. COBB DRIVE
MARIETTA, GEORGIA 30060

2a. REPORT SECURITY CLASSIFICATION
UNCLASSIFIED

2b. GROUP

3. REPORT TITLE
IMPROVEMENT OF A STRUCTURAL FATIGUE SENSOR

4. DESCRIPTIVE NOTES *(Type of report and inclusive dates)*
FINAL REPORT - APRIL 1969 to APRIL 1970

5. AUTHOR(S) *(Last name, first name, initial)*
ROBERT S. HORNE

6. REPORT DATE	7a. TOTAL NO. OF PAGES	7b. NO. OF REFS
APRIL 1971	138	13

8a. CONTRACT OR GRANT NO.	9a. ORIGINATOR'S REPORT NUMBER(S)
F 33(615)-69-C-1593	ER 10655
b. PROJECT NO.	
c. 1347	9b. OTHER REPORT NO(S) *(Any other numbers that may be assigned this report)*
TASK NO.	AFFDL-TR-70-141
d. 134702	

10. AVAILABILITY/LIMITATION NOTICES This document is subject to special export controls and each transmittal to foreign governments and foreign nationals may be made only with prior approval of the Air Force Flight Dynamics Laboratory (AFFDL/FBT) Wright-Patterson Air Force Base, Ohio 45433.

"Approved for public release; distribution unlimited."

11. SUPPLEMENTARY NOTES
Approved for public release; distribution unlimited

12. SPONSORING MILITARY ACTIVITY
AIR FORCE FLIGHT DYNAMICS LABORATORY
WRIGHT-PATTERSON AFB, OHIO 45433

13. ABSTRACT

The annealed Constantan foil materials currently used in bonded fatigue sensing devices have fatigue life and sensitivity limitations which place restraints upon practical application to long life service aircraft. These restraints led to the requirement for further investigation and development of a more compatible material to meet present and future applications to fleet aircraft within the Air Force inventory. Since previous sensor development efforts have been centered around strain gage technology, a new approach oriented toward adapting the most favorable metallurgical and fatigue properties of a bondable resistive material to the fatigue behavior of an aircraft structure seemed the more appropriate course of action. Initially a group of alloys of the most promising thin foil resistive materials were evaluated. When the threshold sensitivity of the annealed foil materials proved inadequate, the effort was directed toward the development of a vacuum deposited sensor of a material having an ordered atomic structural arrangement. A selected composition of a copper-nickel-zinc material was vacuum deposited in a long-range order arrangement so that when disordered by cyclic deformation a relatively large, permanent electrical resistance change was produced. The test results indicated that the vacuum deposited sensor shows a substantially large improvement over annealed foil materials in the important areas of fatigue life and sensor sensitivity. The sensor performance obtained did represent a breakthrough in technology and indicates the potential for diversified application to fleet aircraft.

DD FORM 1 JAN 64 1473

UNCLASSIFIED
Security Classification

14. KEY WORDS	LINK A		LINK B		LINK C	
	ROLE	WT	ROLE	WT	ROLE	WT
(1) INSTRUMENTATION: FATIGUE						
(2) FATIGUE DAMAGE INDICATOR						
(3) FATIGUE MEASUREMENT						
(4) AIRCRAFT STRUCTURAL FATIGUE						
(5) UNIAXIAL TENSILE TEST						
(6) STRUCTURAL TESTING						

INSTRUCTIONS

1. ORIGINATING ACTIVITY: Enter the name and address of the contractor, subcontractor, grantee, Department of Defense activity or other organization *(corporate author)* issuing the report.

2*a*. REPORT SECURITY CLASSIFICATION: Enter the overall security classification of the report. Indicate whether "Restricted Data" is included. Marking is to be in accordance with appropriate security regulations.

2*b*. GROUP: Automatic downgrading is specified in DoD Directive 5200.10 and Armed Forces Industrial Manual. Enter the group number. Also, when applicable, show that optional markings have been used for Group 3 and Group 4 as authorized.

3. REPORT TITLE: Enter the complete report title in all capital letters. Titles in all cases should be unclassified. If a meaningful title cannot be selected without classification, show title classification in all capitals in parenthesis immediately following the title.

4. DESCRIPTIVE NOTES: If appropriate, enter the type of report, e.g., interim, progress, summary, annual, or final. Give the inclusive dates when a specific reporting period is covered.

5. AUTHOR(S): Enter the name(s) of author(s) as shown on or in the report. Enter last name, first name, middle initial. If military, show rank and branch of service. The name of the principal author is an absolute minimum requirement.

6. REPORT DATE: Enter the date of the report as day, month, year; or month, year. If more than one date appears on the report, use date of publication.

7*a*. TOTAL NUMBER OF PAGES: The total page count should follow normal pagination procedures, i.e., enter the number of pages containing information.

7*b*. NUMBER OF REFERENCES: Enter the total number of references cited in the report.

8*a*. CONTRACT OR GRANT NUMBER: If appropriate, enter the applicable number of the contract or grant under which the report was written.

8*b*, 8*c*, & 8*d*. PROJECT NUMBER: Enter the appropriate military department identification, such as project number, subproject number, system numbers, task number, etc.

9*a*. ORIGINATOR'S REPORT NUMBER(S): Enter the official report number by which the document will be identified and controlled by the originating activity. This number must be unique to this report.

9*b*. OTHER REPORT NUMBER(S): If the report has been assigned any other report numbers *(either by the originator or by the sponsor)*, also enter this number(s).

10. AVAILABILITY/LIMITATION NOTICES: Enter any limitations on further dissemination of the report, other than those imposed by security classification, using standard statements such as:

(1) "Qualified requesters may obtain copies of this report from DDC."

(2) "Foreign announcement and dissemination of this report by DDC is not authorized."

(3) "U. S. Government agencies may obtain copies of this report directly from DDC. Other qualified DDC users shall request through _____."

(4) "U. S. military agencies may obtain copies of this report directly from DDC. Other qualified users shall request through _____."

(5) "All distribution of this report is controlled. Qualified DDC users shall request through _____."

If the report has been furnished to the Office of Technical Services, Department of Commerce, for sale to the public, indicate this fact and enter the price, if known.

11. SUPPLEMENTARY NOTES: Use for additional explanatory notes.

12. SPONSORING MILITARY ACTIVITY: Enter the name of the departmental project office or laboratory sponsoring *(paying for)* the research and development. Include address.

13. ABSTRACT: Enter an abstract giving a brief and factual summary of the document indicative of the report, even though it may also appear elsewhere in the body of the technical report. If additional space is required, a continuation sheet shall be attached.

It is highly desirable that the abstract of classified reports be unclassified. Each paragraph of the abstract shall end with an indication of the military security classification of the information in the paragraph, represented as *(TS)*, *(S)*, *(C)*, or *(U)*.

There is no limitation on the length of the abstract. However, the suggested length is from 150 to 225 words.

14. KEY WORDS: Key words are technically meaningful terms or short phrases that characterize a report and may be used as index entries for cataloging the report. Key words must be selected so that no security classification is required. Identifiers, such as equipment model designation, trade name, military project code name, geographic location, may be used as key words but will be followed by an indication of technical context. The assignment of links, rules, and weights is optional.